12-2001

Evolution of Sprague Neck Bar, Machias Bay, Maine

Rebecca A. Nestor

EVOLUTION OF SPRAGUE NECK BAR, MACHIAS BAY, MAINE

By

Rebecca A. Nestor

B.S. Juniata College, 1999

A THESIS

Submitted in Partial Fulfillment of the

Requirements for the Degree of

Master of Science

(in Geological Sciences)

The Graduate School

The University of Maine

December, 2001

Advisory Committee:

    Joseph T. Kelley, Professor of Geological Sciences, Advisor

    Daniel F. Belknap, Professor of Geological Sciences

    Duncan M. FitzGerald, Professor of Geological Sciences, Boston University

EVOLUTION OF SPRAGUE NECK BAR, MACHIAS BAY, MAINE

By Rebecca A. Nestor

Thesis Advisor: Dr. Joseph T. Kelley

Sprague Neck Bar is a recurved barrier spit located in Machias Bay, Maine. Principle geomorphic features associated with Sprague Neck Bar include bedrock, coastal bluffs, till in grounding line (the Pond Ridge Moraine) and washboard moraines, mudflats, sand and gravel beaches, and a salt marsh. Sprague Neck Bar is attached to the western end of the Pond Ridge Moraine (Sprague Neck) and extends northward toward the head of Machias Bay for 845 meters before the system recurves to the southeast for 232 meters. The recurve system forms a broad tidal flat with evidence for northward and eastward migration of the spit.

The main objectives of the project include: identification of major trends in shoreline change based on historic maps and aerial photographs, characterization of the main sedimentary environments of Sprague Neck, determination of the mechanisms influencing cross-shore and longshore transport, and finally an assessment of the relationship between relative sea-level rise and sediment availability and their role in barrier evolution was evaluated. Sprague Neck Bar is a mixed sand and gravel barrier spit. As with most mixed-sediment barriers the surface sediment fits a bimodal distribution, pebbles (-7 to -6 phi) and medium sand (0 to 1 phi). Surface sediment on the northward extension is not distributed in alongshore zones. The coarsest sediment is

Tidal currents reach a greater maximum velocity, approximately 15 cm/s, along the recurve. Ebb and flood tidal currents are nearly equal in magnitude along the northward extension of Sprague Neck Bar and the recurve system. The qualitative historical analysis, c.a. 1776 to present, revealed no significant long-term change in orientation or morphology of Sprague Neck Bar.

Sprague Neck Bar was examined in context of the stepwise-retreat model developed by Boyd et al. (1987), which is often applied to barrier systems in the Gulf of Maine. Sprague Neck Bar differs from the model by Boyd et al. (1987) in one aspect: Sprague Neck Bar does not have two discrete sediment sources and attachment points. The stepwise-retreat model explains barrier evolution in terms of two barrier spits, each attached to a local source deposit, separated by a tidal inlet. According to the Boyd et al. (1987) model, barrier evolution involves closure of the tidal inlet, spit breaching, and two new sediment sources. Therefore, Sprague Neck Bar is not an obvious example of the stepwise-retreat model.

TABLE OF CONTENTS

List of Figures

List of Tables

INTRODUCTION

During the last 20,000 ^{14}C yr. B.P. coastal Maine was covered by the Laurentide

Ice Sheet and experienced two periods of marine transgression as a result of isostatic

adjustments and rising relative sea-level. The Maine coast is still experiencing a marine

transgression at a rate of 2-3 mm/yr. (Belknap et al., 1989). The wide spectrum of coastal

morphology along the coast of Maine is a result of the diverse effects of glaciation and

associated sea-level change (Kelley, 1987; Kelley et al., 1989; Belknap et al., 1989).

Coastal evolution is a cumulative process in which morphological outputs are

included among the inputs for the next cycle of evolution (Cowell and Thom, 1994).

Cumulative evolution occurs on all time scales, but is most significant over geologic

time. Studying coastal morphology within distinct embayments provides useful

information on the main factors influencing a shoreline's geomorphic response and

evolutionary history. On coastlines experiencing marine transgression, geomorphic

response is largely influenced by antecedent geology, rising relative sea level, and

sediment availability (Belknap and Kraft, 1985).

Sprague Neck (Figure 1), located in Machias Bay, consists of bedrock, mixed-

sediment beaches, a recurved barrier spit, coastal bluffs, coarse- and fine-grained flats,

and grounding line and washboard moraines. The main objectives of this project include:

1) qualitative analysis of the shoreline change of Sprague Neck Bar ca. 1776 to present,

based on historic charts, topographic maps, and aerial photographs, 2) identifying the

sources supplying sediment to Sprague Neck Bar, 3) determining the mechanisms

responsible for transporting and eroding sediment, and 4) inferring the evolutionary

history of Sprague Neck Bar with respect to the stepwise retreat model by Boyd et al.

(1987). In addition to the principle objectives three supplementary questions are asked:

1) in the intricate relationship between relative sea-level rise and sediment availability,

which one is the dominant factor controlling shoreline change in Machias Bay?, 2) how

does the evolution of Sprague Neck Bar compare with similar barrier systems in eastern

Maine?, and 3) what does this comparison indicate about shoreline dynamics in the

eastern Gulf of Maine?
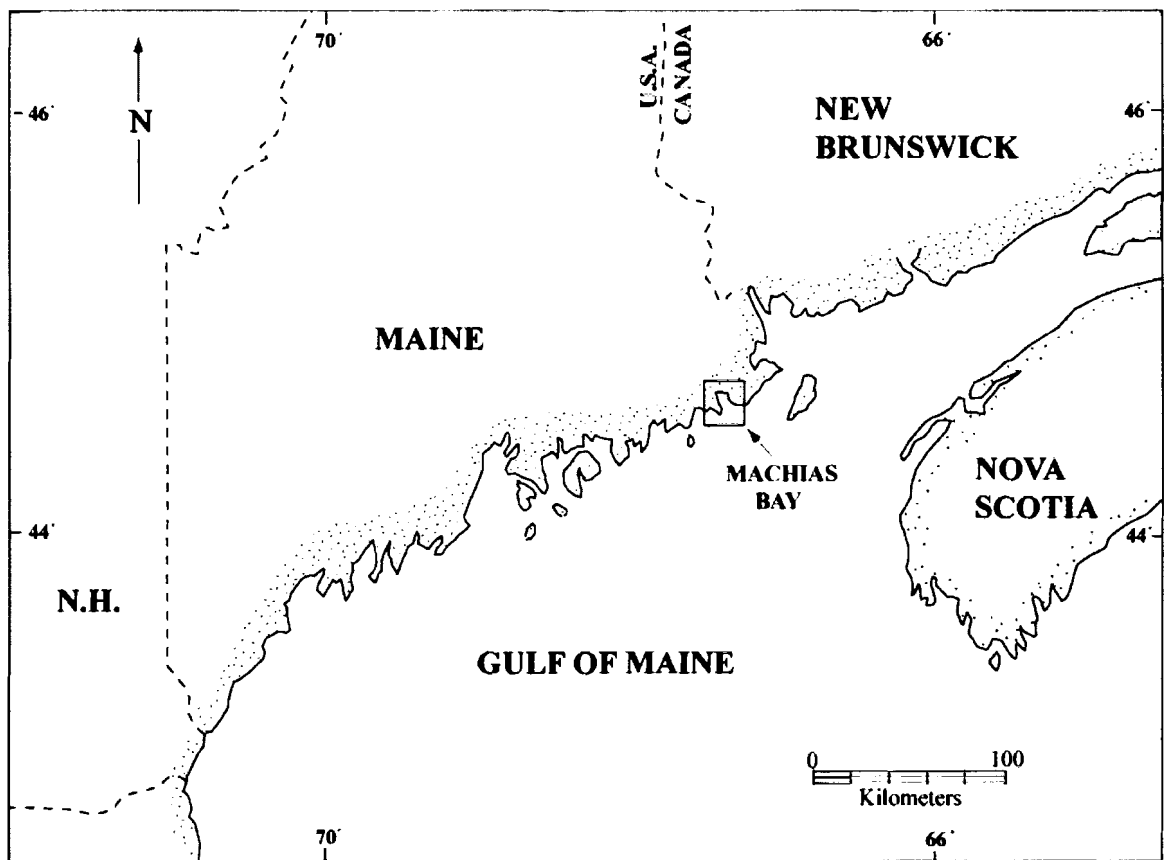
Figure 1. Regional Map of Coastal Maine showing the location of Machias
Bay (modified from Walsh, 1988).

PREVIOUS WORK

Morphodynamics and Barrier Evolution

Coastal evolution is a function of morphodynamic processes that occur in response to changes in external conditions such as waves, tides, sea-level change, and sediment supply. Morphodynamics is defined as the 'mutual adjustment of topography and fluid dynamics involving sediment transport' (Cowell and Thom, 1994, p. 33) and relies on the 'predictability along certain environmental gradients with behavior varying in a deterministic manner' (Carter and Woodroffe, 1994, p.10).

Morphodynamic processes function in a feedback loop between topography and fluid dynamics (Figure 2). Sediment transport is the coupling mechanism between morphodynamic change and fluid dynamics. Positive feedback (or self-organization) is a self-forcing behavior that leads to greater instability and a new mode of operation. Negative feedback (or self-regulation) stabilizes the system for a given range of environmental conditions by acting against fluctuations from a morphodynamic steady state. Reversals from positive to negative feedback (or vice versa) mark a threshold (Cowell and Thom, 1994). Thresholds are intrinsic values of a forcing function that are defined by a system's ability to absorb stress, and are reached when changing inputs drive variables to limiting values. When a threshold is exceeded, adjustments occur and a new set of variables and processes define the system (Carter and Woodroffe, 1994; Cowell and Thom, 1994).

Coarse-grained systems illustrate the ability of coastal systems to control the morphodynamic environment as the systems evolve toward stable, organized forms. As a gravel-dominated beach moves toward a stable morphodynamic state, wave and current

3
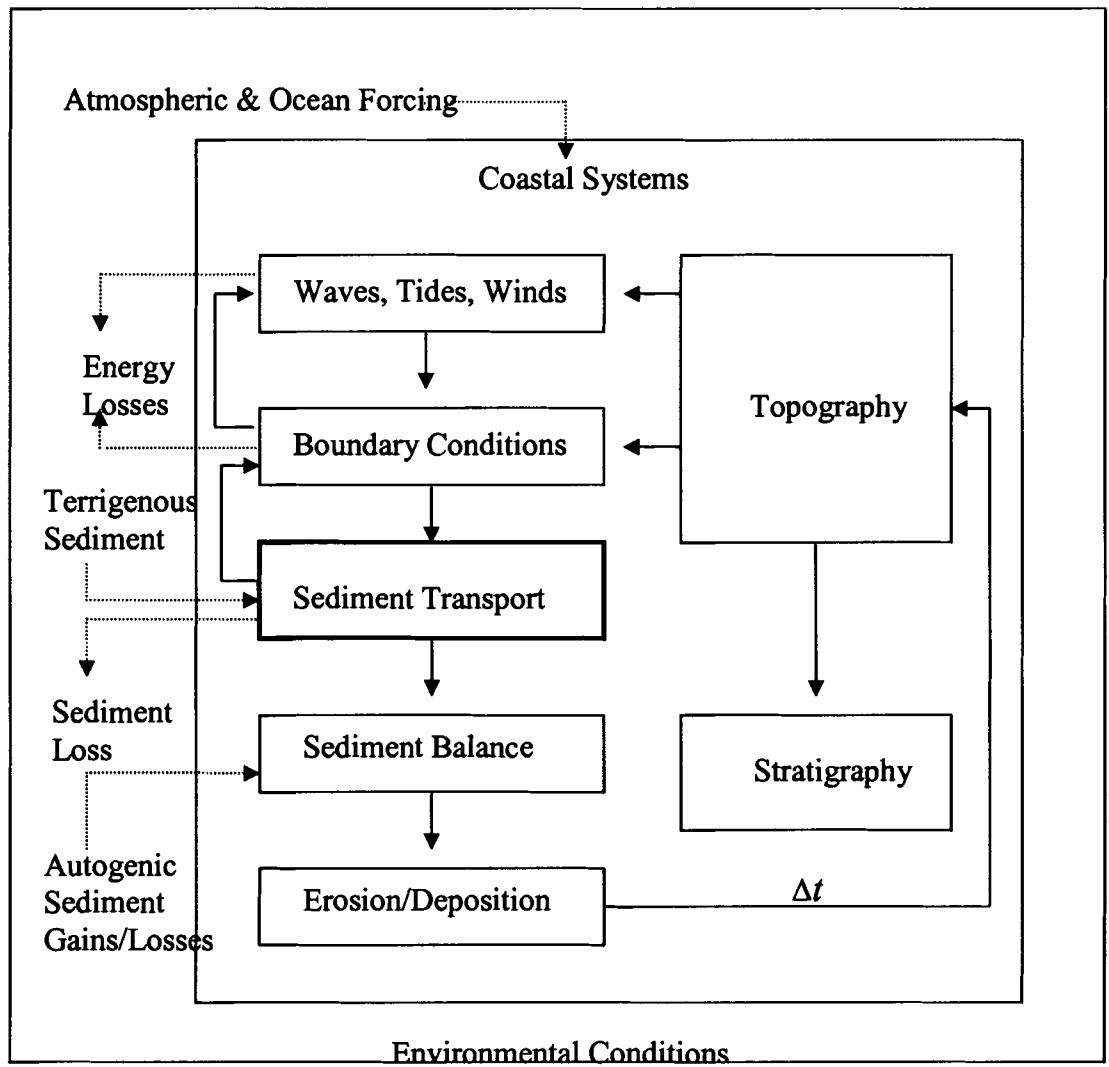
Figure 2. The structure and functions of the morphodynamic model for the coastal system. Boundary conditions refer to spatial and process boundaries for the system. Sediment transport is highlighted because it is the link between fluid dynamics and morphological change. Dashed arrows indicate input-output between the coastal system and environment (after Cowell and Thom, 1994).

4

processes move sediment and landforms in longshore and cross-shore directions. Movement in both longshore and cross-shore directions allows the system to absorb a range of energy inputs. For example, the morphodynamic state of a coarse clastic beach characterized by a concave-up form with a break in gradient near the mid- to low-tide line will alter as the critical wave height-to-depth and depth-to-wavelength ratios vary. The main determining factors of barrier evolution in paraglacial and other temperate environments are: 1) sediment availability, 2) relative sea-level fluctuations, 3) antecedent geology, and 4) wave and tidal climate (Belknap and Kraft, 1985, 1981; Hayes, 1975; Kraft et al., 1979; Kraft and John, 1979).

Sedimentology

Size and volume of glacial sediment sources influence the size and shape of coastal features (Forbes et al., 1995a). The rate of sediment input and proportion of sand and gravel affect storage volume, facies characteristics, and overall stability of littoral systems (Forbes and Taylor, 1987. The type of onshore or offshore source determines the size and amount of available sediment (Forbes et al., 1995a).

Sediment supplying New England barriers is, either directly or indirectly, from inland, updrift, and offshore sources. Inland sources are eroded and transported to the coastline by rivers. Large amounts of sediment bypassed the shoreline after deglaciation and were stored in submerged paleodeltas. Submerged paleodeltas and drowned glacial features comprise the offshore sources (Barnhardt et al., 1997; Belknap et al., 1986). Skeletal carbonates are associated with late Quaternary glacigenic deposits found on the inner continental shelf of Maine. Carbonate-secreting organisms (barnacles, echinoids, mussels) live on the substrate and, with a low input of terrigenous sediments, are the only

5

sediments now accumulating on the inner shelf (Barnhardt and Kelley, 1995). The onshore glacial equivalents and coastal bluffs comprise the updrift sediment sources that have not been previously incorporated into barrier systems (FitzGerald and van Heteren, 1999). Bluffs are composed of unconsolidated sediment that are subjected to marine and subaerial erosion processes (Carter and Guy, 1988; Kelley and Dickson, 2001; Smith, 1990).

A range of particle sizes and shapes and the system's organization determines the actual degree of transport (Carter and Orford, 1993; Hoekstra et al., 1999). The distribution of particle shapes is largely dependent on lithology; size differentiation among lithologies is negligible. Nonspherical shapes (blades and plates) are easily transported by hydrodynamic shear at lower fluid velocities than spheres and rods because of their higher cross-sectional area to volume ratio. When a wave reaches the capacity to transport material the flat particles are transported shoreward. As the wave reaches the highest point of swash the flat particles are again preferentially moved shoreward by sliding. Flat particles remain on the barrier crest because of their resistance to being rolled while spherical shapes are transported to the breaker line by rolling and tumbling (Brenninkmeyer and Nwankwo, 1987; Rosen and Leach, 1987).

As coarse particles accumulate, the rules of mass transport apply and group imposed controls (e.g., position, bed acceptance/rejection, contact stresses) dominate the transport environment. Group-imposed controls may overwhelm transport thresholds and lessen transport potential (Bluck, 1967; Carter and Orford, 1991, 1993). On a gravel beach, progressive clast selection may stop or slow clast entrainment. Thus, it is possible to have a slow transition from an unsorted population toward a sorted subpopulation with

6

a narrow range of size/shape characteristics (Carr, 1969). Size/shape sorting indicates the level of organization (Carter and Orford, 1991).

For a given barrier system, the input population will be sorted according to individual clast characteristics including size, shape, and density. The coarse beach is viewed as a surface of probability in which an individual clast has a range of transport potential (Figure 3a), including incorporation into the surface facies (Px), washover/ejection losses (Pw), entrapment between larger clasts within the matrix (Pc), acceptance into a subpopulation controlled by either size or shape (Pi), offshore losses (Pa), and breakage losses (Pb). As facies and barrier organization evolve the probabilities of each entrapment possibility changes, i.e., probability of clast acceptance into an imbricate frame increases as the frame increases. As acceptance (Pi) increases the probability of remobilization (Pr) decreases (Carter and Orford, 1993, 1991).

Carter and Orford (1991) attempted to explain the longer-term relationships between various entrapment possibilities and time (Figure 3b). With increased organization, the probability of entrapment (Pe) and acceptance (Pi) into subpopulations increases. Breakage opportunities also increase with greater organization because it is more difficult for individual clasts to move downdrift. As the intertidal frame increases, by means of entrapment and acceptance, the system becomes more dissipative and the probability of washover and offshore losses decrease (Carter and Orford, 1991). Transport probabilities vary according to barrier organization into alongshore and cross-shore zones (Carter and Orford, 1991). Each zone may be capable of trapping clasts of a certain size, shape, or lithology, and therefore, to a certain degree these zones control the developing barrier architecture (Moss, 1963; Carr, 1969).

Pa = unit input/output
Px = beach facies
Pw = washover/ejection
Pe = entrapment matrix
Pi = acceptance
Pb = breakage
Po = offshore
Pr = remobilization
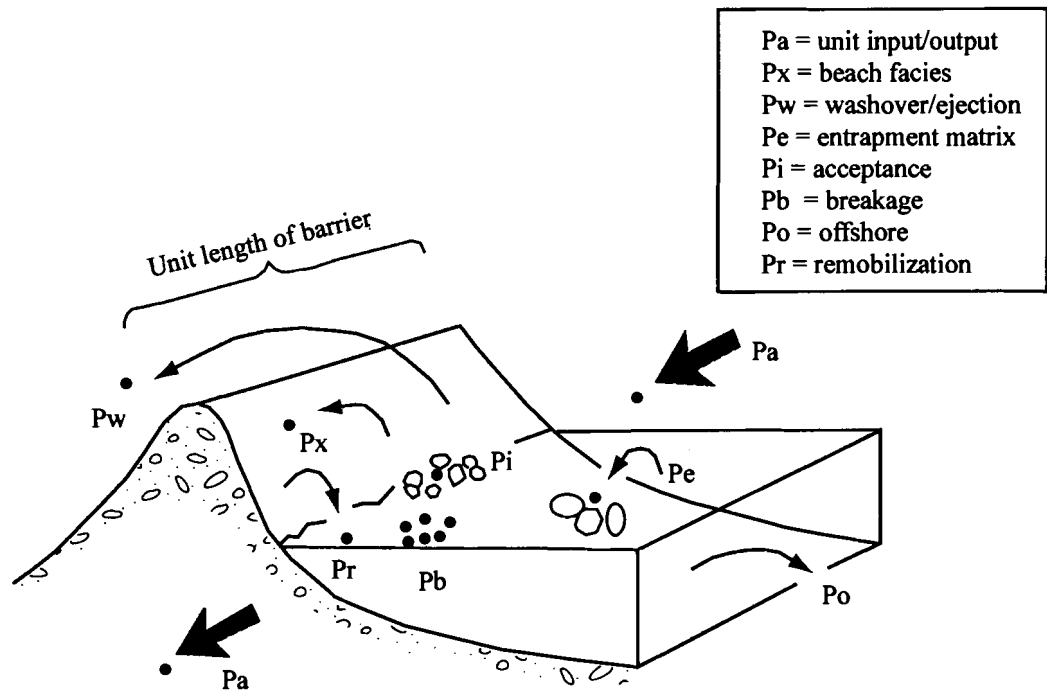
Figure 3a. The probabilistic nature of individual sediment grain transport (modified from Carter and Orford, 1991).
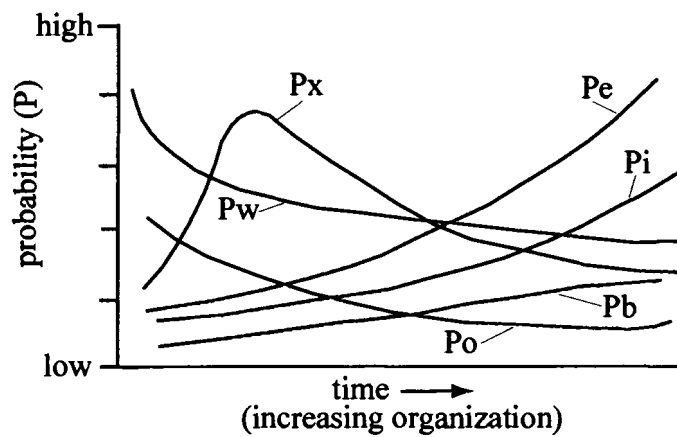
Figure 3b. Long-term probabilistic opportunities for gravel clasts in a barrier system (modified from Carter and Orford, 1991).

Sediment movement is distinguished as longshore and cross-shore transport (Ostrowski et al., 1995). Continual reworking of clasts results in cross- and along-shore facies assemblages and, in the absence of "new" sediment, a reduction in the overall potential for transport (Carter and Orford, 1993). The direction and magnitude of longshore transport are functions of exposure to waves, orientation with respect to waves, and offshore slope (Komar, 1974). Longshore transport is fundamental to creating spatial changes and in the formation and movement of erosional and accretional features (Ostrowski et al., 1995). Quick and Ametepe (1991) proved that for a range of beach slopes and sediment sizes, total longshore transport increases with beach slope, though only minimally with sediment size. A large offshore flux enhances longshore transport. With a continued large offshore movement, and adequate sediment supply, beach slope decreases. The decrease in slope causes a reduction in longshore transport. Reduction in both beach slope and longshore transport results in a system that conserves sediment. If the longshore supply is insufficient, the offshore flux is transported alongshore. The beach slope will not decrease under these conditions and the longshore transport will remain high, supplied by offshore sediment movement. As the offshore flux continues to supply sediment for longshore transport the beach erodes and recedes. Thus, cross-shore transport and slope may play a substantial role in controlling the velocity and magnitude of longshore transport (Quick and Ametepe, 1991).

Relative Sea-Level Fluctuations

Relative sea level (RSL) control is an important factor in the development of coarse-grained barriers (Boyd et al., 1987; Carter et al., 1989; Forbes and Syvitski, 1994). Direction and rate of RSL change affects long-term evolution of barrier and backbarrier

environments (Forbes et al., 1995b) by controlling sediment availability and the timing or location of reworking. Eroding bluffs and headlands last longer under slowly, rather than rapidly, rising RSL because a longer time period exists for the system to reach equilibrium (Forbes and Syvitiski, 1994; McNinch et al., 1999).

Recycling former backbarrier sediments into the active barrier sediment budget allows barriers to keep pace with rising RSL. Recycling operates by exhuming the underlying substrate when the shoreface migrates landward (Belknap, 1991; Belknap and Kraft, 1981, 1985; Duffy et al., 1989; McNinch et al., 1999; Swift, 1975). If the rate of barrier build-up can not keep pace with the rate of RSL rise then overtopping, overwashing, or overstepping may occur (Forbes et al., 1991; Orford et al., 1995).

Orford et al. (1995) attempted to define the relationship between barrier behavior and sea-level rise. In theory, coarse barriers move both horizontally and vertically in response to sea-level rise. Orford et al. (1995) postulated that the horizontal movement of barrier systems indicates a long-term relationship between RSL and barrier stability. Barrier stability is indicated by the height of the barrier crest. As the rate of RSL rise increases, the rate of overwash increases, leading to an increase in the landward transport of crest sediment to the backbarrier. Therefore, overwash drives the barrier rollover processes (Orford et al., 1995).

If the assumption that a barrier rolls over during retreat is correct, then the sediment in the beachface must be raised to the elevation of the crest. If the barrier rollover volume, an estimate of the volume under a barrier cross-section, is multiplied by barrier height, then a measure of barrier stability to retreat rate can be made (Table 1). A barrier with a small rollover volume and low barrier height is the least resistant to change.

10

This suggests that barrier dimensions and RSL rise may be of equal importance, and the smaller the barrier's rollover volume the faster the retreat regardless of the rate of RSL rise (Orford et al., 1995).

Table 1. Characteristics of sample gravel barriers. Barrier height is the vertical difference between the gravel crest and the seaward edge of the barrier. Rollover volume is an estimate of volume under a sample barrier cross-section. Resistance is the rollover volume multiplied by barrier height to provide a measure of barrier stability (Orford et al., 1995). Barrier 3 has the greatest resistance to change.

Barrier	Barrier Height (m)	Rollover Volume (m^3)	SLR rate (mm/yr)	Resistance
Barrier 1	3.5	130	3.8	455
Barrier 2	6.5	325	0.9	2113
Barrier 3	8.0	340	1.5	2720

The relationship between wave activity and barrier stability corresponds with the explanation by Forbes et al. (1991) that storm surge is largely responsible for higher rates of landward migration. Increased storm surge leads to increased overwashing and overtopping events, which enhances barrier instability (Orford et al., 1996). The relationship between RSL change and barrier stability also indicates that barriers may evolve under fluctuating and stable conditions. Gravel-dominated barriers retreat with a rise, and at some point, a fall in RSL. Retreat during a fall in RSL can only occur through strong wave activity in the absence of an adequate sediment supply. The barrier crest eventually fails, and the barrier is translated landward by wave activity (Forbes et

al., 1991; Orford et al., 1983, 1995).

Antecedent Geology

Antecedent geology controls the shape of the coastline by providing the regional slope and establishing the initial orientation with respect to wind and waves (Belknap and Kraft, 1985; Kelley, 1987). Local bedrock controls deposition and preservation of facies, morphodynamics, landward migration of nearshore sediment, reworking, and dispersal (Buynevich and FitzGerald, 1999; Evans et al., 1985). Topographic highs can serve as attachment points and stop landward migration (Fields et al., 1999).

Antecedent geology determines the amount of accommodation space available for deposition in relation to the rate of sediment supply and RSL fluctuations (Belknap and Kraft, 1981, 1985; Cowell and Thom, 1994; FitzGerald and van Heteren, 1999) and affects the thickness of barrier lithosomes. Even with the same rate of sediment supply variations in accommodation space produces different coastal geometries and stratigraphies (Roy et al., 1994); typically thin barrier lithosomes in paleotopographic highs and thick in low areas (Belknap and Kraft, 1985; FitzGerald and van Heteren, 1999). Coastal lithosomes on a topographically varied surface have differential preservation with portions of the stratigraphic column better preserved in valleys (Belknap and Kraft, 1985, Belknap et al., 1994).

Transgressive systems interact with antecedent geology to control the evolution and preservation of barrier systems. A transgressive system is created when the rate of RSL drives a system landward faster than sediment supply builds the barrier seaward (Evans et al., 1985). As the system translates landward and builds upward, the units are truncated by the shoreline at the ravinement surface. The ravinement surface (Swift,

12

1975) represents the depth of shoreface erosion and controls the location and morphology of the coastline (Belknap and Kraft, 1985; Fields et al., 1999). Fluvial and subaerial erosion during sea-level lowstand results in a basal unconformity, which represents the major hiatus between the leading edge of the Holocene transgression and pre-Holocene units. The spatial relationship between the two unconformities determines the degree of preservation (Belknap and Kraft, 1985).

Wave and Tidal Regime

Waves are the main entrainment mechanism and tide/wave/wind-driven currents transport the sediment on coasts (Davis, 1994; Soulsby, 1991). The vertical range of wave action and the frequency of wave attack at a specific intertidal level are a function of RSL changes and tidal currents. The level of wave attack influences the sedimentation pattern by determining access to source deposits (Forbes and Syvitski, 1994).

Local reworking by waves and currents under changing RSL and supply conditions produces different morphologies (Roy et al., 1994). Waves and currents resculpt the topography and change the roughness distribution, which results in a redistribution of wave energy along the shore. Spatial and temporal variations in roughness and topography affect wave height and direction along the shoreline (Hume et al., 1995).

Longshore currents are an important mechanism in distributing sediment along the beach and nearshore environments. Beach form and nearshore slope are two factors in determining a system's morphodynamic response to wave attack (Davis, 1994). While a gravel beach with a single slope remains reflective under most conditions, the morphodynamic characteristics of slopes with a significant break in gradient, near the

low- to mid-tide line, change as the wave height to depth and depth to wavelength ratios vary (Carter and Orford, 1993; List and Farris, 1999). The greater the wave height or longer the period, the greater the depth at which a particle can be transported (Brenninkmeyer and Nwankwo, 1994).

Shoreline configuration may have a "memory affect" in which the system returns to the pre-storm shape as storm intensity decreases (List and Farris, 1999). During storm events, sediment from the nearshore profile is often deposited in the offshore portion of the profile and returned to the nearshore section when the storm ceases. With the transfer of sediment from one section of the profile to another the total sediment volume within the overall system remains constant (Haines et al., 1999).

Evolutionary Models

As the concept of barrier evolution developed, four dominant theories emerged. De Beaumont (1845) first proposed the theory of barrier formation through the upward building of offshore bars, later supported by Otvos (1970). According to this theory waves approaching the nearshore environment disturb sea-floor sediments. When the waves reach the breaker zone and lose energy, sediment settles out, accumulating as an offshore bar. With continued aggradation the barrier eventually encounters sea level and sediment accumulates, forming beaches and dunes (Otvos, 1970). Johnson (1919) used this theory in a situation of emergence. Gilbert (1885) advocated an alternative theory of spit formation through longshore transport and breaching, also supported by Fisher (1968). The third theory is submergence of antecedent topography such as Pleistocene coastal features (Hoyt, 1967). The fourth theory is that barriers formed on the shelf and were separated from the site of origin through landward migration, with the origin

14

obscured after migration (Shepard, 1960; Swift, 1975). With increasing field evidence Zenkovitch (1967) and Schwartz (1971) advocated the idea of multiple causality.

Halsey (1979) combined various aspects of the four dominant theories in the nexus model. The nexus model is the linking of new and old topographies, particularly inlets occurring over paleovalleys, coupled with differing supply rates (Halsey, 1979). This model relies on the rate of RSL rise to overwhelm sediment supply and create a transgressive system (Evans et al., 1985).

The control antecedent geology exerts on sediment dispersal as the shoreline transgresses over irregular topography is also illustrated by the stepwise barrier retreat model. The six-stage coastal sedimentation model for the eastern shore of Nova Scotia is developed around isolated sediment supplies (eroding drumlins) and headland anchor points (Boyd et al., 1987; Johnson, 1919). Along the Nova Scotia coast, each eroding drumlin is in a different stage of evolution. The drumlin with the maximum sediment available controls the sediment transport pathway. Control of the pathway transporting sediment is relinquished when the drumlin is depleted and drowned (Boyd et al., 1987; Carter and Woodroffe, 1994).

The first two stages (Figure 4) explain coastal origin during the early Holocene. Stages 3-6 are cyclic for each compartment with the time scale dependent on rate of RSL rise and the frequency with which sediment sources are encountered. Barrier building begins when the transgressing shoreline encounters sediment sources (Boyd et al., 1987). As the erosional front moves across the drumlins, sediment is distributed parallel and normal to incoming waves (Carter and Orford, 1988). While a large sediment supply is available the barrier progrades seaward. When supply diminishes, the barrier loses

15

2. SEA LEVEL RISE AND ESTUARY DEVELOPMENT

3. BARRIER GENESIS AND PROGRADATION

4. BARRIER RETREAT

CONTINENTAL GLACIER

ICE SHELF

ICEBERG

1. CONTINENTAL GLACIER AND ICE SHELF

6. BARRIER REESTABLISHMENT

5. BARRIER DESTRUCTION

AGE INCREASING

DRUMLIN
GLACIAL TILL
BOULDER RETREAT SHOAL

SUBAERIAL BARRIER
MARSH
BARRIER MIGRATION PATH

OCEAN AND ESTUARY
INTERTIDAL ESTUARINE SEDIMENT
SUBAQUEOUS BARRIER (SHOREFACE, TIDAL DELTAS)

Figure 4. The evolutionary model proposed for transgression on the eastern shore of Nova Scotia (modified from Boyd et al., 1987).

16

contact with the drumlin and reaches equilibrium with the incident waves (Carter and Woodroffe, 1994). RSL rise is again the dominant control and barriers migrate landward. Retreat is dominated by overwash and tidal-inlet processes that remove sediment from the system and deposit the material in flood-tidal deltas, washover and estuarine environments (Boyd et al., 1987; Boyd and Honig, 1992). The development of estuarine sediment sequences is dictated by cycles of barrier progradation and destruction (Boyd and Honig, 1992). Maximum rates of sedimentation occur during transgression and destruction (Boyd et al., 1987). Barrier building may slow or stop the supply of sediment to the estuarine environment, creating a fluctuating sediment supply and a sequence of stacked estuarine facies. The cyclic pattern of facies indicates that fluctuating sedimentation rates are not necessarily the result of RSL oscillations, but may occur through variations in physical parameters during a transgression (Boyd and Honig, 1992; Duffy et al., 1989).

Forbes et al. (1995b) emphasize the ability of barrier systems to self-organize rather than following a distinct model of set pathways. Coarse-grained barriers exhibit self-organization through large-scale morphological evolution and facies differentiation. The process of self-organization involves reworking and textural sorting of material toward transport minima. This produces a stable configuration in which the barrier system is resistant to change under fluctuations in external conditions up to certain limits.

The stages of self-organization include formation, growth, consolidation, and destruction. Progression through the various evolutionary stages depends on external conditions (energy and mass input) and the morphodynamic feedback (internal response) of the system (Forbes et al., 1995a; Orford et al., 1996). A set of environmental controls

17

exists whose interactions create circumstances that allow gravel barriers to develop, organize, and evolve (Orford et al., 1996). External conditions influencing morphosedimentary characteristics include sediment supply, antecedent geology, RSL fluctuations, and wave climate. These characteristics occur on various scales and vary through time. As long as a certain threshold is not exceeded, then self-organization continues (Forbes et al., 1995a). During formation, growth, and consolidation, sediment supply is the most important control. When the source is depleted, wave climate becomes the dominant control with respect to shoreline adjustment. Antecedent topography is important at all times, lessening in importance during growth, consolidation, and initial destruction. RSL change is not predominant in any particular phase. Fluctuations in RSL are most effective during consolidation because of overwash and overtopping processes (Orford et al., 1996).

Barrier Systems on the Northeastern Coast of Maine

New England experienced several episodes of glaciation, which is responsible for the irregular and rocky coast with varied and isolated sediment supplies. The thickness and extent of the Laurentide ice sheet and the timing of deglaciation influenced the varying sea-level histories in New England (FitzGerald et al., 1994). The bedrock headlands that divide the coast into compartments restrict sediment movement. Restricted sediment movement creates short, isolated barriers. Barrier spits are common on New England coasts as a result of the irregular coastline and the high number of local onshore deposits (Duffy et al., 1989; Kelley, 1987).

Along the coast of Maine, barrier system morphology (e.g., spits, tombolos, and pocket beaches) varies greatly because of bedrock geology and the diverse effects of

18

glaciation. The majority of the northeastern coastline is tide-dominated (Figure 5) and sediment-starved, with barrier formation typically restricted to protected embayments with glacial sediment sources (Duffy et al., 1989). The eastern, macrotidal coast of Maine is the only tide-dominated coast in New England (FitzGerald et al., 1994). Composition ranges from fine sand to cobble-size material with mixed-sediment beaches common. Mixed-sediment beaches occur where sediment supply is variable in texture. Barriers on this type of coastline are typically isolated, anchored to bedrock or glacial headlands, backed by fresh- to salt-water lagoons or marshes, low in relief, and transgressive (Duffy et al., 1989). Transgressive systems are characterized by washover deposits of sand and gravel in the backbarrier area and exposed peat on the beachface (FitzGerald et al., 1994; FitzGerald & van Heteren, 1999).

Jasper Beach – Jasper Beach is a pocket, gravel, barrier system that is transgressive in nature. Profiles of Jasper Beach are characterized by a steep beachface slope, high berm, and coarse material. The barrier is retreating over lagoon or backbarrier marsh sediments exposing peat on the beachface (Duffy et al., 1989). Gehrels et al. (1996) determined the higher high marsh and high marsh have existed since at least 4.795 ± 0.080 ka. This vertical sequence reflects RSL rise and the resulting landward translation of marine environments (Duffy et al., 1989; Gehrels et al., 1996).

Lubec Embayment – Lubec Embayment (Figure 6) is a coastal re-entrant in eastern Maine, adjacent to the international boundary with Canada. Lubec and Quoddy Spits are shore-parallel features generated within a low wave-energy environment. Lubec Embayment is an embayment sheltered to the west and south by the mainland and West Quoddy Head, respectively. Wave generation is fetch-limited for all wave approach
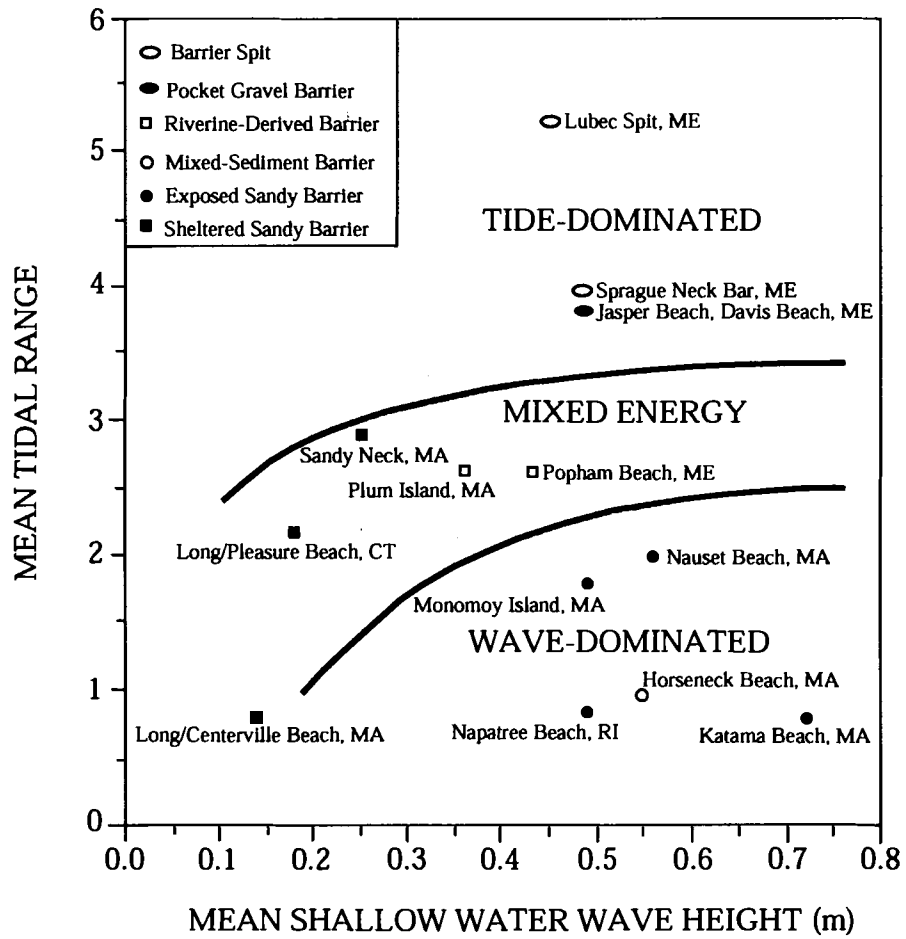
Figure 5. Shoreline classification based on mean tidal range and mean shallow water wave heights (modified from FitzGerald et al., 1994, p. 323).
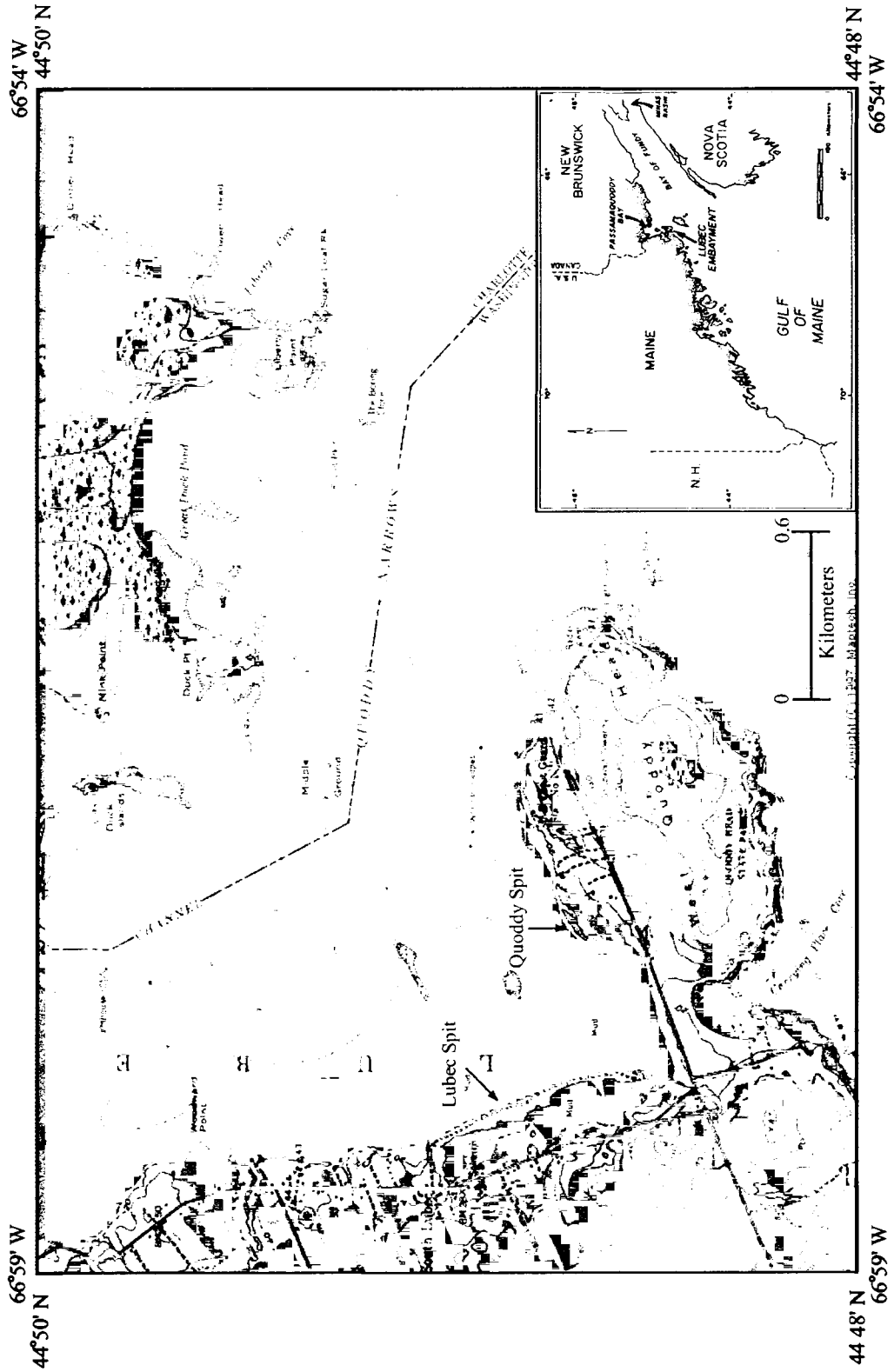
Figure 6. Location of the Lubec Embayment (Terrain Navigator, 1998). The regional map of Maine is from Walsh, 1988.

directions (Walsh, 1988). In fetch-limited conditions waves cannot attain the maximum

wave energy for a given wind speed and duration (Komar, 1974). Maximum fetch is

from the ENE and is approximately 4.5 km at MHW, and minimum fetch is 1.7 km at

MLW. The predicted maximum wave height during average wind speed conditions is

0.24 m. In the Lubec Embayment mean tidal range is approximately 5.3 m, exceeding 6

m on spring tides. The macrotidal environment fosters the development of large tidal

flats and high velocity bi-directional currents (Walsh, 1988). Walsh (1988) determined

that tidal current flow within the embayment was ebb dominated, based on current sensor

data and intertidal morphology.

Principle geomorphic elements include coarse-grained barrier spits, a backbarrier

salt marsh, and coarse-grained tidal flats. Landward transfer of sediment from intertidal

source areas to modern depositional sites occurs by swash bar migration, seaweed

transport, and ice-rafting. Migration of intertidal swash bars and seaweed transport of

gravel-sized clasts are the most important transport mechanisms in the Lubec

Embayment. Walsh (1988) determined that seaweed transport is an effective mechanism

transporting gravel-sized clasts from the low-mid intertidal source areas to sites of

modern-day accretion. The net transport is onshore for the mid-high intertidal locations,

while the low intertidal flat and channels show bi-directional and offshore transport.

Walsh (1988) suggested clast movement with seaweed is episodic because clasts become

trapped in gravelly sediments. High-energy events or ice-rafting disperse the clasts and

allow continued transport (Walsh, 1988). The attachment of seaweed may also enhance

ice-rafting because of the larger surface area around which ice can form (Dionne, 1965).

Ice transport is important in marsh sedimentation and largely responsible for the growth

of Quoddy Spit (Walsh, 1988).

Evolution of the Lubec Embayment was rapid through historic time and cyclical in nature (Walsh, 1988), fitting the evolutionary model proposed for transgression on the eastern shore of Nova Scotia by Boyd and others (1987). From late Pleistocene time to present, evolution involved the formation and destruction of two ancestral barriers, followed by the growth of the modern Lubec Spit during a period of reformation (Walsh, 1988). During reformation, sediment depleted from one barrier is relocated landward and concentrated in a new barrier (Orford et al., 1996). During late Holocene time, evolution was rapid and complex. Retreat can be summarized by three main processes: 1) spit breaching and destruction, 2) sediment reworking by waves and tides resulting in landward translation of the relict spits, and 3) spit regeneration into forms stable under contemporary marine conditions (rate of sea-level rise and sediment supply). The growth of the Lubec and Quoddy Spits is primarily a result of marine reworking of relict barriers in a relatively sheltered environment. Internal sediment recycling and conservation of relict barrier sediments, with minimal sediment supplied from outside the embayment, led to the development of the modern-day spits. Most or all of the sediment present in the earliest mapped barrier in Lubec appears to have been conserved in the present barrier systems (Walsh, 1988).

PHYSICAL SETTING

Geography

Machias Bay, the study area, is located in the northern Gulf of Maine and is rectangular in shape (Figures 1, 7). Sprague Neck divides the bay into two halves. North of Sprague Neck lies the mouth of the Machias River, fronted by several smaller islands, and Holmes Bay. The southern half of Machias Bay is more open to the Gulf of Maine. Cross Island and a group of smaller islands sit at the mouth of Machias Bay.

Geology

Bedrock Geology– The Machias area is composed of Silurian and Devonian metasedimentary and metavolcanic rocks (Figure 8, Table 2). There is a minor amount of intrusive rock that is predominantly gabbro to ultramafic in composition. Two major fault systems cut the Machias region. The intersecting fault systems are Paleozoic and Mesozoic in age (Osberg et al., 1985). Location and trend of the fault systems control the shape of Machias Bay (Kaplan, 1994).

Quaternary Geology – The Laurentide Ice Sheet (LIS) advanced into Maine from Quebec between 30,000 and 24,000 ^{14}C yrs. B.P. (Dorion et al., in press). The LIS continued the southward advance until it reached a terminal position in the Gulf of Maine between 20,000 and 22,000 ^{14}C yr. B.P. (King, 1996; Bothner and Spiker, 1980). The ice sheet retreated across the Gulf of Maine at approximately 19,000-15,000 yrs. B.P. in a north-northwest direction, depositing laminated marine mud and outwash (Dorion, 1997). By 15,300 ^{14}C yrs. B.P. the LIS retreated from the continental shelf (LePage, 1982) with the grounding line reaching eastern Maine by 14,000 ± 85 ^{14}C yrs. B.P. (Kaplan, 1994,

24
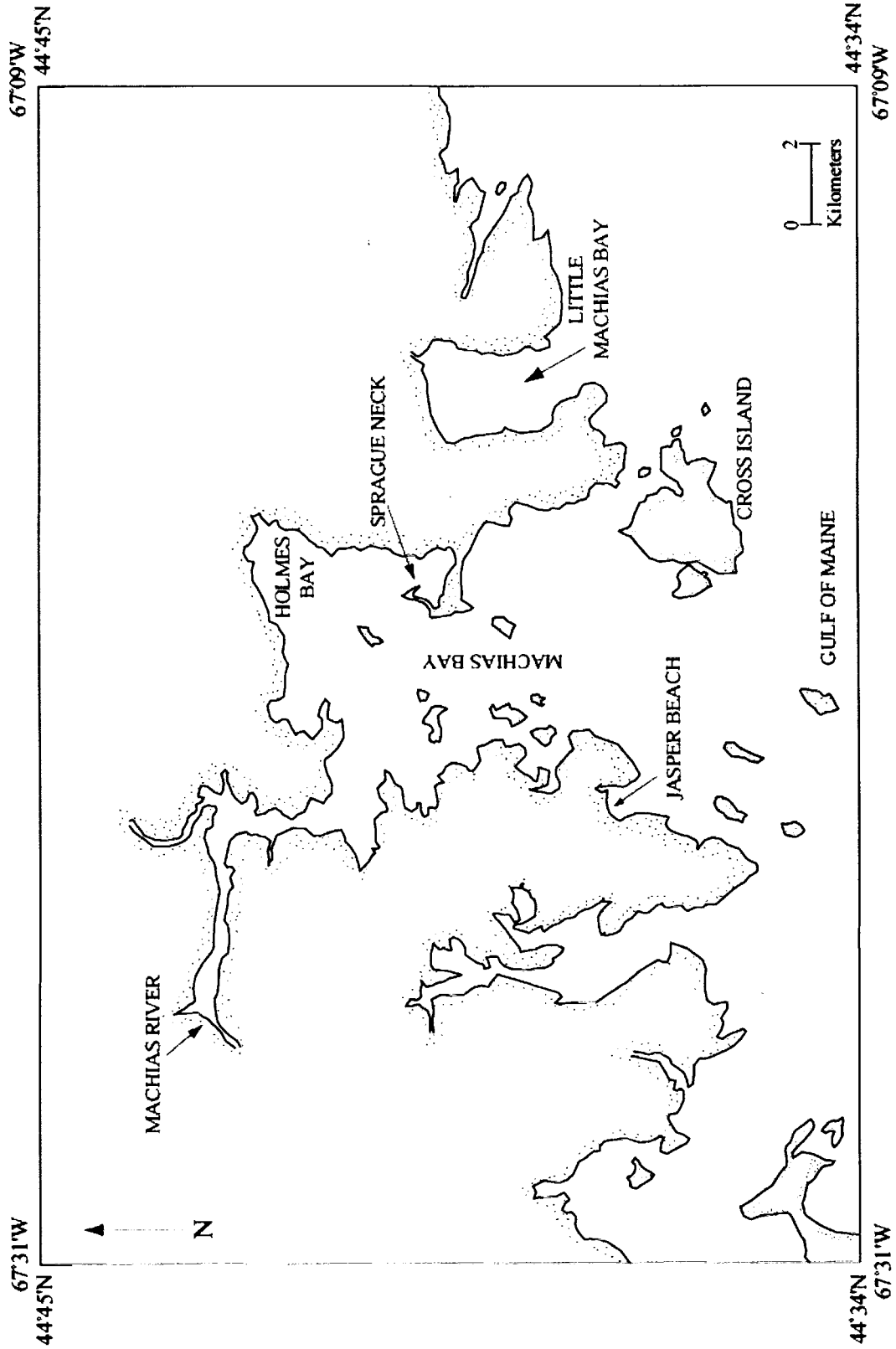
Figure 7. Geography of the region surrounding Sprague Neck (modified from Terrain Navigator, 1998).

25
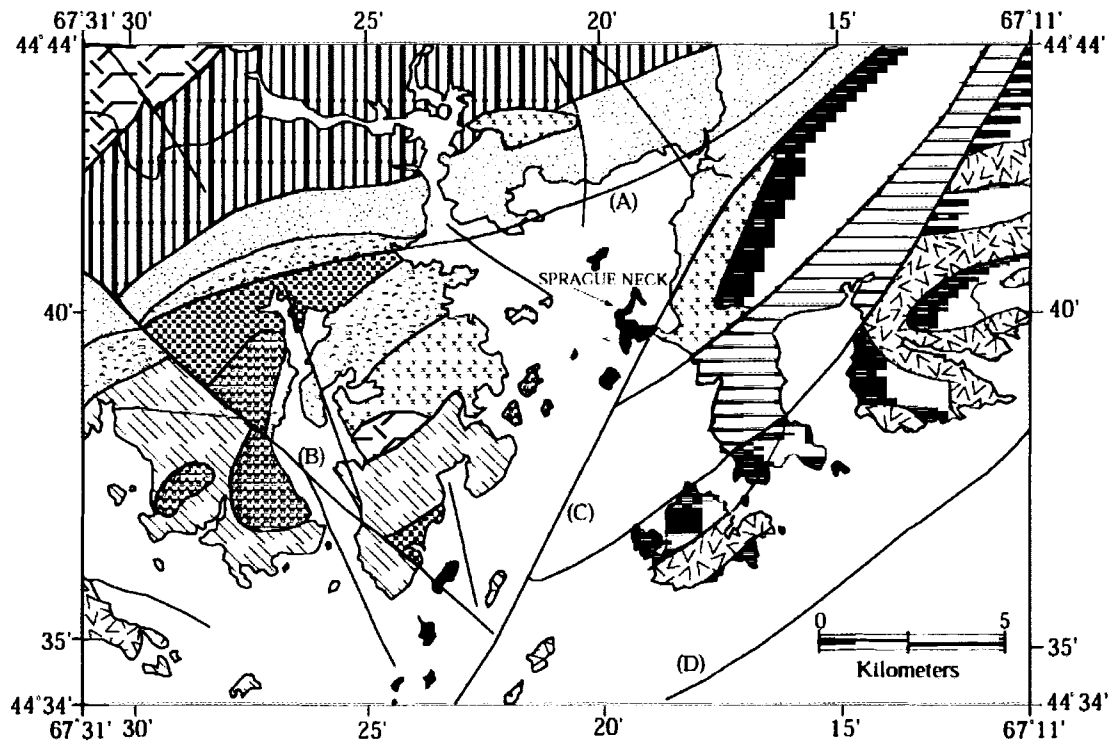
Figure 8. Bedrock Geology Map for the Machias Bay region. Faults are: A-Machias Bay Fault; B-Starboard Fault; C-Lubec Fault Zone; and D-Fundian Fault (modified from Osberg et al. 1985). Bedrock units described in Table 2.

Symbol	Unit Name	Composition	Symbol	Unit Name	Composition
	Pluton	Granite		Leighton Fm. Pelite Mbr.	Pelite
	Pluton	Gabbro		Leighton Fm. Basalt Mbr.	Basalt
	Cutler Pluton	Gabbro		Edmunds Fm.	Volcanics
	Eastport Fm. Basalt & Pelite Members	Basalt		Denny Fm. Volcanic Mbr.	Volcanics
	Eastport Fm. Volcanic Mbr.	Volcanics		Quoddy Fm. Pelite Mbr.	Pelite
	Hersey Fm.	Pelite & Sandstone		Quoddy Fm. Volcanic Mbr.	Volcanic-Mafic to felsic

Table 2. Key to the Bedrock Geology Map in Figure 8.

1999).

The Pond Ridge Moraine formed between 13,810 ± 55 yrs and 13,660 ± 90 yrs B.P. at the grounding line in a marine environment (Dorion, 1997; Kaplan, 1994, 1999; LePage, 1982). Water depth, which varied locally as the grounding line retreated across a hummocky topography, was an important factor influencing grounding line dynamics in eastern Maine (Kaplan, 1994; LePage, 1982). Kaplan (1999) suggested that high calving rates in deep water of topographically low areas and changes in bed slope caused grounding line instability. The grounding line was relatively more stable at topographic highs, such as Sprague Neck.

The Pond Ridge Moraine (Sprague Neck) is the most continuous glacial landform in the Machias Bay region. In eastern coastal Maine, ice striae are concentrated in the Machias Bay and Lubec Embayment areas. The dominant striae orientation in Machias Bay indicates ice movement toward the southeast. In the vicinity of the Pond Ridge Moraine there are two sets of ice striae. The youngest striae indicate southward ice flow. In contrast, the oldest striae indicate a more southeastward ice flow (Kaplan, 1999; LePage, 1982). LePage (1982) suggested a southeastward ice flow preceded a more southward flow in the Machias Bay region, based on differences in the till underlying and interbedded with the Pond Ridge Moraine. Kaplan (1999) supported LePage's (1982) conclusion that the Pond Ridge Moraine represents a readvance position of the LIS. The next major pinning point was the northern margin of Holmes Bay. Several smaller moraines were deposited and mantled with layered gravel deposits. The ice sheet continued to retreat in a north-northwest direction depositing washboard moraines (LePage, 1982; Stuiver and Borns, 1975).

27

Between 13,500 and 12,500 yrs B.P. the LIS retreated from the coast, creating a period of submergence (Mickelson and Borns, 1972). At the time of deglaciation in eastern Maine, the landscape was depressed by the weight of the ice and RSL at the present coastline was approximately 70 m above sea level (Belknap et al., 1987a). Marine conditions dominated Machias Bay until 12,000 yrs. B.P. (Davis and Jacobson, 1985) when the region rebounded and relative sea level reached a lowstand of -60 m (Figure 9) at approximately 10,800 ^{14}C yr. B.P. (Barnhardt et al., 1995).

A second period of submergence began in the early Holocene. The rate of submergence varied through time (Barnhardt et al., 1995). Thompson (1973) collected radiocarbon dates from salt-marsh peats in Addison, Maine and suggested that SL rose at a rapid rate of 11.5 mm/^{14}C yr. prior to 3000 yrs. ago, slowing to an average rate of 0.3 mm/^{14}C yrs. over the last 1,500 yrs. Anderson and Race (1981) and Anderson and Borns (1983) supported Thompson's (1973) findings for eastern Maine and calculated a SLR rate of 8.9-9.8 cm/century for western Maine. Anderson et al. (1984, 1989) stated that postglacial subsidence affected eastern Maine, resulting in a very rapid SL rise. Based on salt marshes in Machiasport, Gehrels and Belknap (1993) proved that no postglacial subsidence affected eastern Maine during the late Holocene.

In contrast to the idea that the rate of SL rise consistently slowed until recently, Belknap et al. (1987a) suggested that SL rose at a rate of 1.22 m/ 1,000 yrs. between 4.2-1.5 ka. After 1.5 ka the rate slowed to half the mid-Holocene rate and accelerated to 2-3 mm/yr. for the last 60-80 yrs (Belknap et al., 1987a). Belknap et al. (1989) revised the rate of SL rise for Addison to 1.33 mm/^{14}C yrs. between 4 ,000 and 1,500 yrs., arguing that previous dates were obtained from displaced or contaminated salt marsh peat.
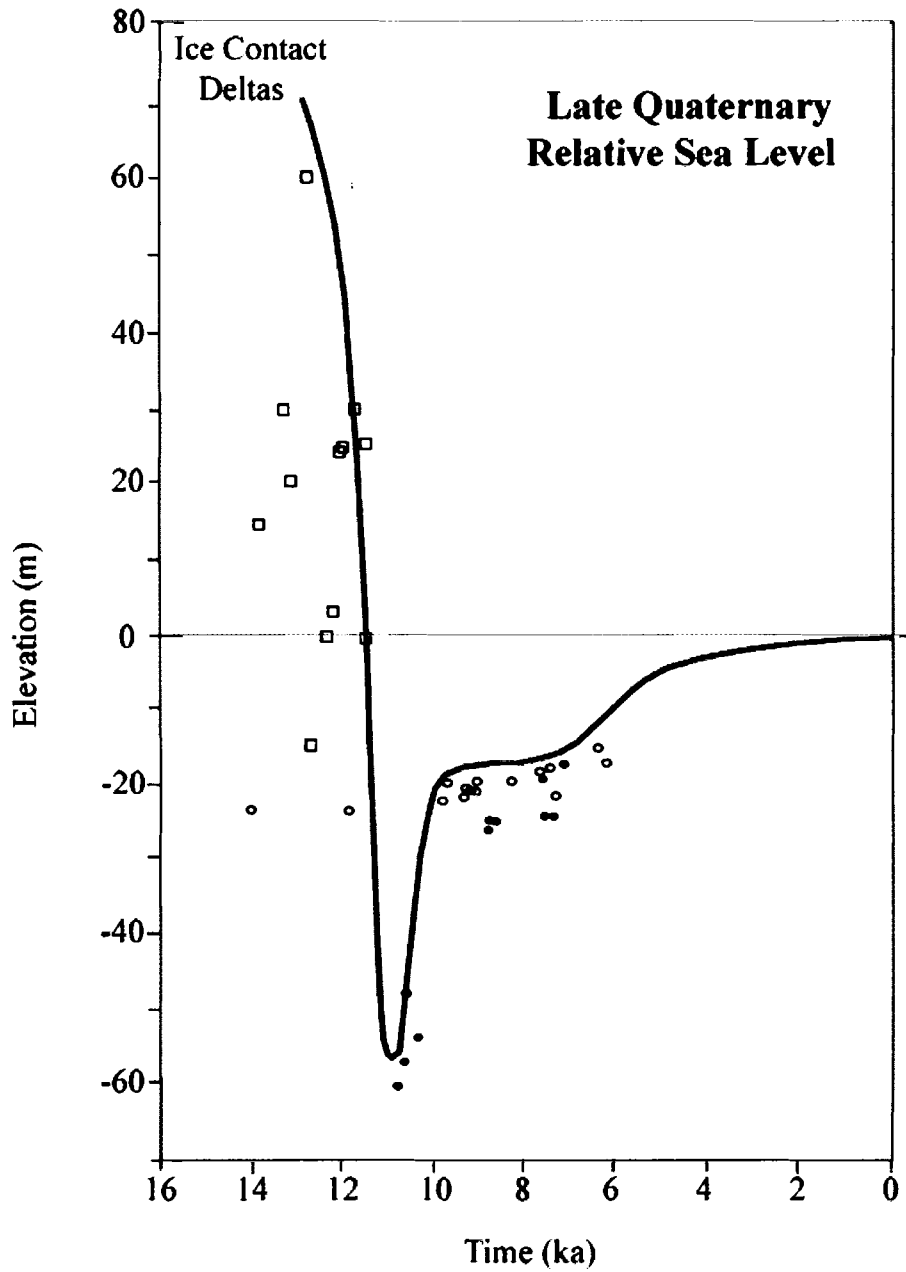
Figure 9. Late Quaternary relative sea-level curve for coastal Maine (modified from Barnhardt et al., 1995). Squares are published dates from Belknap et al, 1987a and Anderson et al., 1990, open and solid circles are dates from Kelley et al., 1992 (open circles between 10 and 5 ka and all solid circles are offshore dates).

According to Belknap et al. (1989) SL rose 1.44 mm/^{14}C yr. between 5,500 and 1,500 yrs. and slowed to 0.3 mm/^{14}C yr. after 1,500 yrs, based on all Maine data.

The resolution of the SL curve by Belknap et al. (1989) was limited because a small number of dates were obtained from nondisplaced basal peats, peats were assumed to represent paleo-mean high water based only on plant identification, and elevations were estimated from tide predictions. Gehrels et al. (1996) used foraminifera for more detailed paleoenvironmental identifications, as well as surveyed levels and tidal range modeling, to produce a more sophisticated sea-level curve. These findings support the conclusions of Belknap et al. (1989) and Gehrels and Belknap (1993), that no postglacial subsidence affected eastern Maine. Maximum SLR rates did not exceed 1.5 mm/yr during the middle to late Holocene. Recent rates of SL rise exceed the maximum late Holocene rates at Wells and at Machiasport (Gehrels, 2000). Explanations for varying rates of RSL change along the Maine coast remain speculative. One explanation for the varying rates is continuing isostatic readjustments following deglaciation (Gehrels et al., 1996).

Stratigraphy in eastern Maine below the marine limit is characterized as follows. Paleozoic bedrock is overlain by lodgment till. Ice-proximal deposits including subaqueous outwash and flowtill overlie the lodgment till. On top of the ice-proximal units is glacial-marine mud of the Presumpscot Formation. The Presumpscot Formation is typically covered by a layer of coarse material that has been reworked by nearshore processes during regression (Dorion et al., in press).

Fine-grained glaciomarine silt and clay, the Presumpscot Formation (Bloom, 1963), covers the majority of the Machias Bay region (Figure 10, Table 3). Numerous,

Pond
Ridge
Moraine

Sprague Neck
Bar

Little
Machias
Bay

Machias
Bay

Jasper Beach

0   5
Kilometers
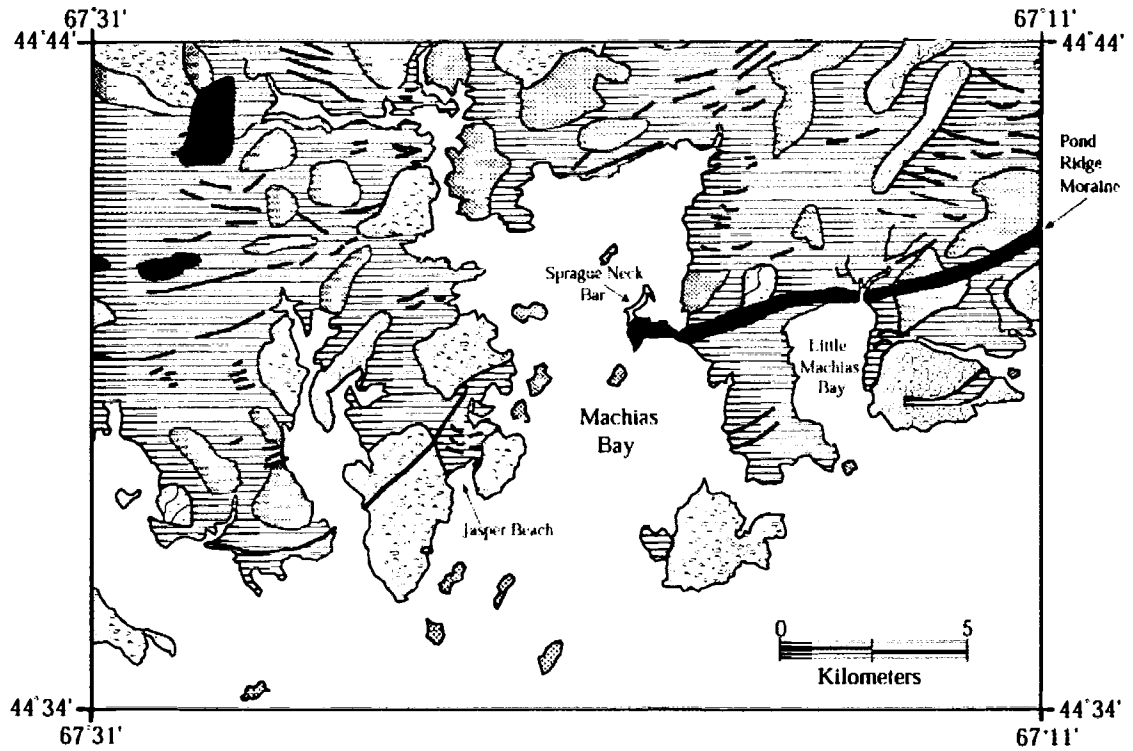
Figure 10. Surficial Geology Map for the Machias Bay region (modified from Thompson and Borns, 1985). Surficial features described in Table 3.
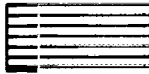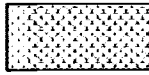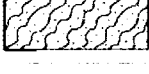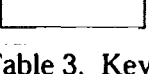
SYMBOL	FEATURE	MATERIAL
	Glaciomarine deposits	Presumpscot Fm. silt and clay
	Till	Diamicton
	End Moraine	Sand and gravel
	Thin drift	Thin layer of sediment and bedrock outcrops
	Thin drift-undifferentiated	Thin layer of sediment and bedrock outcrops
	Washboard Moraines	Diamicton
	Modern coastal sediments	

Table 3. Key to Surficial Geology Map in Figure 10.

31

discontinuous deposits in the area are mapped as till, thin drift, and undifferentiated thin

drift. Flat to depressed topography is filled with marsh, swamp, or bog deposits

(Thompson and Borns, 1985). Numerous washboard moraines oriented ENE-WSW

indicate a NNW retreat (Stuiver and Borns, 1975).

The Pond Ridge Moraine is mapped as a distinct glacial feature in the Machias

Bay region. The moraine crosses the eastern shore of Machias Bay and extends

approximately 15 km to the east, where the orientation of the longitudinal axis changes

from east-west to east-northeast (LePage, 1982). LePage (1982), Dorion (1997), and

Dorion et al. (in press) described the stratigraphy of the Pond Ridge Moraine. Four

stratigraphic units comprise the moraine: basal till, glacial-marine sediment, till along the

proximal slopes, and littoral deposits. Dorion et al. (in press) examined the proximal side

of the Pond Ridge Moraine and found that the glaciomarine mud deposits are, first,

conformably overlain by glacial-marine mud with interbedded sand, and, which, in turn,

are overlain by massive to cross-bedded sand and gravelly sand (Dorion et al., in press).

Coastal Geology - Maine's coastline exhibits variations in morphology and

nearshore dynamics over a short distance. Bedrock geology, tidal range, morphology,

and sediment type vary dramatically from the southwest to the northeast. A classification

scheme dividing the coast into distinct categories is based on these variations (Figure 11).

The four compartments are: 1) SW-Arcuate Embayment; 2) WC-Indented Shoreline; 3)

EC-Island-Bay Complex; and 4) NE-Cliffed Shoreline (Belknap et al., 1987; Duffy et al.,

1989; Kelley, 1987).

Machias Bay falls on the boundary between the Island-Bay Complex and Cliffed

Shoreline and exhibits characteristics of both compartments (Duffy et al., 1989; Shipp,
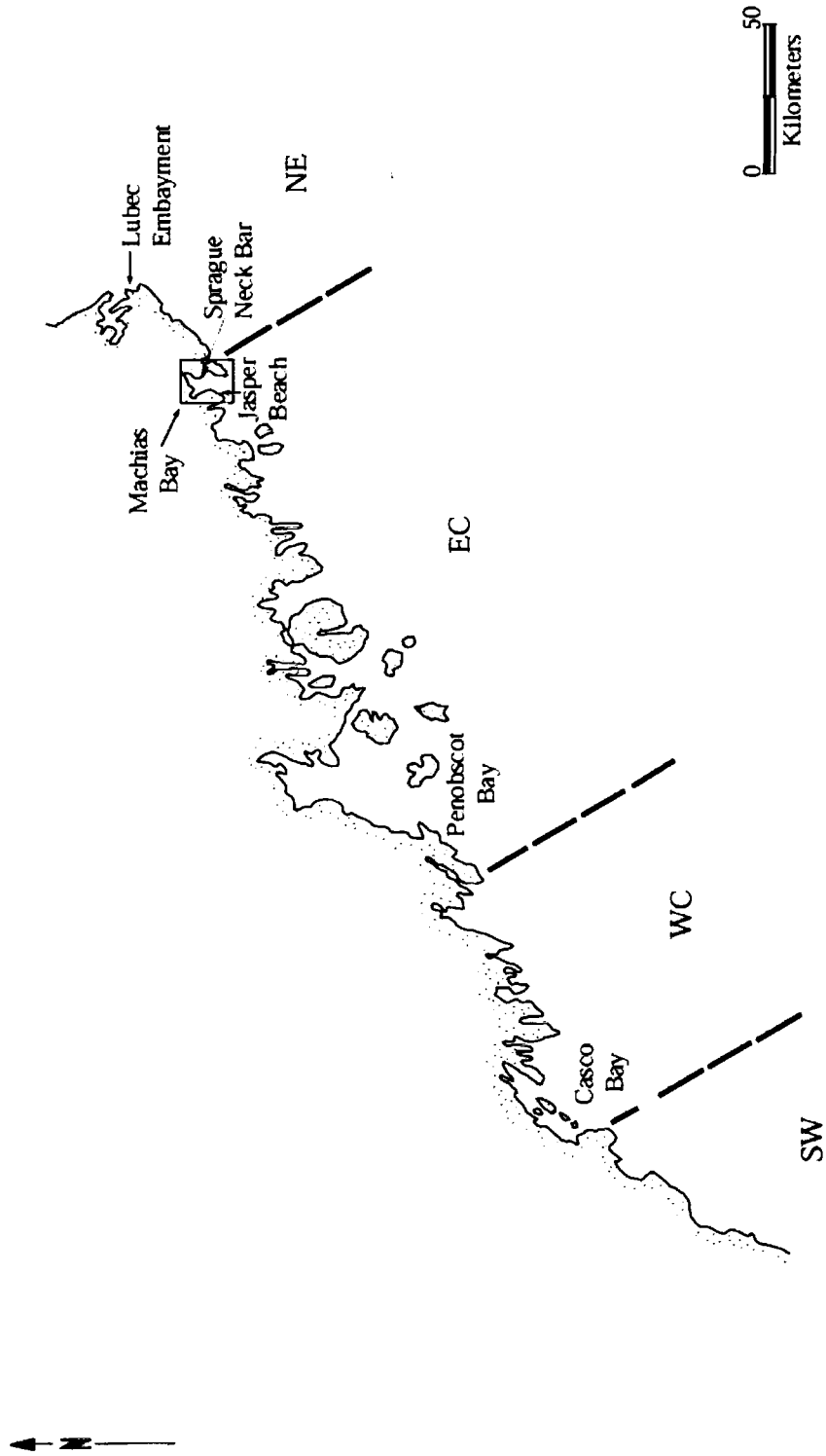
Figure 11. The coastal classification scheme that divides coastal Maine into four distinct compartments: 1) SW-Arcuate Embayment, 2) WC-Indented Shoreline, 3) EC-Island Bay Complex, 4) NE-Cliffed Shoreline (modified from Duffy et al. 1989).

1989). Low-grade metasedimentary rocks intruded by granitic plutons, broad estuaries, and granitic islands characterize the EC compartment. High wave energy, low sediment supply, and the presence of coves produce the coarse-grained pocket beaches found in the EC compartment. Well-protected embayments composed of metasedimentary and volcanic rocks comprise the high-cliffed coast of the NE compartment. The highly resistant volcanics produce the cliffed shoreline while the less resistant metasedimentary rocks form protected estuaries (Duffy et al., 1989; Kelley, 1987). Machias Bay sits largely in the island-bay complex even though the bedrock composition is metasedimentary and metavolcanic (Shipp, 1989).

Shipp (1989) divided Machias Bay into three distinct zones (Figure 12) according to intertidal geomorphology. The intertidal estuarine zone (Zone I) consists of mudflats and fringing marshes. Zone I extends from the mouth of the Machias River to the head of the Machias and East Machias Rivers. Seaward of Zone I is an intertidal zone (Zone II) located in the upper half of Machias Bay. The characteristic environment of Zone II is extensive mudflats, and occasional sandflats. South of Sprague Neck to the mouth of Machias Bay is Zone III. Ledges and coarse-grained beaches (i.e., Jasper Beach and Davis Beach) characterize the lower half of Machias Bay (Shipp, 1989).

Wind, Wave, Tide Regime

The pattern of prevailing winds is related to the distribution of air pressure systems. In winter Maine is situated between (Icelandic) low pressure and (North America continental) high pressure. This condition results in northwesterly and westerly winds. During the spring and early summer the two pressure systems weaken, and the wind blows mainly from the southwest.
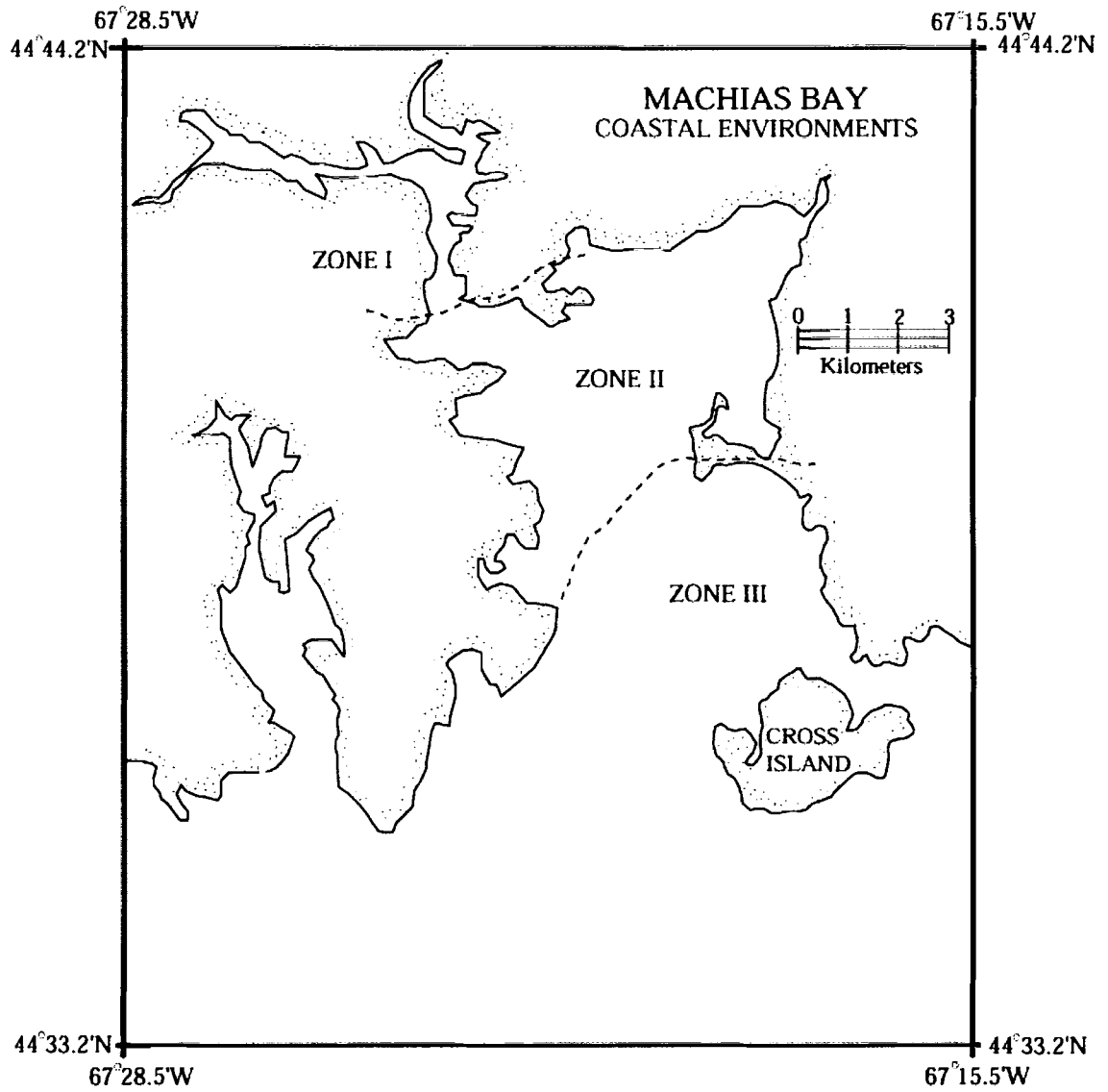
Figure 12. Three zones of Machias Bay based on intertidal geomorphology (modified from Shipp, 1989).

The Maine coast is susceptible to two types of cyclonic storms: frequent extratropical storms and infrequent hurricanes. The most common extratropical storm is the "Northeaster" which tracks east of Cape Cod and Nova Scotia. Northeasters generate strong northeast winds and waves. The southwesterly and southeasterly extratropical storms are less common and occur when low-pressure systems travel west of New England. Hurricanes are rare along the New England coast. By the time hurricanes reach New England most of the energy is dissipated (Kelley, 1987; FitzGerald et al., 1994).

Machias Bay is a well-mixed system that receives a freshwater input of 25 m^3/s from the Machias River and is open to the Gulf of Maine. The tidal prism is significantly greater than 25 m^3/s (Fefer & Schettig, 1980). The open exposure of Machias Bay results in a hydrodynamic regime where waves and tides are codominant (Belknap et al., 1987b). Shipp (1989) described Machias Bay as the transition boundary between meso- and macro- tidal conditions. The semidiurnal North Atlantic tide controls tidal forcing in the Gulf of Maine. Amplification of tides in the Gulf of Maine/Bay of Fundy system is a result of basin geometry (Scott and Greenberg, 1983). The mean tide range is 3.8 m, and the spring tide range is approximately 4.4 m (NOS, 2000). Times of high and low tide at the head of Machias Bay lag behind the mouth by 12-37 minutes (NOS, 2000).

Bathymetry

In the upper half of Machias Bay a channel oriented north-south splits at Sprague Neck. The main branch is a broad, shallow depression that splits around Hog Island (Figure 13). The eastern channel is between Sprague Neck Bar and Hog Island, and the western channel leads to the Machias River (Shipp, 1989; Timson, 1976). The Machias River follows the narrower and steeper branch, which joins the main channel west of Hog
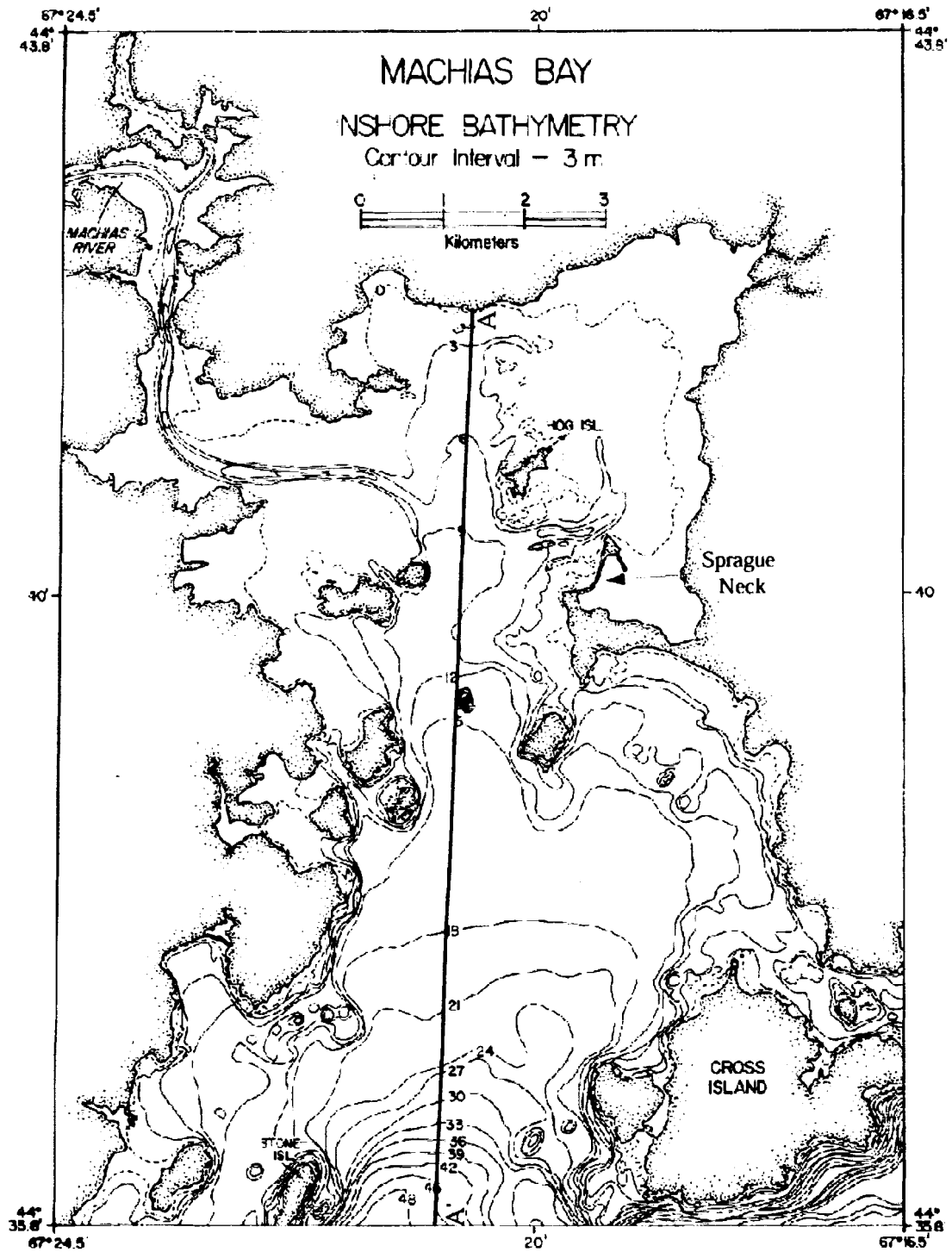
Figure 13. Bathymetry of the inshore Machias Bay area (Shipp, 1989, p. 6-17, Figure 6-5). Line A-A' is the location of the seismic profile shown in Figure 15.

Island. South of Sprague Neck is a broad, gently sloping submarine plain. At the mouth of Machias Bay the bay floor deepens to the inner shelf.

Sediment Distribution

The inshore sediment prism is relatively large and highly variable (Figure 14). Sandy mud to muddy sand is the dominant sediment texture in Machias Bay. Local deposits of sand and gravel exist throughout the bay. Seismic profiles (Figure 15) along the main N-S axis of Machias Bay illustrate the dominance of glacial drift (Belknap et al., 1987b; Shipp, 1989). Three distinct moraines separated Machias Bay at different times. For each moraine glaciomarine mud and stratified outwash was deposited seaward of the grounding line. Major sediment was deposited when the ice stranded at Sprague Neck, producing the Pond Ridge Moraine, with the Presumpscot Formation accumulating along the margins (Belknap et al., 1987b).

Numerous coarse-grained deposits exist in Machias Bay in the form of eroding moraines located at Sprague Neck, Holmes Bay, and Cross Island Narrows (Shipp, 1989). One reason for the thick sediment cover is the connection of the East Machias River to the esker/delta complex. The Machias and East Machias Rivers are part of the esker/delta drainage system and transport Pleistocene deposits to Machias Bay. Additional sources for coarse material include the moraines located in Holmes Bay, the submerged segment of the Pond Ridge Moraine (Shipp, 1989; Thompson and Borns, 1985), and subaqueous outwash associated with glacial tunnel fans (Ashley et al., 1991; Kaplan, 1994, 1999). The coarse material was not strongly reworked as RSL fell. With rising RSL the morainal bluffs were eroded and recycled, supplying coarse-grained sediment to Machias Bay (Shipp, 1989).
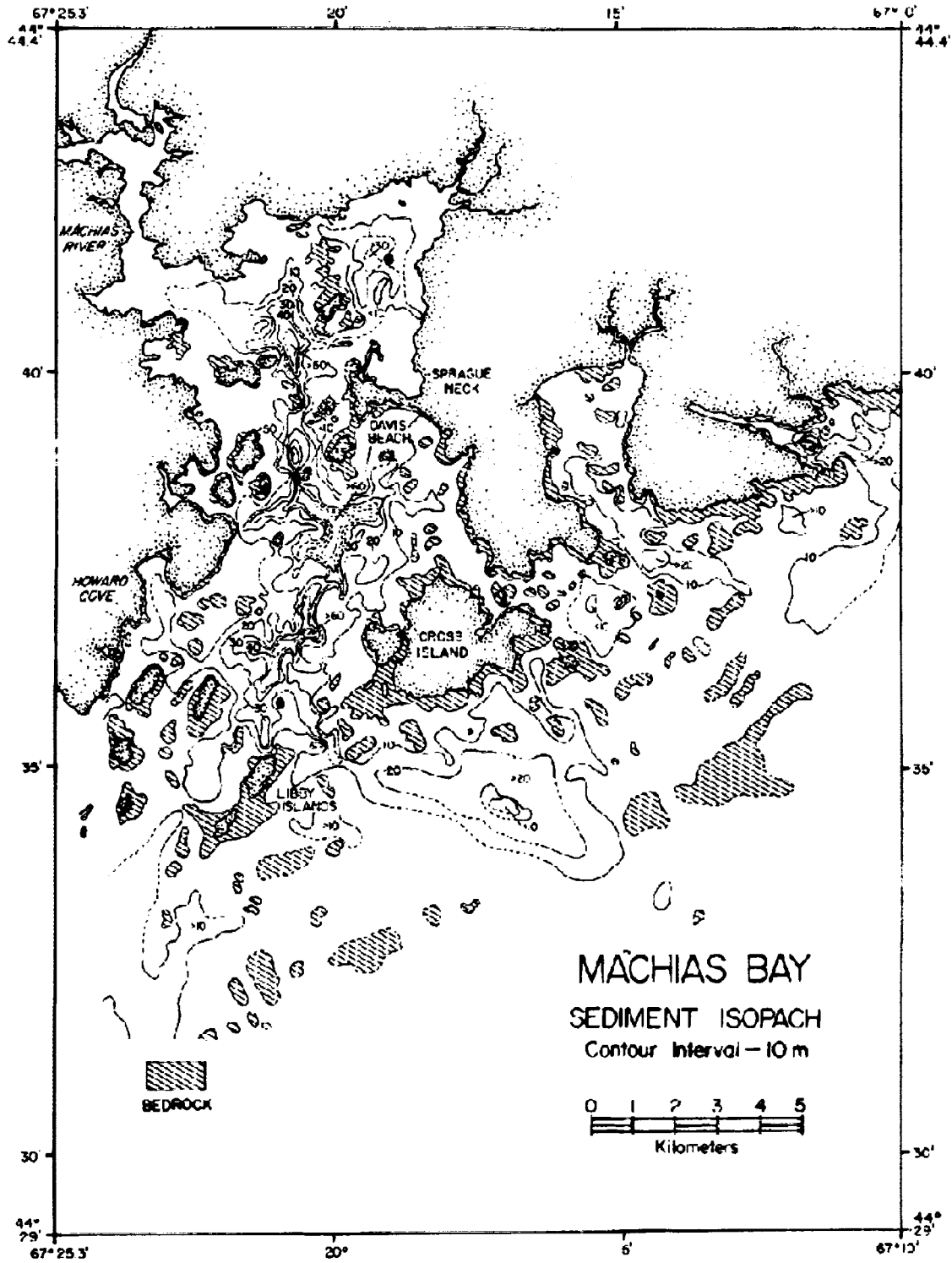
Figure 14. Sediment isopach map of total sediment thickness in Machias Bay, based on seismic profile data (Shipp, 1989, p. 6-29, Figure 6-13).

39
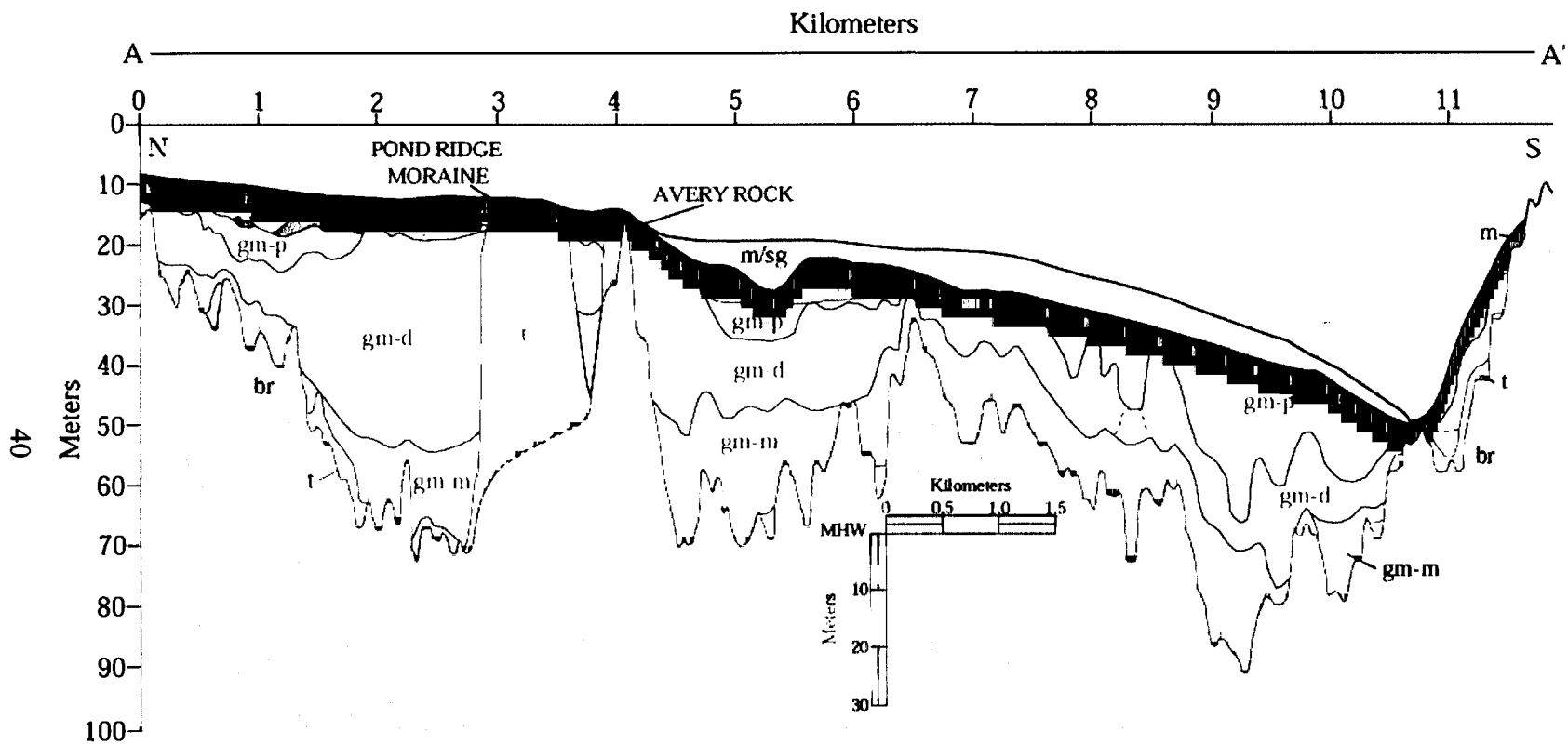
Figure 15. Line drawing of 3.5-kHz seismic profile along the central N-S axis of Machias Bay, x50 vertical exaggeration. Location of the profile. A-A', is shown in Figure 13 (modified from Shipp, 1989). Units are: br=bedrock, m/sg=mud/sandy gravel, sg=sandy gravel, s=sand, m=mud, t=till, gm=glaciomarine sediments (p=ponded, d=draped, m=massive).

Geomorphic Elements of Sprague Neck

Sprague Neck is bordered by mixed sand and gravel beaches, gravel beaches, and coastal bluffs (Figure 16). The offshore area (on the western and southern sides of Sprague Neck) is composed of coarse-grained flats and seaweed-covered coarse-grained flats. Sprague Neck Bar is a mixed-sediment barrier spit with a vegetated dune ridge and preserved recurved system forming a broad flat. Multiple swash bars are located at the end of the recurve. The backbarrier environment is characterized by mudflats and algal flats (Timson, 1976). Several minor eroding moraines, oriented east-west, extend from the western side of Sprague Neck and Sprague Neck Bar. Boulder ramps are associated with these moraines.

Sprague Neck Bar - Sprague Neck Bar (Figure 17) is a drift-aligned, mixed-sediment, recurved barrier spit attached to the western end of Sprague Neck. The system extends in a northerly direction into the head of Machias Bay. The recurve system is oriented in a southeasterly direction, forming a broad flat (Figure 18). Surface sediment comprising the preserved recurve system is characterized by gravel and clusters of cobble-sized clasts. The dominant plant species colonizing the flat environment are *Limonium carolinianum* (sea lavender) and *Salicornia bigelovii* (dwarf glasswort). Two linear structures (Figures 16, 19), oriented perpendicular to Sprague Neck Bar, extend from the western side of the barrier spit and are exposed during low tide. These structures have been interpreted as barrier spits by Timson (1976) and as the cores of eroded moraines (Kelley, pers. comm.).

Sprague Neck Bar is approximately 1 km in length, varying in width from 45 m at flag SB3 to 53 m at flag SB8, to 61 m at flag SB10 (Figure 20). Relief (above MLW)

B1 Mixed-sediment beach   F3 Algal flat
B2 Coarse-grained beach   L Ledge
B3 Gravel beach   M Moraines
Br Boulder ramp   G Gravel flat
V Vegetated dune ridge   SB Swash bars
F Mudflat
F1 Coarse-grained flat
F2 Seaweed covered coarse-grained flat
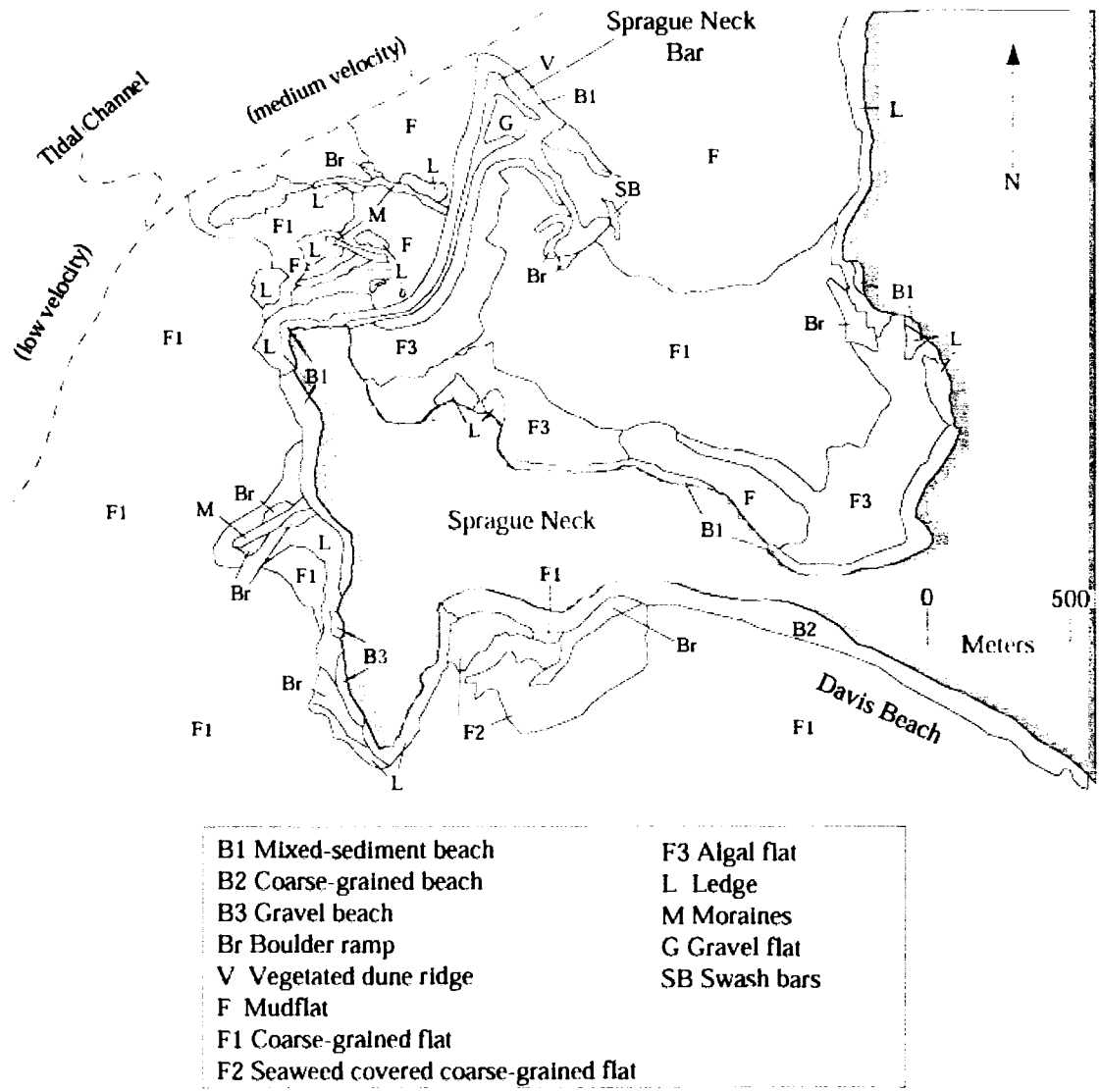
Figure 16. Coastal environments of Sprague Neck (from Timson, 1976). Coastal bluffs border Sprague Neck but are too small to depict on this map.
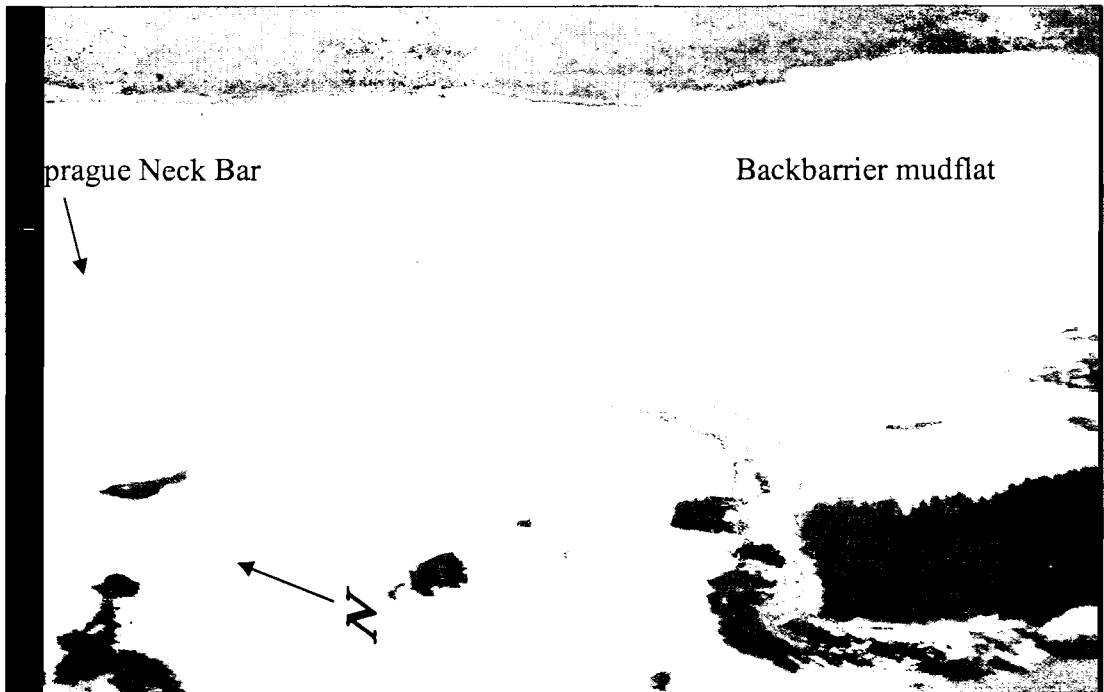
Figure 17. Air photo of Sprague Neck Bar (Kelley, 1983).
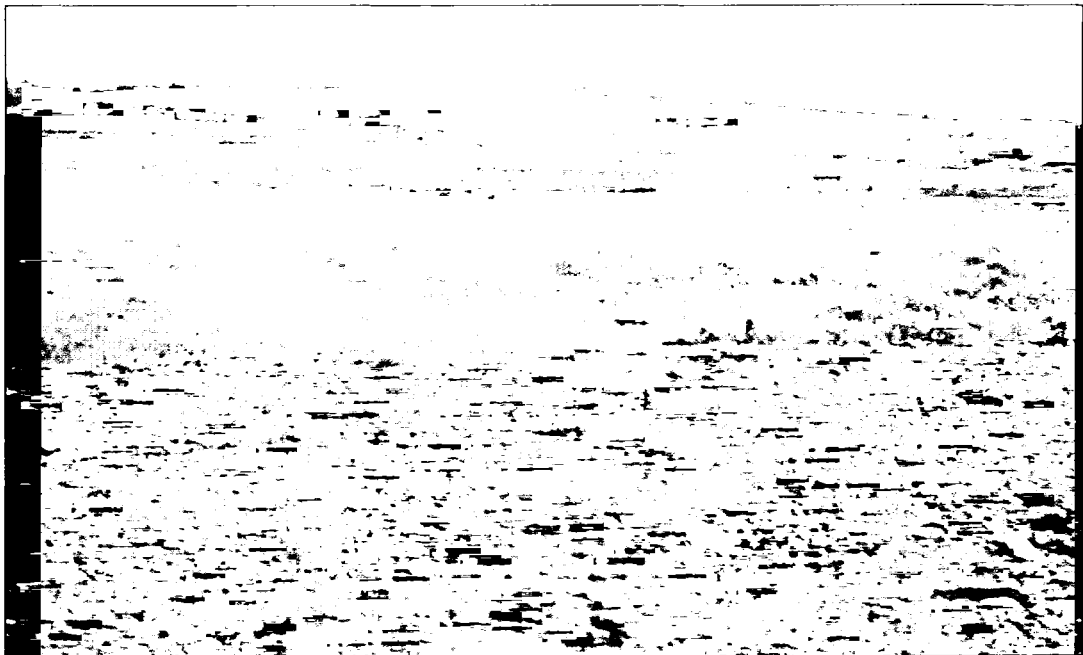
Figure 18. The preserved recurve system, view to the southeast (July, 2000).
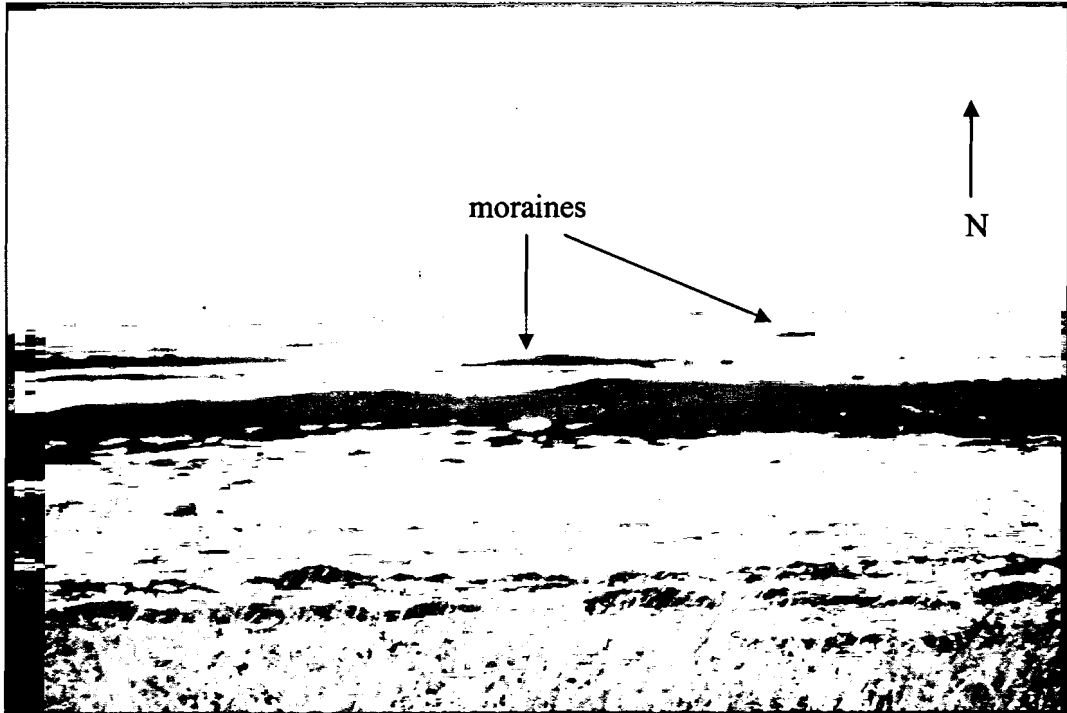
Figure 19a. The eroded moraines oriented perpendicular to Sprague Neck Bar (November 2000).
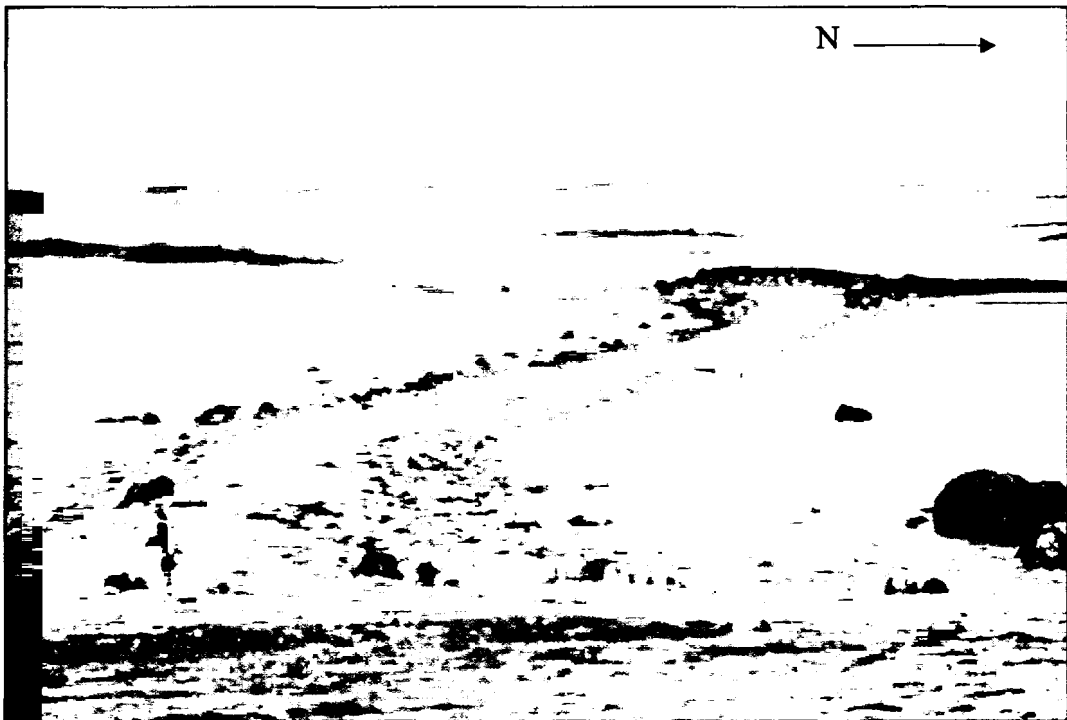
Figure 19b. Photograph of a moraine at low tide (November, 2000).
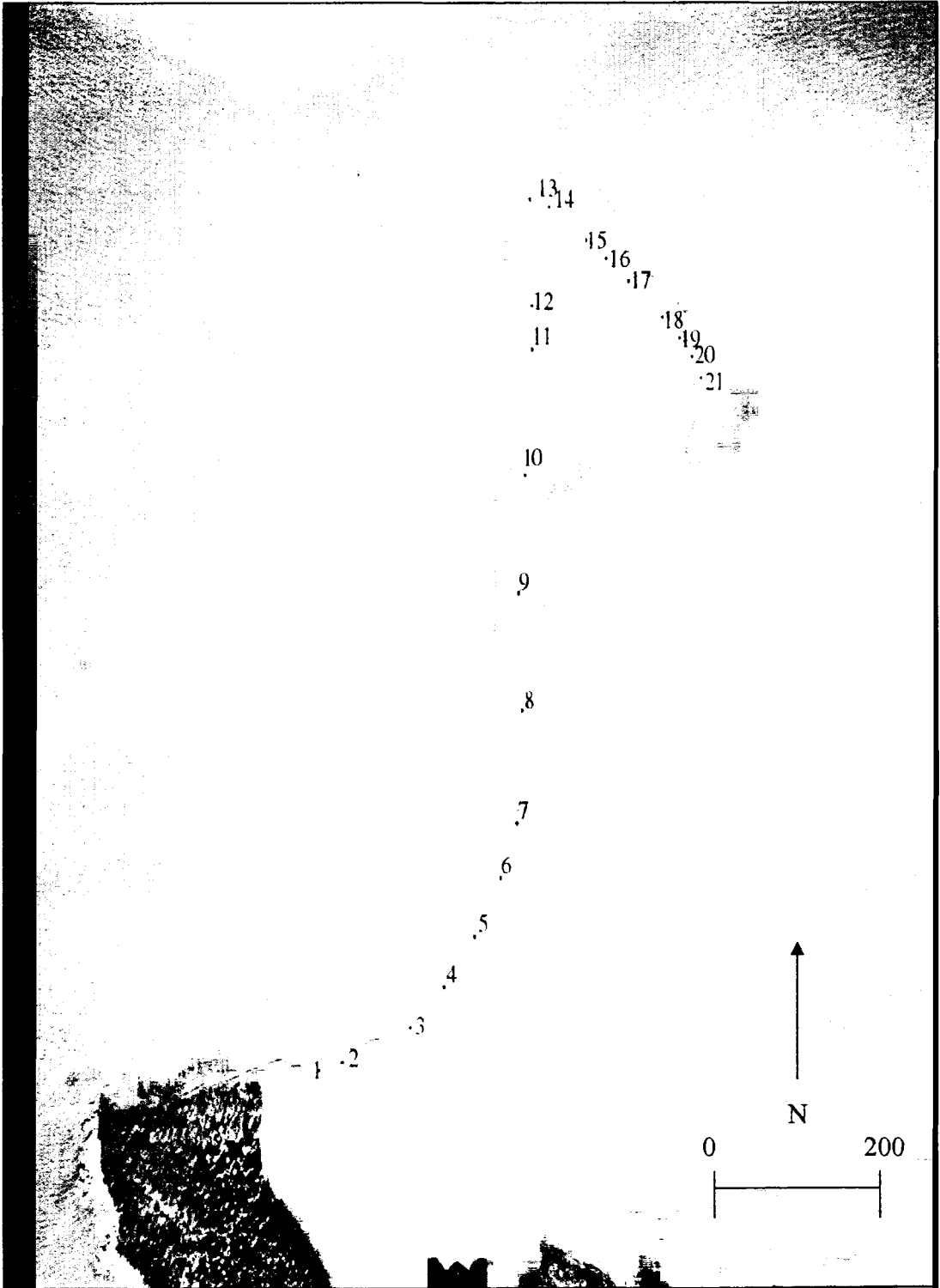
Figure 20. Location of the main survey flags (SB1, SB2, etc.)

ranges from 4.0 m proximal to the Pond Ridge Moraine (SB3), where overwash occurs, to 5.5 m at the spit tip, to 1.8 m on the swash bars. Surface sediment texture grades alongshore from pebbles and cobbles proximal to the Pond Ridge Moraine to sand and gravel patches between flags SB8 and SB9 (Figure 20). Between flags SB8 and SB9 the grading begins to reverse and sediment grades into cobble-sized clasts at flag SB13. Grain size on the current recurve is more uniform, consisting predominately of pebble-sized clasts. The surface sediment changes to gravel and coarse sand on the swash bars. Cross-shore grain size trends typically show a coarse-fine-coarse zonation, with the coarsest material located on the lower intertidal zone. Pebbles and cobbles are located on the barrier crest and backbarrier (eastern) side of Sprague Neck Bar.

A diverse plant community colonizes Sprague Neck Bar (Table 4). Grain size variation correlates with changes in vegetation. *Ammophila breviligulata* (American beach grass) colonizes the barrier crest where the sediment is predominately fine sand. In locations where the sediment is a mixture of sand, pebbles, and cobbles, vegetation consists of plant species that are more tolerant of marine exposure such as *Lathyrus japonicus* (beach pea), *Artemisia stellerianna* (dusty miller), and *Rosa rugosa* (wrinkled rose).

Mudflats - Mudflats are the predominant coastal environment in Machias Bay (Timson, 1976; Shipp, 1989; Smith, 1990). Three potential sources exist to supply the modern mud: offshore deposits, the Machias River, and glaciomarine mud bordering the shoreline (Smith, 1990). Timson (1976) characterized the backbarrier environment of Sprague Neck Bar as algal flats, mudflats, and coarse-grained flats. Mudflat and algal flat environments are located along the shoreline (Figures 16, 21). Away from the

46

Table 4. List of Plant Species Colonizing Sprague Neck Bar.

Scientific Name	Common Name
Achilles millefolium	Yarrow
Ambrosia chamissonis	Beach bur
Ammophila breviligulata	American beach grass
Arenaria peploides	Seabeach sandwort
Artemisia stellerianna	Dusty miller
Atriplex patula	
Cakile edentula	Sea rocket
Convolvulus sepium	Morning-glory
Lathyrus japonicus	Beach pea
Limonium carolinianum	Sea lavender
Oenothera biennis	Evening primrose
Rosa rugosa	Wrinkled rose
Salsola kali	Common saltwort
Salicornia bigelovii	Dwarf glasswort
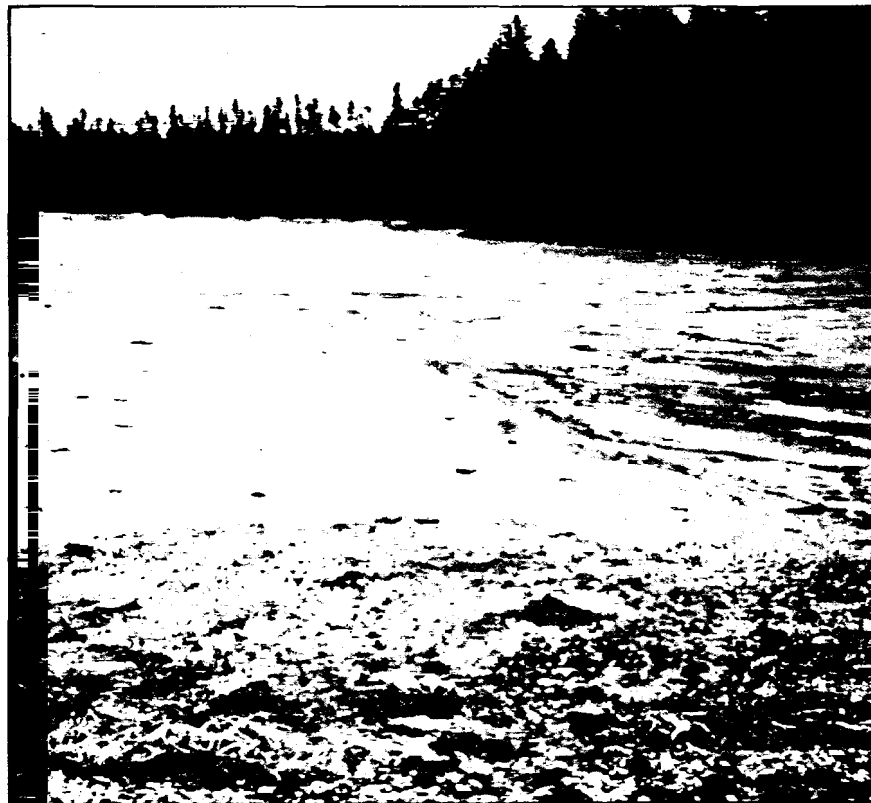
Figure 21. The backbarrier mudflat of Sprague Neck Bar (August, 2001).

shoreline the mudflat and algal flat environments grade into a coarse flat. West of Sprague Neck Bar the mudflat changes to a coarse-grained flat near the tidal channel (Timson, 1976).

Coastal Bluffs - Minor bluffs extend along Sprague Neck, contributing sediment to the coastal systems. The largest bluff at Sprague Neck is Sprague Neck Bluff (Figure 22), part of the Pond Ridge Moraine. A cobble beach, with abundant large boulders, fronts the unvegetated bluff. The lack of vegetation results in active subaerial erosion, producing a sandy beach at the bluff toe. The bluff is relatively sheltered from marine erosion, except during coastal storms, due to the long distance from the bluff toe to MHW (Smith, 1990).

Pocket Beaches – All pocket beaches derive sediment directly from the eroding bluffs along the Pond Ridge Moraine. Several small, mixed-sediment pocket beaches are located along the western edge of the Pond Ridge Moraine (Figure 16, 23). Pebbles to cobble-sized clasts dominate the lower intertidal zone. The upper beachface is predominately sand. Outcrops of metasedimentary and metavolcanic rocks separate the beaches. Davis Beach (Figure 16, 24) is located along the southern margin of Sprague Neck. The swash-aligned pocket beach is composed of metasedimentary and metavolcanic cobbles and boulders. Davis Beach occupies a less sheltered environment than the mixed-sediment beaches on the western side of Sprague Neck.

Figure 22. Sprague Neck Bluff and Davis Beach, view to the north
(August, 1986).

Figure 23. Pocket beach located on the western side of Sprague Neck, view to the
north (June, 2000).

Figure 24. Davis Beach, view to the east (August, 2000).

METHODS

Three aspects of Sprague Neck Bar were evaluated to determine its evolution: 1) qualitative historical shoreline change, 2) geomorphic elements, and 3) modern processes. Analyzing the historical shoreline change involved comparing the shape and location of Sprague Neck Bar through the use of aerial photographs, topographic maps, and nautical charts. Identifying the geomorphic elements and past/present sedimentary environments entailed ground penetrating radar (GPR) and sediment grain-size analysis. Establishing the modern processes shaping Sprague Neck Bar included analysis of the tidal regime and studying the role of algal fronds and ice as a transport mechanism of individual clasts.

Historic Shoreline Analysis

Historic maps, nautical charts, and aerial photographs were collected from various sources (Table 5) and used to qualitatively analyze shoreline change from 1776 to 1991. Examination of the air photos revealed little significant change during the time of coverage. Therefore, the use of five photos (1940, 1958, 1966, 1979, and 1991) was deemed sufficient. The nautical charts from 1776 and 1886 were not used in the digitized overlay analysis because of uncertain mapping accuracy. The photos were scanned into a computer and registered in MapInfo using GPS data points located on Sprague Neck. Once the images were registered, the maps and air photos were layered and compared.

Sprague Neck Bar was surveyed with the Sokia Total Station. The base station was positioned at a point halfway between the moraine and spit tip. Sprague Neck Bar was not surveyed in to benchmarks, thus the survey data points are relative only to each

51

Table 5: Historic maps and air photos used in the shoreline change analysis of Sprague Neck Bar. (* indicates maps used and shown in text)

Date	Type	Approx. Scale	Description	Source
1776	chart	----------	Atlantic Neptune navigation chart	Osher Map Library USM, Portland
1886*	map	1:10000	USC&GS # 1687*, # 1688	
1919*	map	1:62500	topographic map 7.5' Quadrangle	Osher Map Library USM, Portland
8/8/1940*	photo	1:44000	GSM 186	
1951*	map	1:24000	topographic map	Osher Map Library USM, Portland
5/1958*	photo	1:15840	CBT-3-4*, 3-5	Sewall Co., Old Town
1960*	map	1:10000	USC&GS # 8857	
11/5/1966*	photo	1:30000	196-7-5 & 7-6*	Sewall Co., Old Town
11/21/1966	photo	-----------	196-6-3, 6-4, 6-5	Sewall Co., Old Town
6/26/1969*	photo	------------	ETR-2-186,187*, 188	Maine Geological Survey
5/1979*	photo	1:36000	CCBT-11-5*, 11-6	Sewall Co., Old Town

Table 5 (continued): Historic maps and air photos used in the shoreline change analysis of Sprague Bar. (* indicates maps used and shown in text)

Date	Type	Approx. Scale	Description	Source
10/1979	photo	----------	179-82, 83	Sewall Co., Old Town
11/1991*	photo	1:6000	A4752-44-5*, 44-6	Sewall Co. Old Town

other. First, the main transect along the crest was surveyed. The flat environment and cross-sections at each main flag (labeled SB1, SB2, etc., Figure 20) were surveyed. Elevations were determined for each survey point and incorporated with the GPR records. Elevations are relative to MLW, which was approximated from tidal predictions.

Ground Penetrating Radar

Ground penetrating radar (GPR) utilizes electromagnetic (EM) waves to probe the subsurface. Records are interpreted based on the knowledge of how EM waves behave in various lithologies. The two main characteristics of EM waves are velocity and attenuation, which are functions of conductivity and relative permittivity. The signal can not extend into brackish or salty water (van Heteren et al., 1998).

The Sensors and Software GPR unit with 200 MHz antennas was used to examine Sprague Neck Bar. The GPR unit was programmed to collect data at 0.5-meter intervals at a median velocity of 0.100 m/ns, a value halfway between dry and saturated sand. GPR transects were run across the width of Sprague Neck Bar at flags SB1-SB10 and along the length of the barrier spit (Figure 20).

The GPR data was managed in the software package GPR IxeTerra. The raw data were converted into profile data. Profiles begin as time sections that can be converted to depth or elevation. To create the elevation profiles, the y-axis was first converted from time into depth by creating a velocity profile (using the median velocity). Depth was then converted into elevation by inputting the elevations determined from the survey data. The record is displayed as distance versus elevation above MLW.

Sediment Analysis

Sediment analysis characterizes sediment and provides information on depositional mechanisms and environments. For this analysis grain size and grain-size parameters were examined. Grain-size parameters include sorting, skewness, and mean. Trends in grain size are used to infer direction of sediment dispersal, with grain size decreasing away from the source. The Udden-Wentworth grain-size scale divides sediment into seven class intervals: clay, silt, sand, gravel, pebbles, cobbles, boulders (Table 6). The arithmetic scale of phi units is based on the geometric Udden-Wentworth scale ($\Phi = -\log_2 d$, d is diameter) (Tucker, 1991).

Table 6. Grain-size Scale (Tucker, 1991).

mm	phi	class interval
		boulders
256	-8	
		cobbles
64	-6	
		pebbles
4	-2	
		gravel
2	-1	
		sand
0.062	4	
		silt
0.004	8	
		clay

Classification of sedimentary environments was based on: 1-topographic relief and morphology, 2-size distribution of sediment, 3-the influence of waves and tides, and 4-flora. Grain size was the principal factor in determining environments. Samples were collected from each morphologically and sedimentologically distinct environment. Large

areas with a similar sediment texture were sampled more than one to ensure a representative sample was collected. The mixed-sediment barrier was sampled along the main survey transect and several of the cross transects. The long, intermediate, and short axes of the pebble- and cobble-sized clasts were measured in the field. Some coarse samples were photographed. Only the long and intermediate axes were measured on the photographed samples. The intermediate axis was used to determine the representative mean grain size. Lab analysis of the fine samples included dry and wet sieving and settling tube analysis. Samples with a significant percentage of mud were wet sieved to separate sand from the mud fraction. After the samples were desalinized, a dispersing agent was added to break up floccules of mud.

Sand samples with a gravel component were dry sieved at 0.50 phi intervals from -1.5 phi to 0 phi. Sediment texture of the sand was determined by running the sample (approximately 10-15g) through the settling tube. The settling tube operates on the terminal settling velocities of individual particles in water at a constant temperature (Stokes Law). The settling rate is a function of particle diameter, particle and fluid density, acceleration due to gravity, and fluid viscosity (Selley, 1994). Sediment will accumulate on the bottom scale in order of decreasing hydraulic equivalence. The sand-fraction grain size distribution is based on the accumulated mass at the bottom of the tube. Analyses of the sediment with the rapid sediment analyzer reflects grain shape, density, and degree of roundness, which is not obtained with sieving (Komar and Cui, 1982). The settling tube computer program calculated statistical parameters including grain size, sorting, skewness, and kurtosis (Belknap, unpub.). These parameters were calculated for coarse samples based on the method of moments.

Samples were characterized according to percent mud, sand, gravel, pebbles, and cobbles. The percentages were plotted on ternary diagrams based on: 1) percent sand, gravel, mud (Folk-Ward classification); 2) percent pebbles, cobbles, sand; and 3) percent pebble gravel sand.

Ice and Algae Transport

Ice and the attachment of algal fronds to rocks are effective transport mechanisms for barrier systems in the Gulf of Maine (Walsh, 1988). Algae adhere to the rock with a root-like "holdfast" when the plant begins to grow. Seaweed has air pockets that allow the algae to remain erect under water, providing buoyancy to plant and rock. As strong currents rush over the rock with the attached algal frond the buoyancy and hydrodynamic drag of the plant allows the rock to be carried with the current. The movement of rocks with attached algae is noted by drag marks on the beachface (Carter and Orford, 1991) and tidal flat (Walsh, 1988). Ice processes are an important seasonal factor in deposition and erosion, typically from late December or January to March. The effects of ice processes include transport and deposition of sediment incorporated in the ice, protection from wind and wave erosion, and topographic changes as the ice moves over the substrate. The influence of ice and algae on the movement of pebble- and cobble-sized clasts was measured during the winter months (November to May). Five groups of ten rocks were placed along Sprague Neck Bar (Figure 25, 26). Each group contained rocks with and without attached algae. The rocks were painted with a fluorescent paint, labeled, and covered with a marine durable varnish. GPS points were taken in order to determine the distance and direction of transport of each clast.
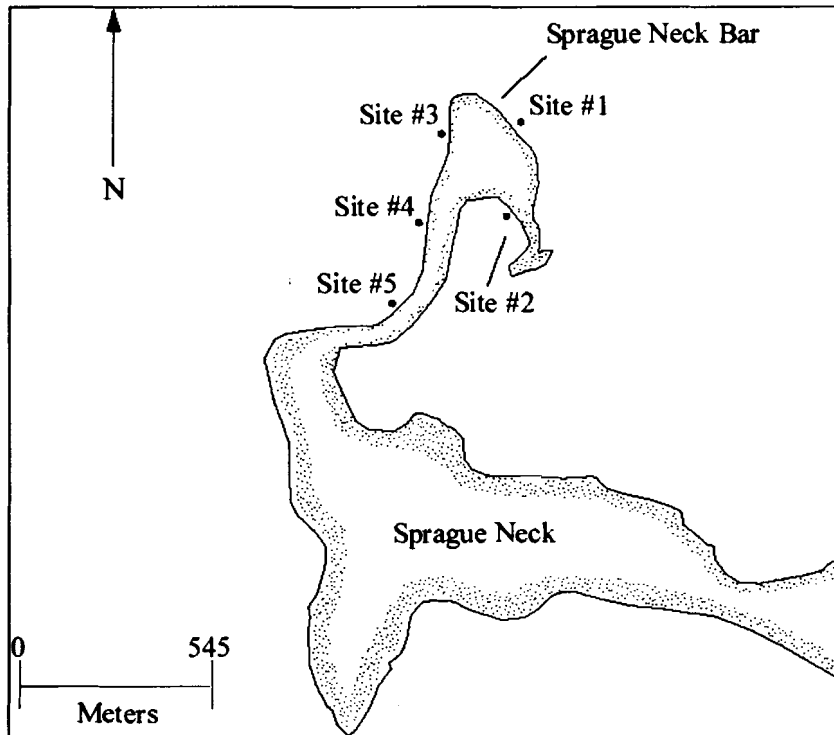
Figure 25. Location diagram for the five groups of clasts in the seaweed and ice transport experiment on November 21, 2001.
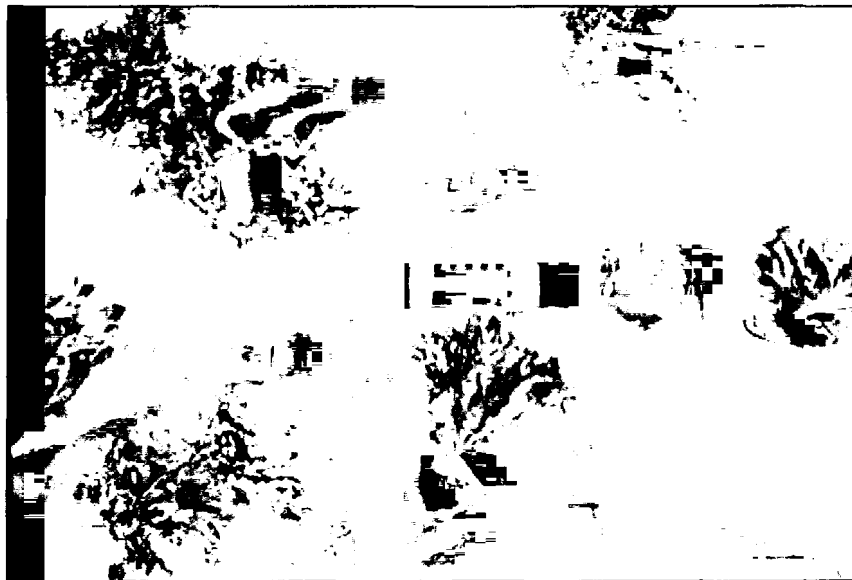
Figure 26. Group #3 in the transport experiment beginning on November 21, 2001.

3-D Acoustic Current Meters

The 3D Acoustic Current Meters (3D-ACM) collect current velocity data in three dimensions. The instrument measures velocity along four acoustic paths, three orthogonal magnetic vectors, and two orthogonal gravity vectors (tilt). From these parameters the 3D-ACM calculates velocity relative to the earth. Water flow along the four acoustic paths is calculated by using the transmission of sound from one transducer to another. There are a total of eight acoustic transducers on the sensor head. Water flow calculations are based on the acoustic phase shift of sound, i.e., the advance of sound travelling in the same direction as the water and the slowing down of sound travelling against the flow of water (Falmouth Scientific Instruments, 3D Acoustic Current Meter Manual, 2000).

A fixed platform, consisting of a wooden rod attached to a cement anchor, was used to hold the current meters in position. A wooden rod was used to ensure compass accuracy. The fixed platform was necessary because of the shallow water. The platform also provided a stable base, which eliminated movement of the instrument. Current meters were placed in the nearshore environment along the northern extension (3D-ACM 1601) and recurve (3D-ACM 1600) (Figure 27). The tidal regime was sampled over a 24-hour period on June 11-12, 2001. The instruments were programmed for a delayed start on June 11 at 8:00 a.m. Measurements were taken continuously for 59 minutes of every hour, and averaged every 15 seconds. Measured parameters include sea temperature, N velocity, E velocity, Up velocity, tilt, and direction. The north and east velocities were plotted to determine direction and magnitude of the currents. In addition

59

to the vector plots, the horizontal and total scalar speeds were plotted for each current meter. The horizontal scalar speed is a function of the east velocity and north velocity, providing a measure of the horizontal speed. Total scalar speed is calculated using the 3-dimensional velocity. The total scalar speed includes the upward movement of the water, and may provide a measure of turbulence.
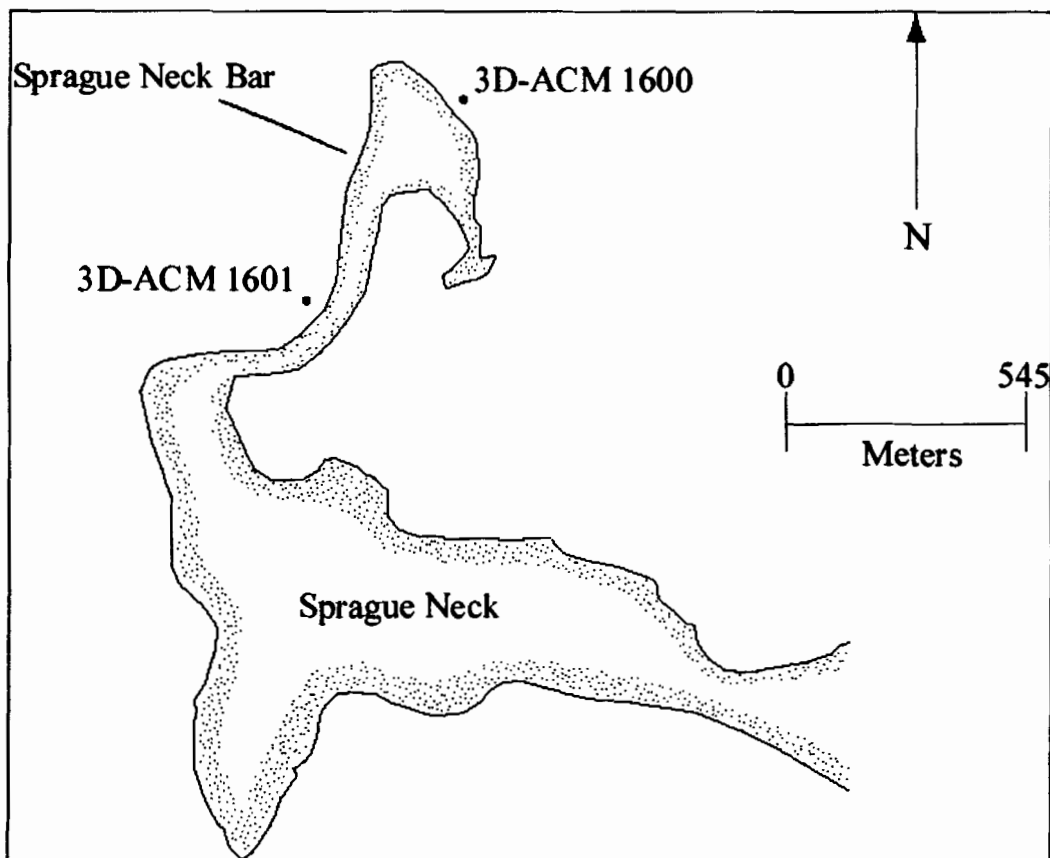
Figure 27. Location of the 3D-acoustic current meters on June 11-12, 2001.

RESULTS

Surface Sediment Distribution

Coarse sand (S) and pebbles (P) are the dominant surface sediment textures of

Sprague Neck Bar. Muddy sand (mS) is significant only in the backbarrier environment.

Surface sediment of Sprague Neck Bar fits a polymodal distribution. The two most

abundant class intervals are -5 to -6 phi (16.8%), pebble-sized clasts, and 2 to 1 phi

(16.5%), medium sand (Figure 28; Table 7). Approximately 48% of the surface sediment

falls within the range of 0 to -4 phi, very coarse sand to small pebbles. The surface

sediment of Sprague Neck Bar is well sorted and negatively skewed. Major sedimentary

facies of Sprague Neck Bar are (Figure 29, 30, 31): 1) sand (S, gravel <5%, mud < 10%

by wt.), 2) pebbles and cobbles (P/cP facies, cobbles < 50%), 3) sandy mud/muddy sand

(sM/mS facies), 4) sandy gravel and gravelly sand (sG/gS facies, < 50% by wt.), and 5)

gravel and pebbles (pG/gP facies, gravel < 50). Boundaries between all sedimentary

facies are gradational in the field.

The two predominant sediment facies of Sprague Neck Bar are sand (S facies)

and pebbles and cobbles (P/cP facies) (Figure 31). Sand (S facies) is the most abundant

sediment texture, accounting for 22% of the surface sediment. The S facies occurs in two

barrier environments along the northern extension of Sprague Neck Bar: 1) intertidal

zone and 2) the barrier crest. Sand is an interstitial component at the spit tip and recurve.

The S facies is found on the mid- to upper intertidal zone on the western side of Sprague

Neck Bar. On the backbarrier side of the spit, the S facies predominately occurs in the

lower intertidal zone. The coarsest sand, -0.05 phi, is located on the lower intertidal

Table 7. Statistical Data for Sediment Samples obtained from Sprague Neck Bar.

Sample	Mean	Std. Dev.	Sorting	Skewness	%S	%G	%M	%P	%C	Facies
SB 1-5	-4.6163	0.5280	0.2788	-0.2946	----	----	----	90.48	9.52	P
SB 1-6	1.6407	0.3859	0.1489	1.3030	100.00	----	----	----	----	S
SB 1-9	1.5634	0.3226	0.1041	2.2364	100.00	----	----	----	----	S
SB 1-12	1.5340	0.3763	0.1416	0.8746	100.00	----	----	----	----	S
SB 1-14	-0.0462	0.1020	0.0104	-1.9618	100.00	----	----	----	----	S
SB 1-15	-7.0351	1.0485	1.0994	-0.1372	----	----	----	15.00	85.00	pC
SB 2-2	0.9518	0.6136	0.3765	1.7155	93.51	6.49	----	----	----	gS
SB 2-3	1.5283	0.9254	0.8563	1.7276	95.20	4.80	----	----	----	gS
SB 2-5	1.8365	0.4523	0.3267	1.8620	100.00	----	----	----	----	S
SB 2-8	1.8409	0.5150	0.2653	0.6472	94.43	5.57	----	----	----	gS
SB 3-4	1.3960	0.3668	0.1345	2.0534	100.00	----	----	----	----	S
SB 3-5	-6.1259	0.4888	0.2389	0.2863	----	----	----	33.00	67.00	cP
SB 3-7	-5.6243	0.5587	0.3121	0.0767	---	----	----	78.00	22.00	cP
SB 3-8	-5.8345	0.7083	0.5016	-0.7789	----	----	----	62.00	38.00	cP
SB 3-11	0.6460	0.6312	0.3984	2.3980	100.00	----	----	----	----	S
SB 4-2	-2.0340	0.5899	0.3546	1.3427	50.00	----	----	36.00	14.00	csP
SB 4-8	-5.0401	0.6841	0.4681	0.1484	----	----	----	76.00	24.00	cP
SB 4-9	-6.1537	0.7027	0.4938	0.0791	----	----	----	42.00	58.00	cP
SB 4-10	2.3978	0.5717	0.3266	-2.1016	100.00	----	----	----	----	S
SB 4-11	0.4378	0.6630	0.4396	3.2629	39.09	60.91	----	----	----	sG
SB 5-2	-2.1186	0.5953	0.3592	1.7967	50.00	----	----	35.00	15.00	csP
SB 5-3	-5.9222	0.4503	0.2028	1.2804	---	----	----	82.00	18.00	P
SB 5-7	-5.7654	0.6177	0.3816	-0.4936	---	----	----	62.00	38.00	cP
SB 5-8	1.6930	0.4181	0.1748	1.0960	100.00	----	----	----	----	S
SB 12	-7.0921	0.9627	0.9267	-0.2143	----	----	----	80.00	20.00	cP
SB 13	-5.6544	0.6489	0.4211	-0.2299	----	----	----	73.00	27.00	cP
SB 14	-5.1446	0.9540	0.9100	-0.1000	----	----	----	84.00	16.00	P
A	-1.9840	0.3662	0.1341	-1.1619	14.53	42.17	----	43.30	----	pG
B	0.4367	0.5526	0.3053	1.5607	85.72	---	----	14.28	----	pS
C	-0.1899	0.2934	0.0861	1.8838	61.11	19.94	----	18.95	----	gpS

Table 7 (continued). Statistical Data for Sediment Samples obtained from Sprague Neck Bar.

| Sample	Mean	Std. Dev.	Sorting	Skewness	%S	%G	%M	%P	%C	Facies
D	-0.8323	0.9494	0.9014	-1.1070	56.41	----	----	43.59	----	sP
E	-4.4689	0.7206	0.5193	-0.0063	----	----	----	100.00	----	P
F	-3.2598	0.4752	0.2947	-0.2017	10.98	27.38	----	59.64	2.00	gP
H	-0.0332	0.1540	0.0237	0.5976	55.00	45.00	----	----	----	sG
I	-1.8211	0.5919	0.3735	0.9919	50.00	----	----	47.00	3.00	sP
J	1.5579	0.5382	0.2870	2.0769	100.00	----	----	----	----	S
K	1.7412	0.6175	0.3813	1.1959	100.00	----	----	----	----	S
L	-4.8136	0.5715	0.3266	0.0458	----	----	----	100.00	----	P
O	-5.4514	0.5140	0.2642	-0.4303	----	----	----	90.00	10.00	P
M	-2.0399	0.5627	0.3296	1.1999	50.00	----	----	41.00	9.00	csP
N	1.4944	0.6423	0.4126	0.9590	100.00	----	----	----	----	S
P	-2.3681	0.8971	0.8047	-1.6571	----	23.20	----	76.80	----	gP
Q	-5.0120	0.7192	0.5180	-0.1457	----	----	----	94.00	6.00	P
R	1.6836	0.3189	0.1017	1.2605	100.00	----	----	----	----	S
S	-5.5573	0.6310	0.3982	0.6594	----	----	----	82.00	18.00	P
T	1.7573	0.5954	0.3545	1.4309	100.00	----	----	----	----	S
U	5.4432	0.4000	0.8990	-0.0800	11.00	2.00	87.00	----	----	sM
V	5.2200	0.5670	0.9250	-0.0312	10.20	2.80	87.00	----	----	sM
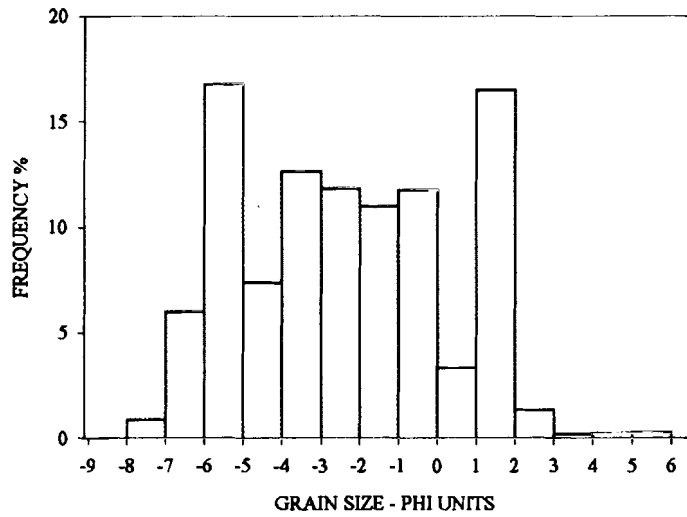
Figure 28. The histogram illustrates the frequency of surface sediment occurring in each size interval and represents a consolidated set of samples. The surface sediment of Sprague Neck Bar fits a polymodal distribution.
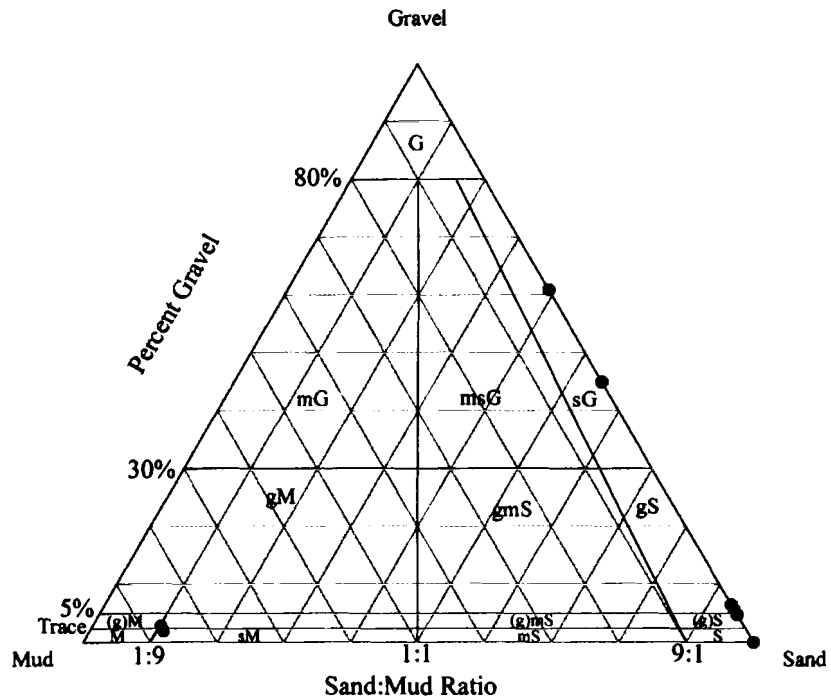

Figure 29. Surface sediment description of Sprague Neck Bar according to percent sand, gravel, and mud. The ternary plot is based on the Folk-Ward Classification.
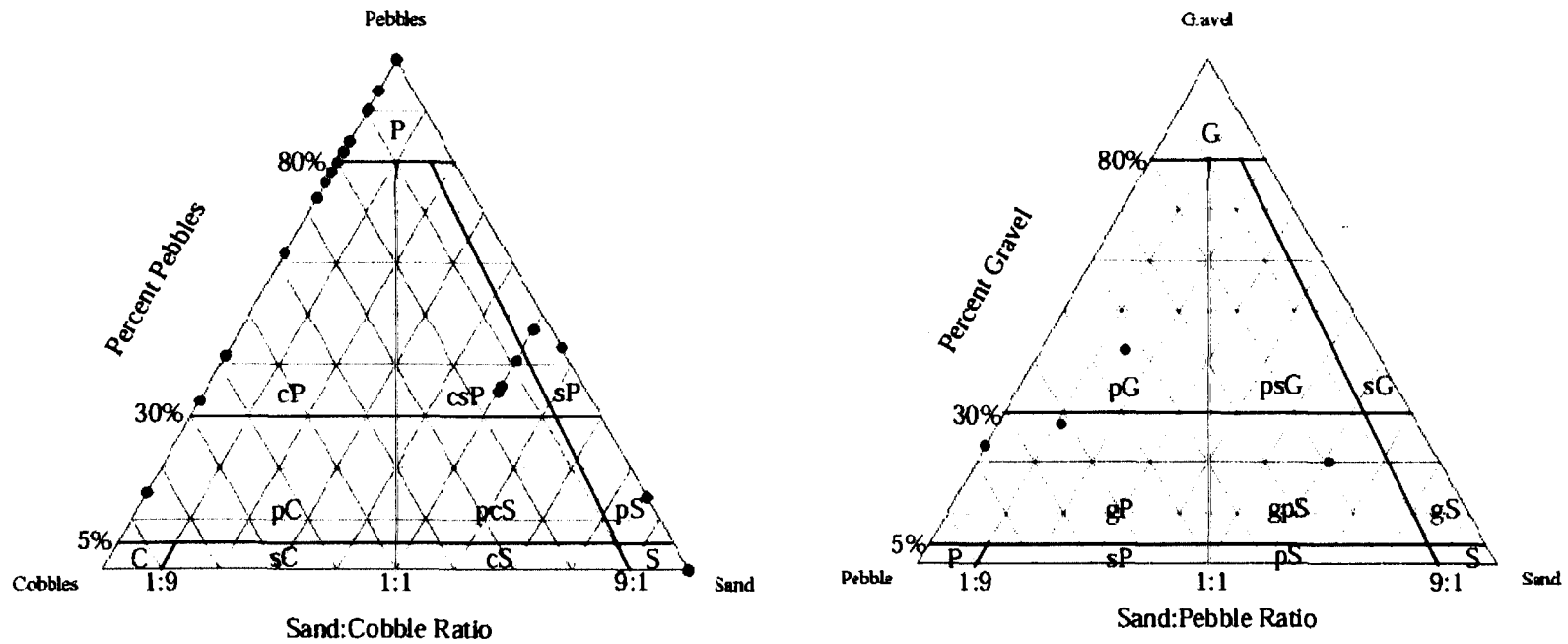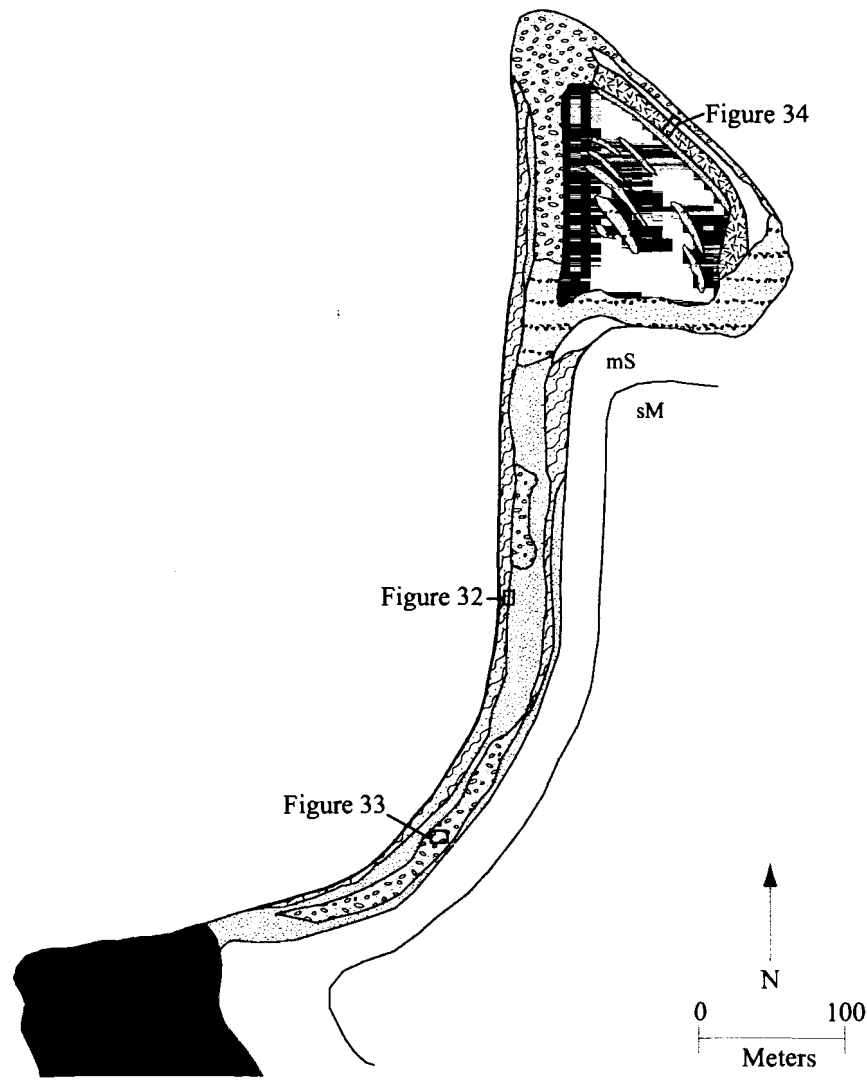
64

Figure 30. Ternary plots for sediment samples obtained from Sprague Neck Bar. The plots are a variation of the Folk-Ward classification. Sediment categories are described in Table 6: Sand: 4 to -1 phi, Gravel: -1 to -2 phi, and Pebble: -2 to -6 phi.
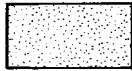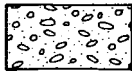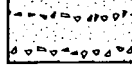
Figure 31. Distribution of the surface sediment facies of Sprague Neck Bar.
Map depicts approximate mean low water setting.

zone. Sediment on the mid- to upper intertidal zone is well sorted and positively skewed ranges from 0.65 phi to 1.7 phi, fining toward the crest. Sediment on the barrier crest is well sorted, positively skewed, and mean sediment size ranges from 1.8 phi to 2.4 phi, medium to fine sand. Fine sand is associated with the colonization of *Ammophila breviligulata.*

The P facies and cP facies (Figures 31) combined account for 32% of the surface sediment, each representing 16%. The P facies (Figure 32) describes the lower to mid intertidal zone of Sprague Neck Bar. Clast size ranges from -4.5 phi to -5.9 phi, 22.2 mm to 60.6 mm. The facies is moderately to well sorted near Sprague Neck, becoming poorly sorted and more negatively skewed toward the spit tip. The cP facies occurs on the northernmost spit tip, the lower intertidal zone of the recurve, and barrier crest near the broad flat and proximal to Sprague Neck (Figure 31, 33). Mean clast size ranges from -5.0 phi to -7.1 phi, 32.9 mm to 136.4 mm. The facies is negatively skewed at the spit tip, but positively skewed on the barrier crest closer to Sprague Neck.

Sandy gravel/gravelly sand (sG/gS) in located on the barrier crest near the preserved recurve system and interior of the flat (Figure 31). Approximately 10% of the surface sediment are described by this facies. On the barrier crest, the sG/gS facies forms a transitional unit between the S and cP facies. Sandy gravel forms distinct ridges on the flat interior. Mean grain size ranges from 1.8 phi to -0.03 phi, medium to coarse sand. The sediment is finely skewed and moderately to well sorted. The coarsest sediment occurs on the barrier crest.

Pebbles and gravel (pG/gP facies) describe approximately 6% of the surface sediment (Figure 31, 34). The pG/gP facies is significant because the unit is found only
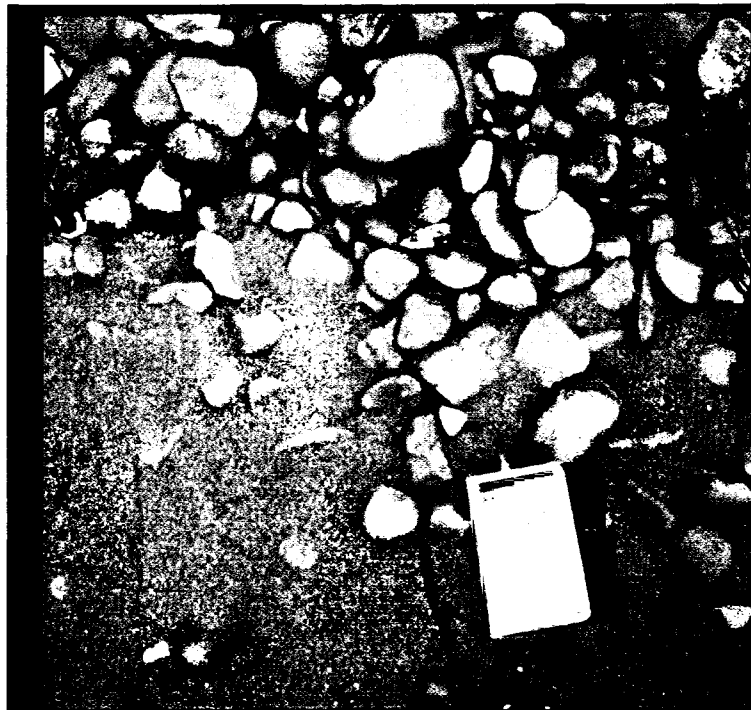
67

Figure 32. Field photograph of the sand (S) facies and the pebbles (P) facies (June, 2001). See Figure 31 for sample location.

Figure 33. Field photograph of the cobbles and pebbles (cP) facies. See Figure 31 for sample location.

68
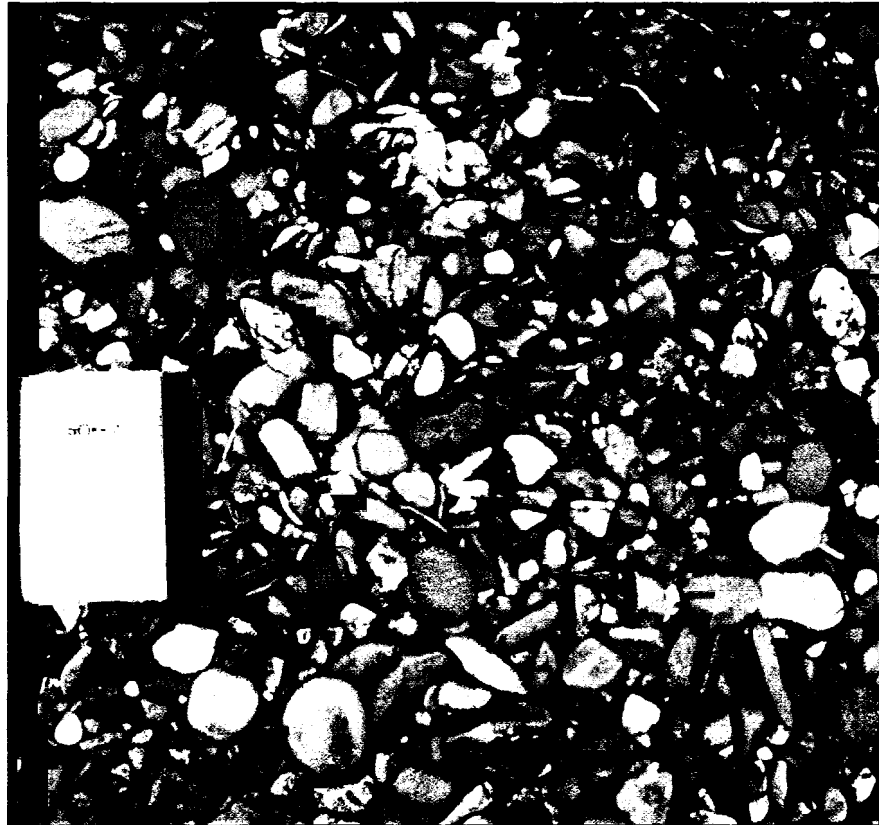
Figure 34. Field photographs of the pG/gP facies. See Figure 31 for sample location on Sprague Neck Bar.

on the current recurve. The gP facies comprises the lower to mid- intertidal zone and grades into the pG facies on the barrier crest. Sediment is well sorted and skewness varies with sample location. Positively skewed samples tend to occur on the crest, while negatively skewed samples are located on the mid- to lower intertidal zone.

Sandy mud occurs in two morphologically distinct environments: 1) the broad flat/salt marsh and 2) the backbarrier mudflat (Figure 31). Mud characterizes the largest percentage of the salt marsh, with sand and gravel being locally significant (i.e., gravel ridges). Boundaries between the salt marsh and gravel ridges are well defined. A unit of muddy sand occurs at the boundary between the barrier spit and mudflat.

Topography

Sprague Neck Bar extends 845 m to the north before the barrier spit recurves to the southeast for 232 m (Figure 35). Extending northward from the Pond Ridge Moraine, for approximately 230 m, Sprague Neck Bar is characterized by steep slopes, narrow crest, and an elevation ranging from 4.8 m to 5 m above MLW. A distinct change in elevation occurs between 230 m and 280 m in which the elevation increases to 6 m. Elevation remains between 5.5 m and 6.1 m for the continued northward extension of Sprague Neck Bar. Along the recurve, elevation decreases to less than 3 m on the developing spit platform. Beachface slopes are steep in profile, with grades of approximately 9-10%, suggesting relatively reflective conditions. The landward-facing slope is less steep with an average relief of 2.3 m. Minimum elevation of the landward-facing slope is approximately 1-2 m higher than the minimum elevation of the beachface slope.

The preserved recurve system, forming a broad flat, has a total perimeter of 574.6
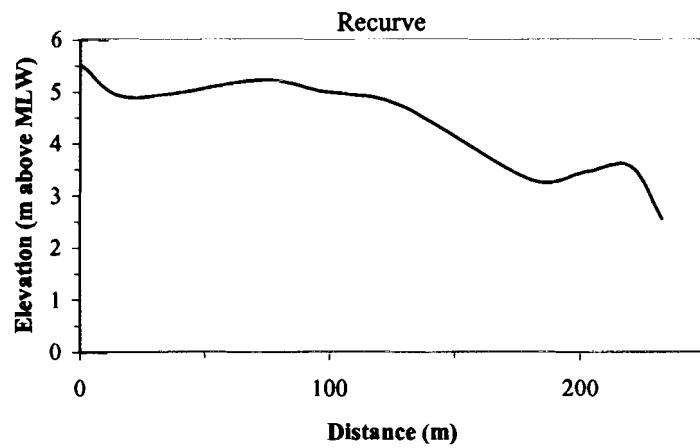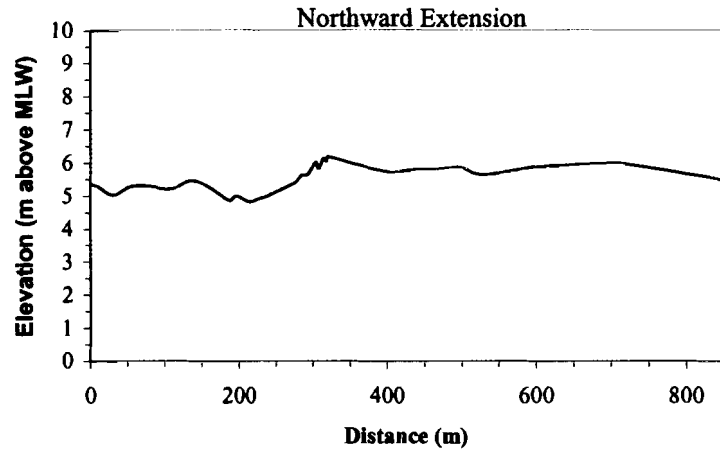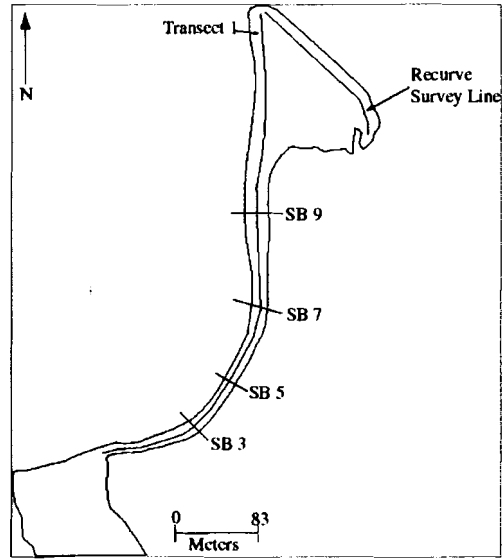
Figure 35. Topographic profiles for Sprague Neck Bar.
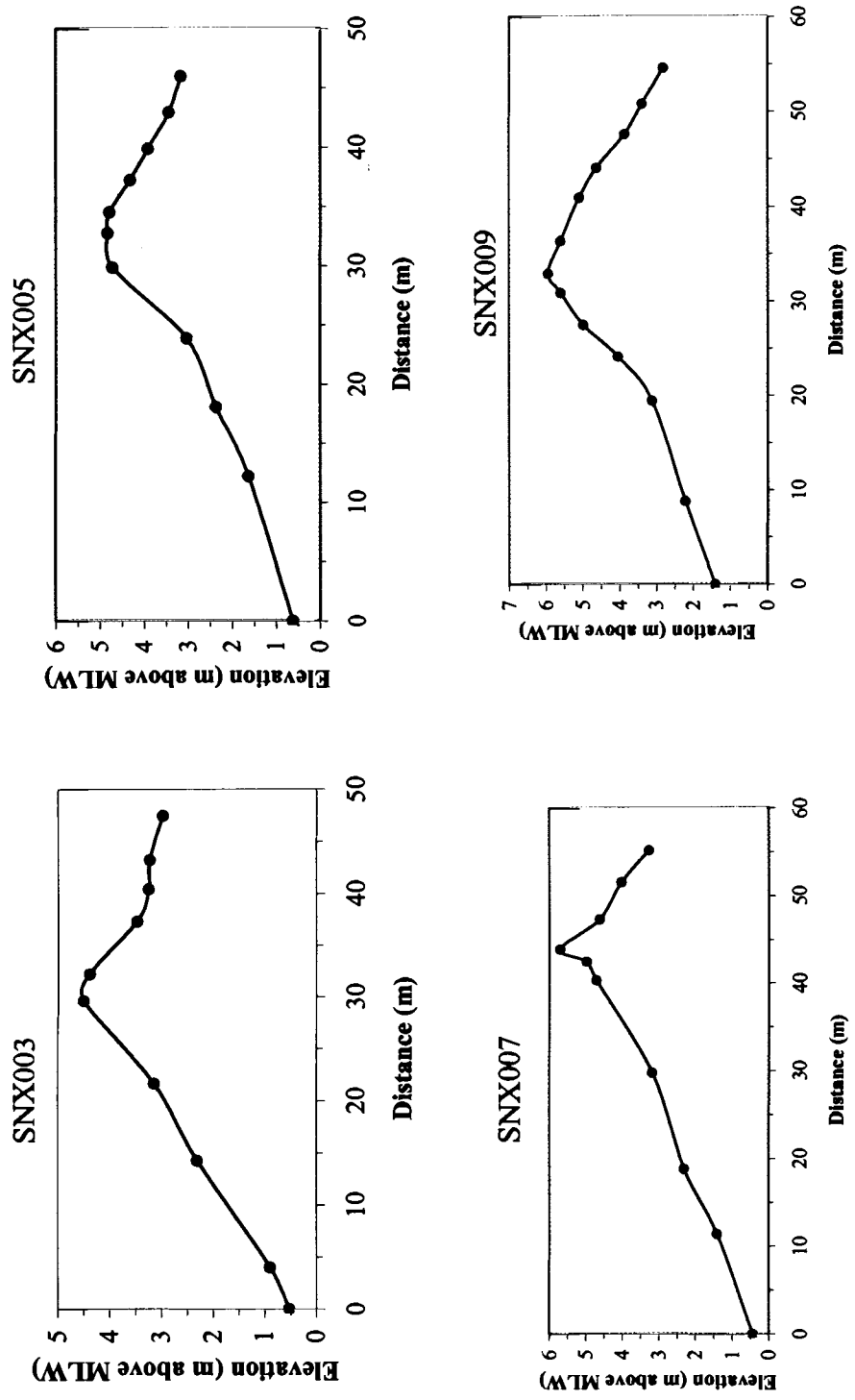
Figure 35 continued. Topographic profiles for Sprague Neck Bar. The vertical is in meters above mean low water.

72

m, ranging in elevation from 3.5 m to 4.1 m. Elevation is greatest on the western edge of the recurve system, averaging 3.9 m above MLW, and decreases along the northeastern, eastern, and southern boundaries. The southern margin of the flat is intertidal and has an average elevation of 3.5 m. While the elevation of the flat perimeter is relatively constant, the interior of the flat is more variable in elevation. Elevation is lowest in the southwestern portion of the broad flat and increases 0.7 m in a northeast direction toward the spit tip and current recurve. Average elevation of the recurve system is approximately 3.3 m above MLW, and the gravel ridges have an average elevation of 3.7 m above MLW. Elevation of the gravel ridges increases 0.4 m toward the current recurve. Relief varies across the flat, averaging 0.35 m difference between the gravel ridges and flat.

Barrier Stratigraphy

A reflection-free configuration (Figure 36) was produced for each of the cross-sectional and recurved transects. The top three reflectors (the thick alternating black-white-black lines) represent the signal travelling through the air and along the surface (Figure 36). For 1.1 m below the surface on cross transect SN 3 the reflectors are multiples of the surface. Below this depth no signal is returned.

The GPR line along the northward extension of Sprague Neck Bar revealed a structure at 220.5 m to 283.5 m (Figure 37). At approximately 220.5 m a reflector located 4.7 m above MLW separates from the reflector above, which represents the surface of Sprague Neck Bar. The reflector parallels the surface for 5 m before dipping 0.1 m away from the surface. A minimum elevation of 4.9 m above MLW is reached at 259.0 m. At 259.0 m the reflector dips toward the surface. At 283.5 m the reflector
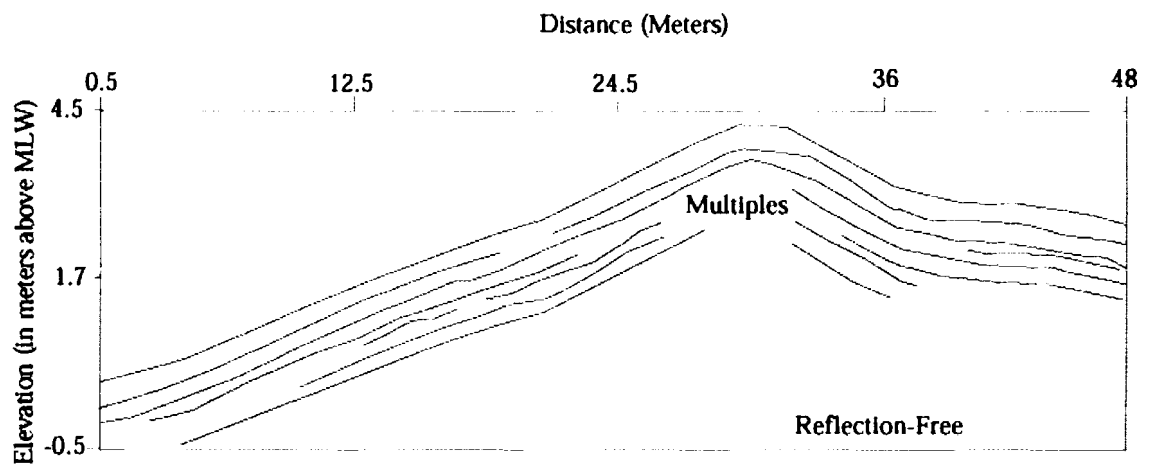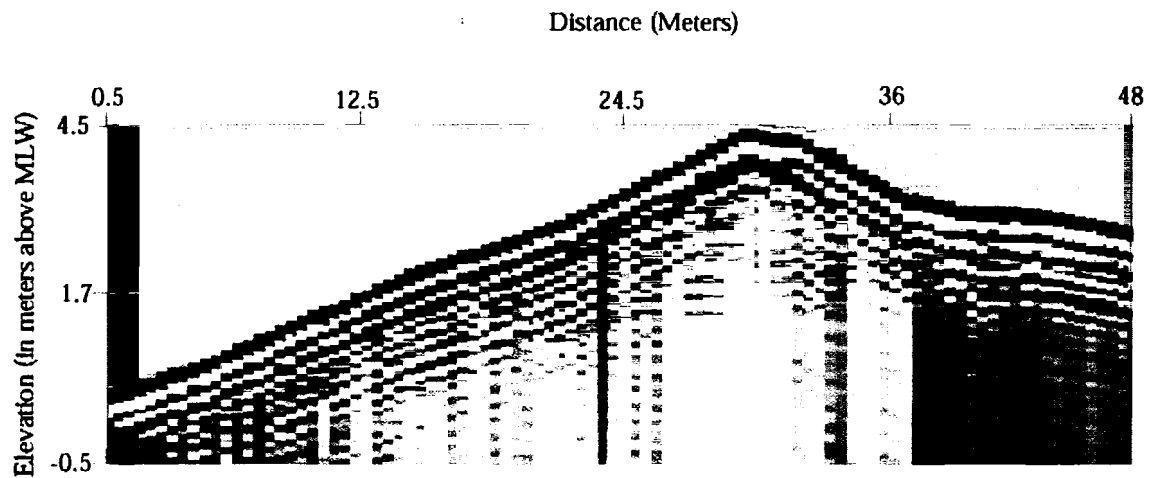
Figure 36. Ground penetrating radar record for transect SN3 across the width of Sprague Neck Bar, x20 vertical exaggeration. See Figure 20 for location of Flag SN3.
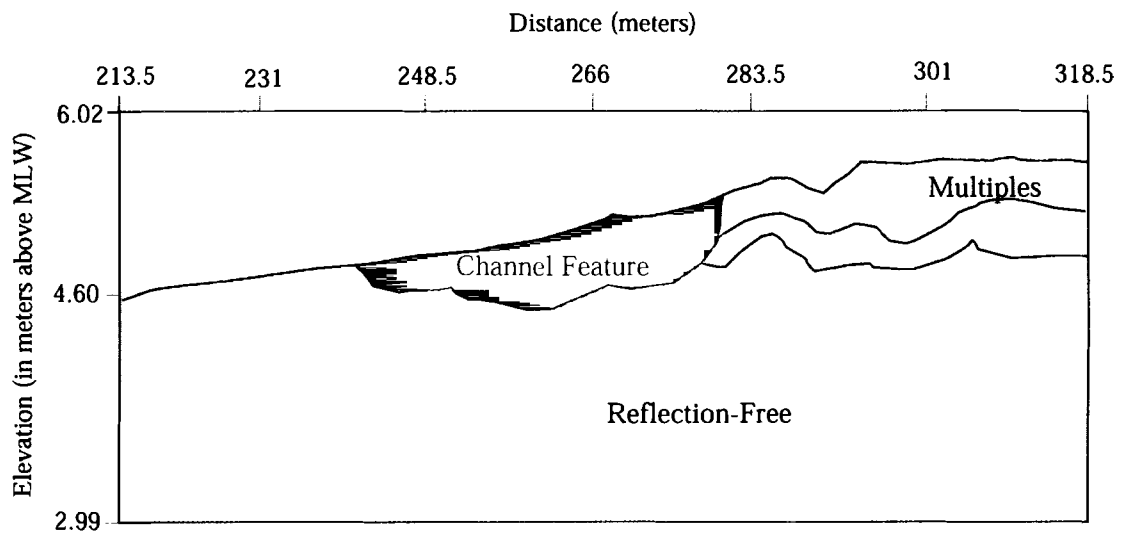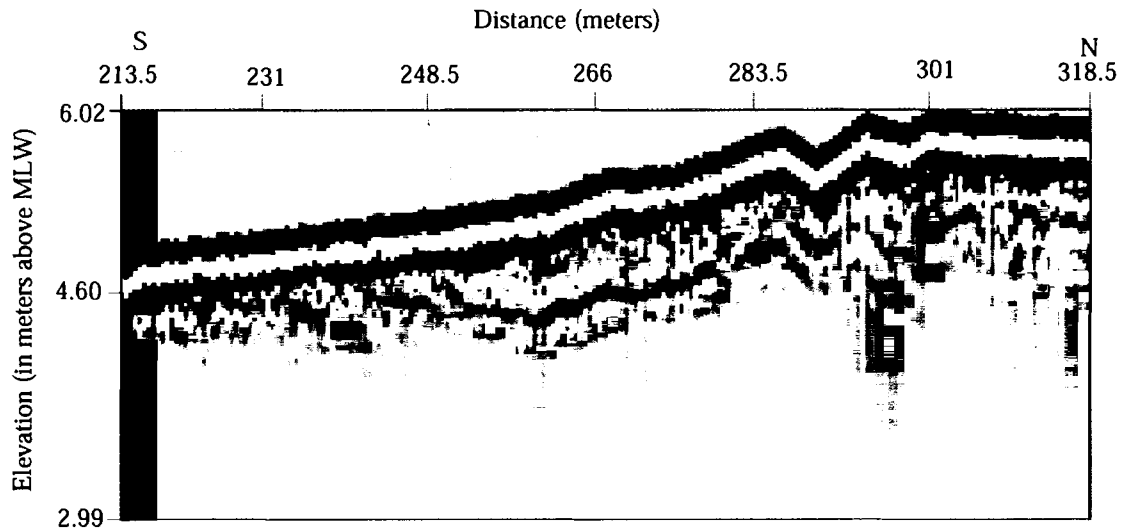
Figure 37. Ground penetrating radar record for the northward extension of Sprague Neck Bar, x18 vertical exaggeration. The GPR record is located on the barrier crest 213.5 m from Sprague Neck, between the two moraines.

reaches an elevation of 4.7 m above MLW. From 283.5 m to the spit tip the reflectors are more closely spaced and parallel the surface.

3-D Acoustic Current Meters

The current meters, placed along the northward extension (3D-ACM 1601) and recurve (3D-ACM 1600) on June 11, 2001 at 8:00 a.m., were exposed at low tide. On June 11, the current meters were submerged at 11:30 a.m. and exposed at 8:15 p.m. The predicted tides for June 11 were at 3:30 p.m. (high tide) and 9:20 p.m. (low tide). The predicted high tide for June 12 was at 3:30 a.m., and the predicted low was at 9:45 a.m. On June 11 the current meters were submerged between 10:30 and 11:15 p.m. and emerged on June 12 at 8:15 a.m. The 3D-ACM 1600 was submerged before the 3D-ACM 1601. Water temperature averaged between 7°C and 12°C (Figures 38, 39). Temperature varied with water depth and was coldest at high tide 7-9°C.

3D-ACM 1601-The direction of the flooding tide is from southwest to northeast (Figure 40). Magnitudes range between 0-5 cm/s, with average velocities of approximately 3 cm/s. The direction of the flooding tide becomes more east-northeast closer to slack high tide. Direction and magnitude varies throughout high tide. The ebbing tide is from northeast to southwest. Velocity ranges between 1-9 cm/s, averaging approximately 4-5 cm/s. Currents of this magnitude suggest a very quiet water environment.

The horizontal scalar speed (Figure 41) is variable during high tide, ranging between 0-16 cm/s. Horizontal scalar speeds greater than 15 cm/s occur when the current meter is exposed to the air during emergence. Several outliers exist near the time of
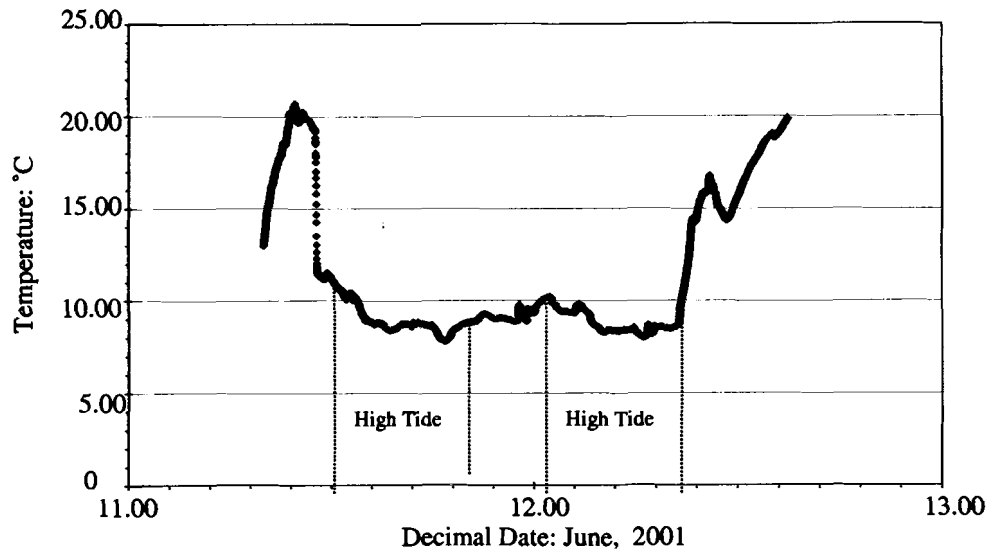
Figure 38. Water temperature data obtained from the 3D-ACM 1601, along the northern extension of Sprague Neck Bar. Predicted high tide on June 11 was at 3:30 p.m. and 9:20 p.m. Predicted high tide for June 12 was 3:30 a.m. and 9:45 a.m.
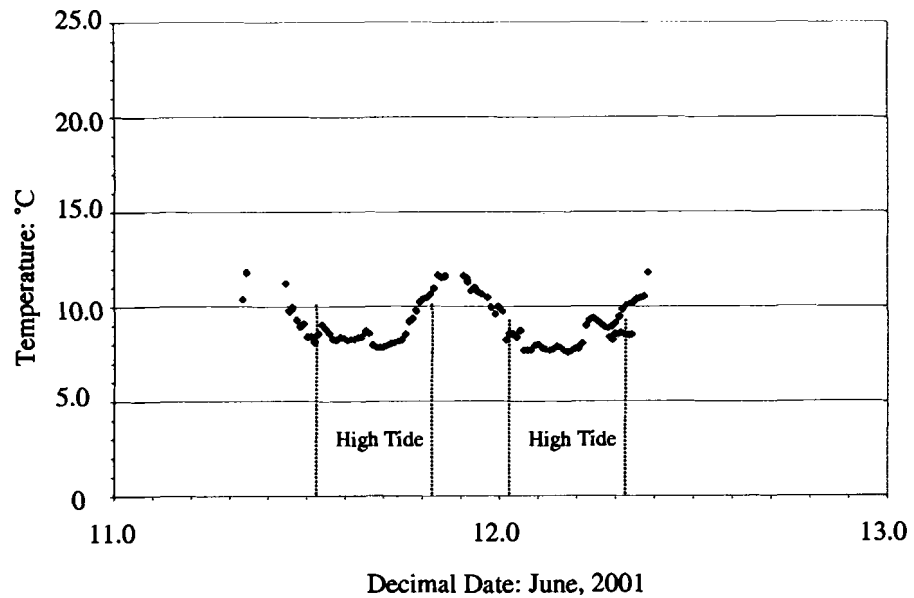
Figure 39. Water temperature data obtained from the 3D-ACM 1600, along the recurve of Sprague Neck Bar. Predicted high tide on June 11 was at 3:30 p.m. and 9:20 p.m. Predicted high tide for June 12 was 3:30 a.m. and 9:45 a.m.

77

SPRAGUE NECK: CURRENT METER 1601
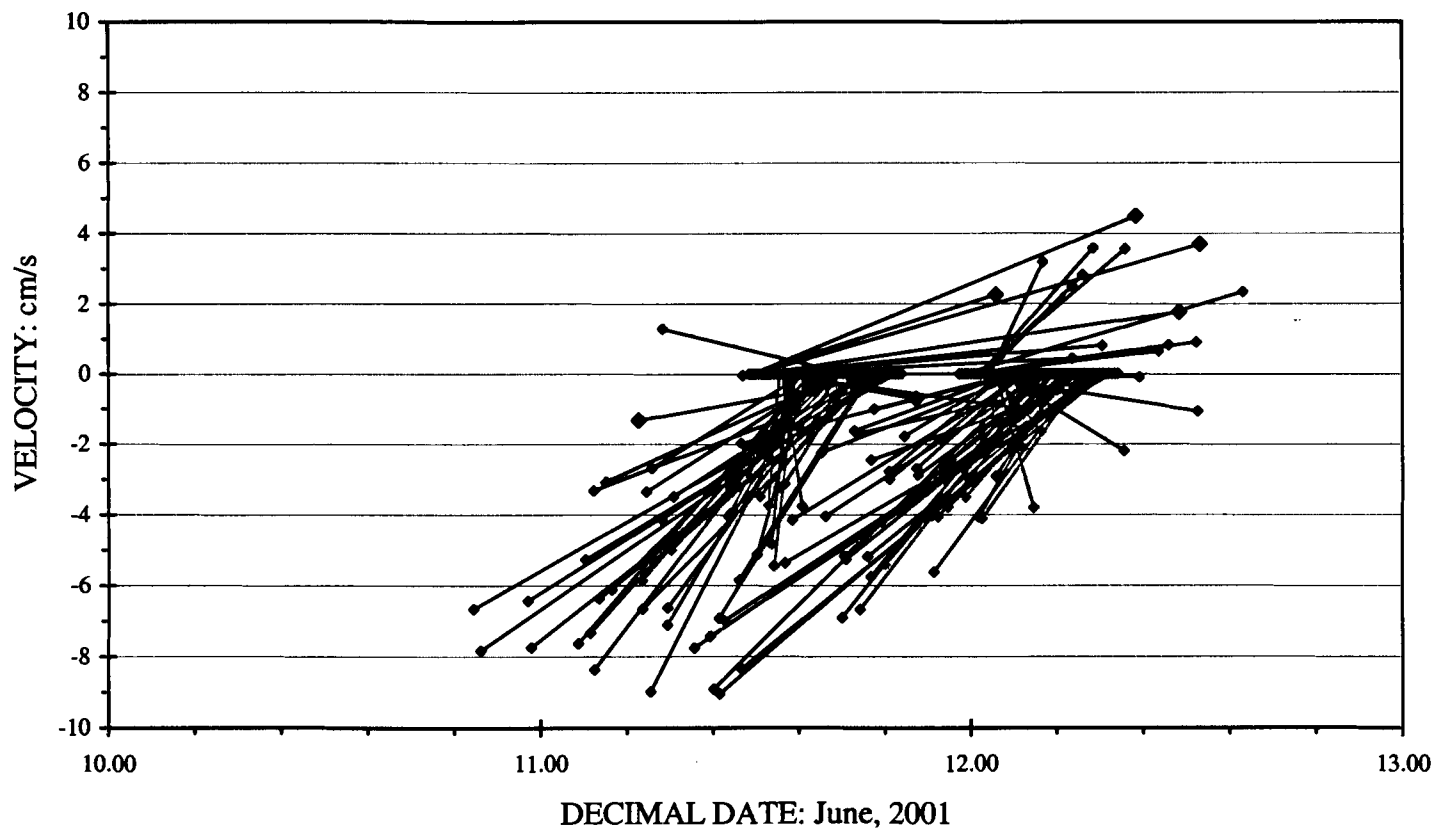
Figure 40. Direction and magnitude of tidal currents on the western side of Sprague Neck Bar. North is toward the top of the plot. Vectors indicate the direction of current flow. The current meter was submerged from (decimal date) 11.5 to 11.8 and 12.0 to 12.3.

Current Speeds: 3D-ACM 1601

Decimal Date: June, 2001
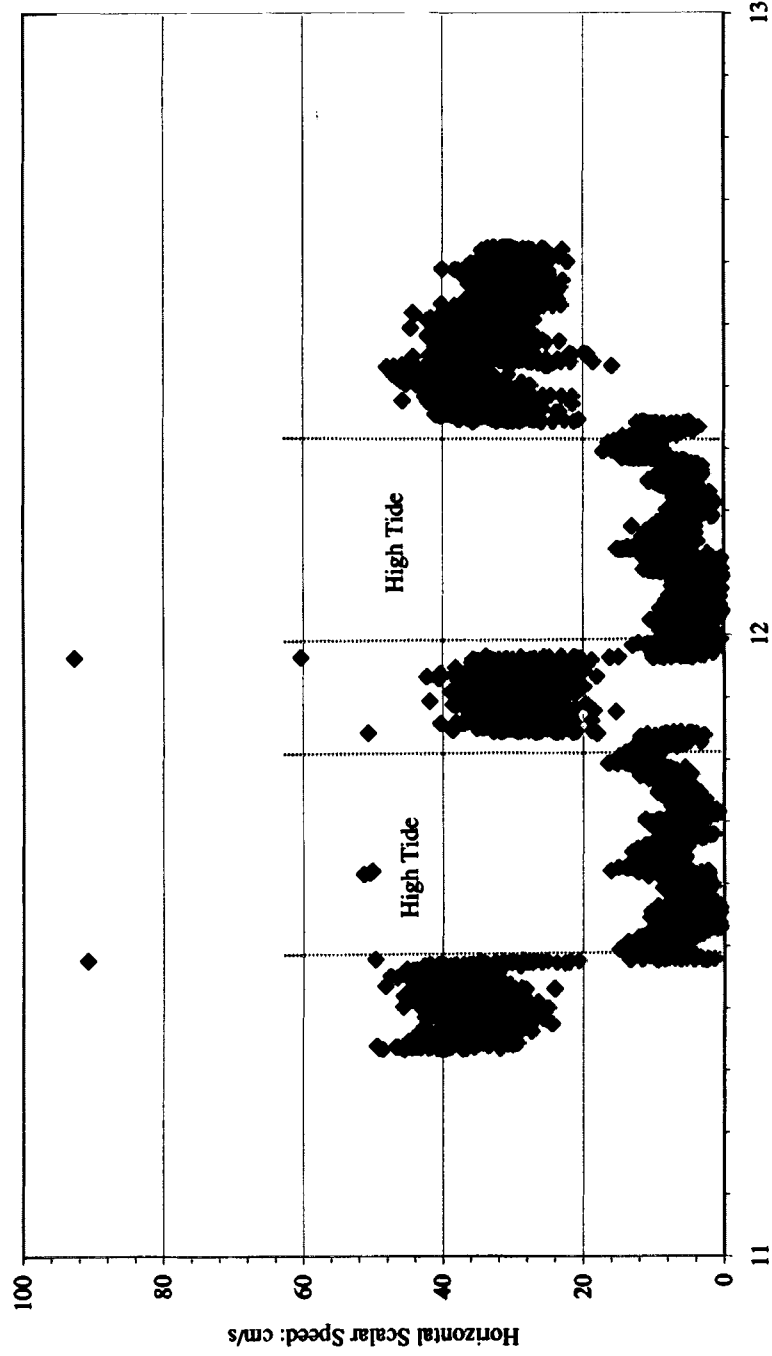
Figure 41. Horizontal scalar speed for the tidal currents on the western side of Sprague Neck Bar. The transient points between 60 and 100 cm/s are wave slap events as the current meter is submerging or emerging. The current meter was submerged between 11.5-11.8 and 12.0-12.3.

submergence and emergence with speeds ranging from 52 cm/s to 93 cm/s. Total scalar speed (Figure 42) is slightly greater and less variable than the horizontal scalar speed. During high tide the total scalar speed ranges between 8-20 cm/s. Horizontal and total scalar speeds reach a maximum speed just before slack high tide.

3D-ACM 1600-Along the current recurve the flooding tidal current is strongest to the southeast (Figure 43). The ebbing tidal current is from southeast to northwest. Flood tidal current velocities are between 3-12 cm/s, averaging 5 cm/s. Ebb tidal current velocities range between 1-24 cm/s and average 14 cm/s, exhibiting a slight ebb dominance.

During high tide the horizontal scalar speed (Figure 44) ranges between 0-38 cm/s, which is slightly greater than the horizontal scalar speed determined for the northward extension. Horizontal scalar speed reaches a minimum speed, 0-2 cm/s, at slack high tide and increases in speed during the ebbing tide. Outliers on the plot of horizontal scalar speed vary between 80-160 cm/s. Total scalar speed (Figure 45) falls between 12-42 cm/s. Total scalar speed and horizontal scalar speed follow a similar trend. The total scalar speed reaches maximum velocities during flooding and ebbing tides. Outliers exist near times of submergence or emergence of the current meter. Speeds for the transient points range between 72-188 cm/s.

Historic Evolution of Sprague Neck Bar

Historic Charts and Maps- The earliest chart of Machias Bay and Sprague Neck is a 1776 Atlantic Neptune navigation chart, an approximate scale of 1 cm = 235 m (Table 5, Figure 46). On this chart only the shape and orientation are discernible due to

80

Current Speeds: 3D-ACM 1601
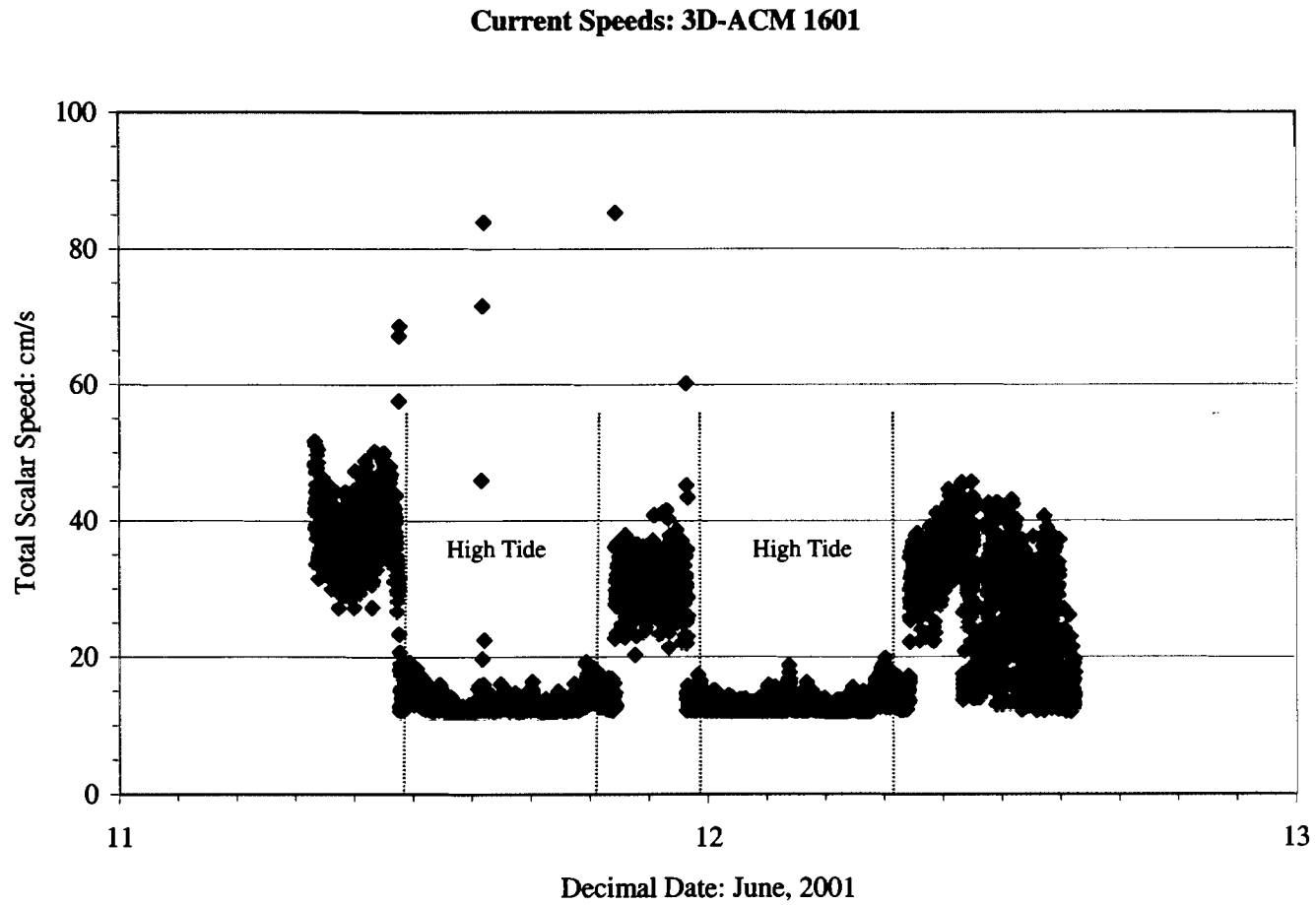
Figure 42. Total scalar speed calculated for the tidal currents on the western side of Sprague Neck Bar. The current meter was submerged between 11.5-11.8 and 12.0-12.3.

Sprague Neck Bar: Current Meter 1600
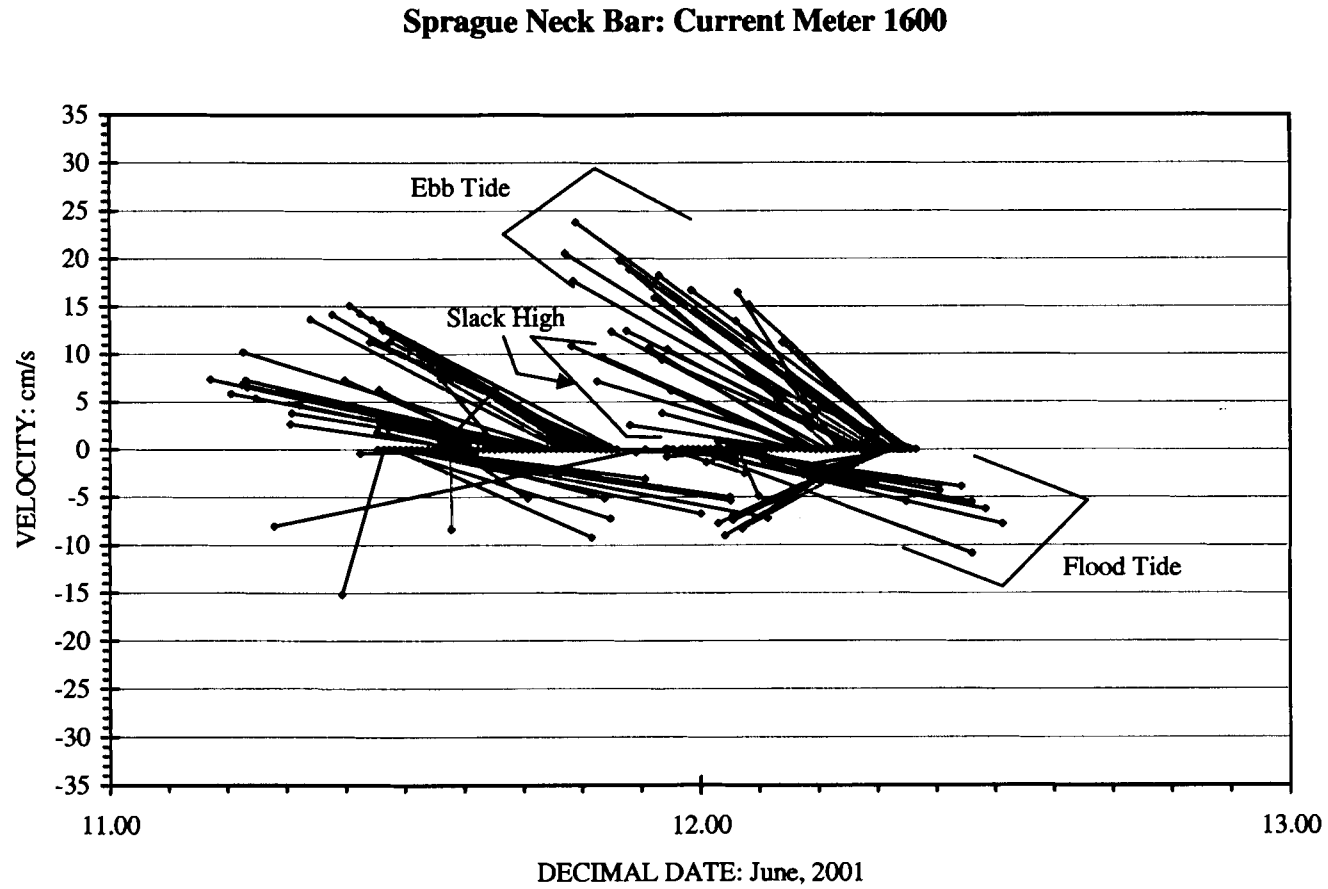
Figure 43. Direction and magnitude of tidal currents along the current recurve of Sprague Neck Bar. North is toward the top of the plot. Vectors indicate the direction of current flow. The current meter was submerged from (decimal date) 11.5-11.8 and 12.0-12.3.

Current Speeds: 3D-ACM 1600
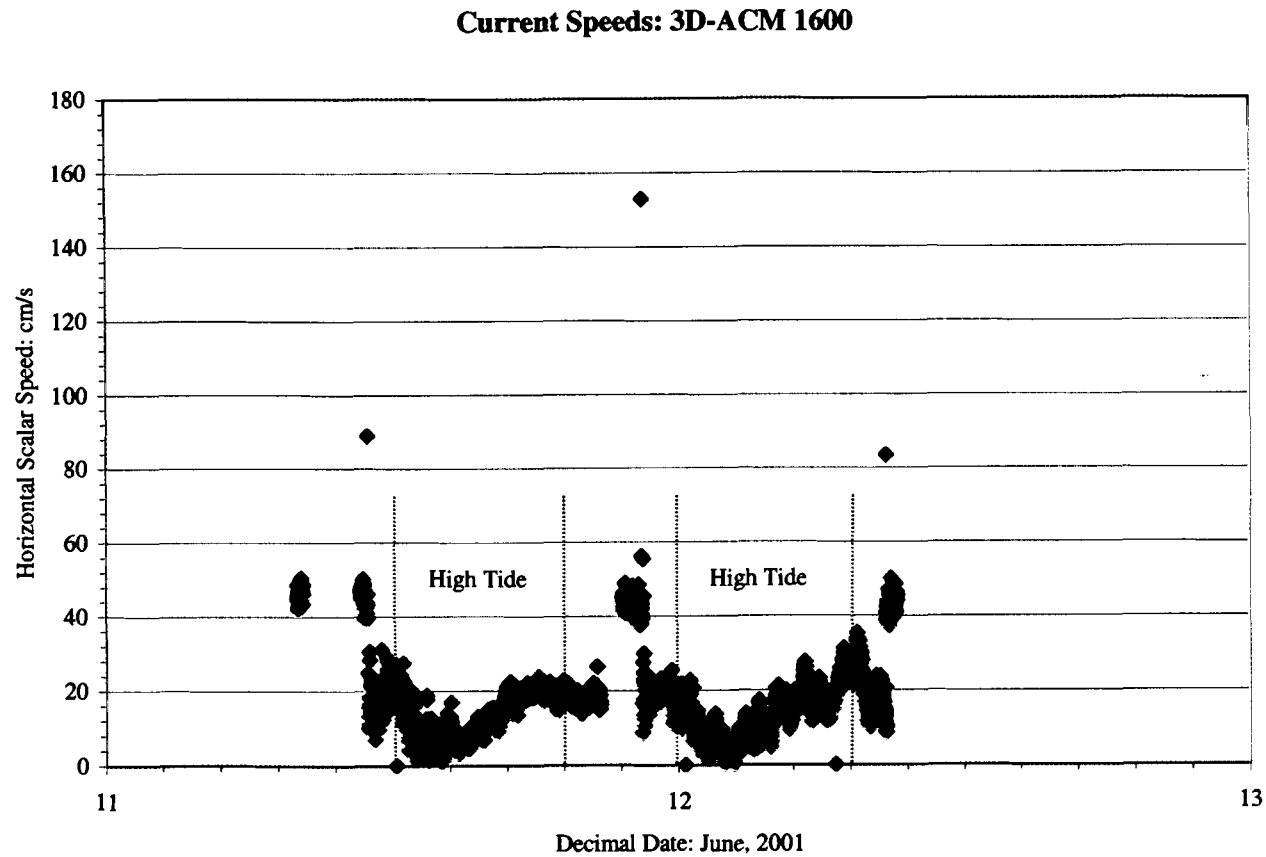
Figure 44. Horizontal scalar speed for the tidal currents along the current recurve of Sprague Neck Bar. The transient points between 80 and 160 cm/s are wave slap events as the current meter is submerging or emerging. The current meter submerged between (decimal date) 11.5-11.8 and 12.0-12.3.

Current Speeds: 3D-ACM 1600
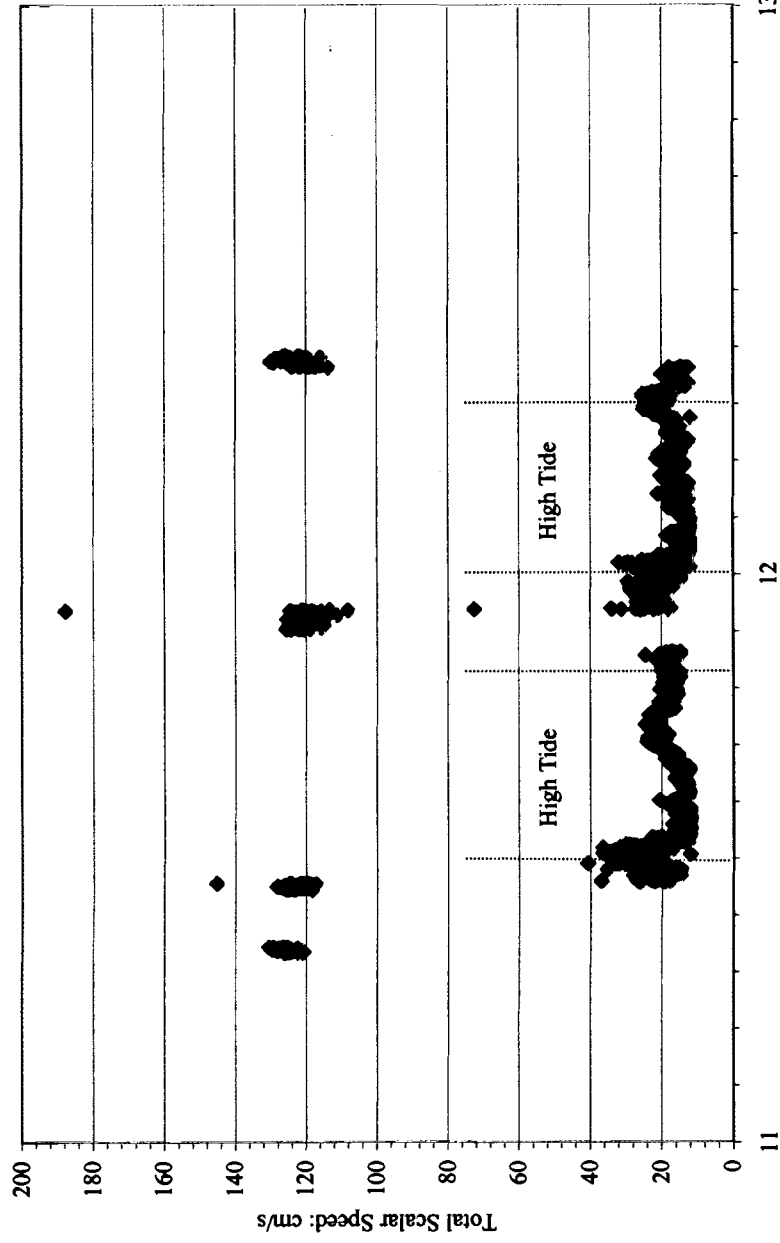
Figure 45. Total scalar speed calculated for the tidal currents along the current recurve of Sprague Neck Bar. The current meter was submerged between (decimal date) 11.5-11.8 and 12.0-12.3.
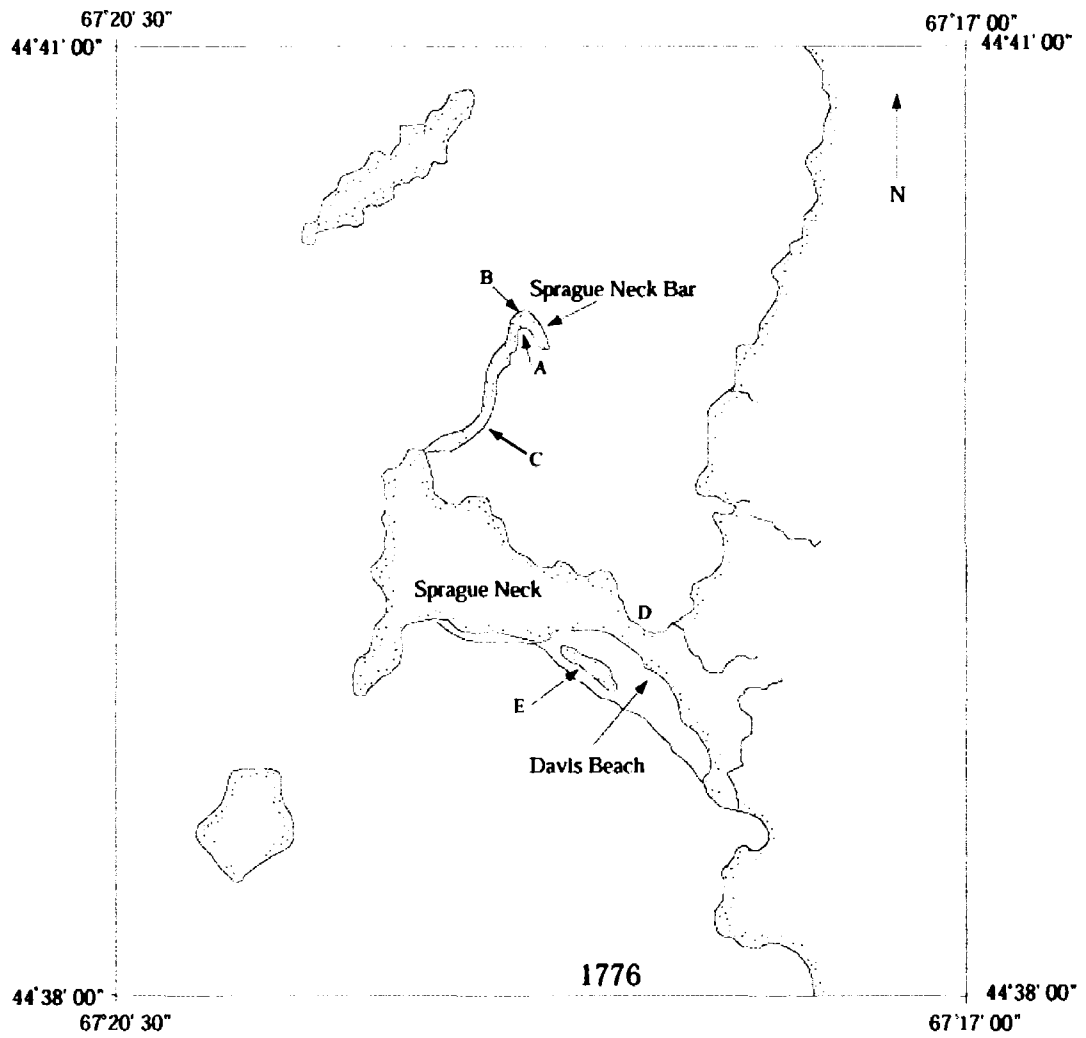
Figure 46. Map based on the 1776 Atlantic Neptune Navigation chart obtained from the Osher Map Library at the University of Southern Maine. Letters A, B, C, D, and E are explained in text. Approximate scale is 1 cm = 235 m.

the small scale of the chart. Sprague Neck Bar is attached to the western end of the Pond

Ridge Moraine and extends northward toward the head of Machias Bay before recurving

to the south-southeast. The broad flat (A in Figure 46), rounded tip (B in Figure 46), and

progressive narrowing of Sprague Neck Bar to the south are evident in the 1776 chart. A

distinct bend (C in Figure 46) in the barrier occurs in the southern segment of Sprague

Neck Bar. Equally prominent is the eroding northern rim of the Pond Ridge Moraine (D

in Figure 46) and an island (E in Figure 46) fronting Davis Beach. The island fronting

Davis Beach does not correspond with a modern day geomorphic feature.

A chart surveyed in 1886 (Table 5, Figure 47) depicts the bathymetry of Machias

Bay and only the principle geomorphic elements are evident. Sprague Neck Bar is

similar in shape and orientation to the 1776 chart. The broad flat (A), rounded tip (B),

and progressive narrowing to the south are clearly identified in the 1886 chart. There is

no land (E in Figure 46) fronting Davis Beach. The 1886 surveyed shoreline is the

shoreline depicted in all topographic maps.

Topographic map documentation began in 1918 and is lacking from 1918 to the

earliest coverage of air photos (1940). The 1918 (Figure 48) and 1951 (Figure 49)

topographic maps show Sprague Neck Bar as similar in shape and orientation to

representations in the earlier charts.

Aerial Photography- Few remarkable changes are noticeable during the period of

air photo coverage (1940 to 1991). This may be due in part to the small scale of the

photos, thus preventing observation of minor changes. Sprague Neck Bar had an

approximate total area equaling 53,245 sq. meters at low tide and an approximate area of
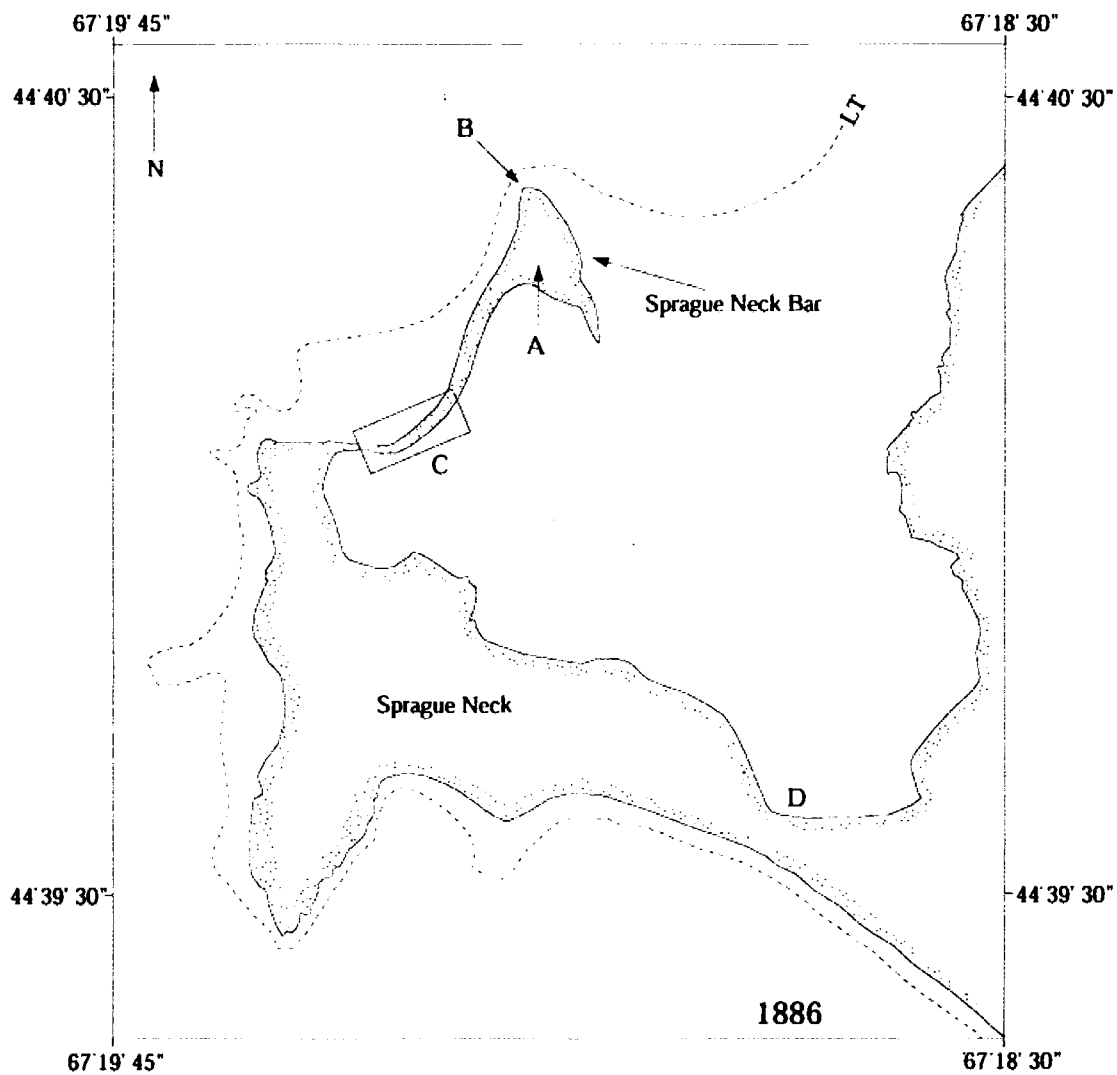
Figure 47. Map of Sprague Neck Bar in 1886. The dashed line represents the low tide line (LT). Approximate scale of 1 cm = 154 m. Note the similarity in shape and orientation, erosion of Sprague Neck, and the broader flat environment to the 1776 chart. Letters A, B, C, and D are described in text.
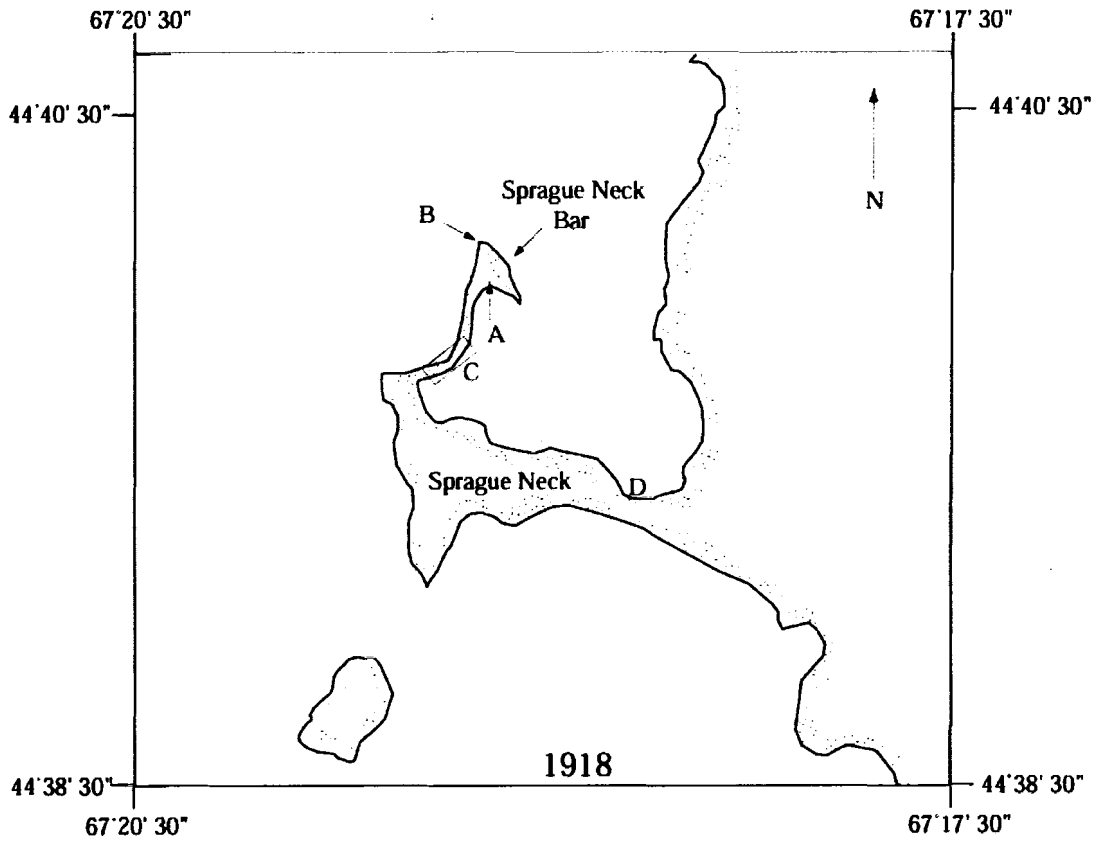
Figure 48. Depiction of Sprague Neck Bar in 1918, the earliest topographic map showing Sprague Neck. Note the rounded tip (B), broad flat (A), and bend (C) of Sprague Neck Bar and the similarity to the chart produced in 1886. Approximate scale is 1 cm = 450 m.
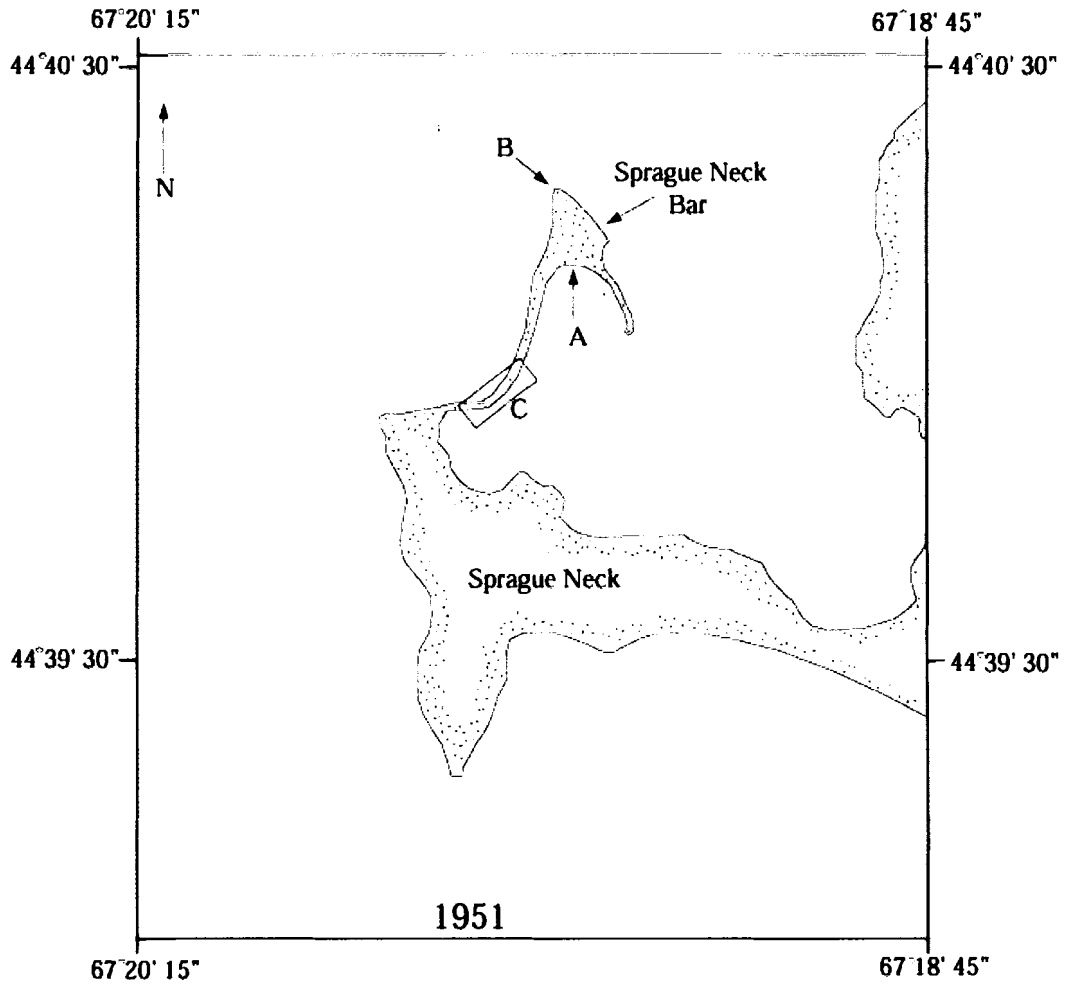
Figure 49. Map of Sprague Neck in 1951. Approximate scale is 1 cm = 240 m. Letters A, B, and C are described in text.

15, 310 sq. meters at high tide (1991 air photo). The total perimeter for the barrier spit from 1940-1991 ranges from 2,434 m to 2,572 m. The much smaller area in the 1991 air photo shows the majority of Sprague Neck Bar is tidally influenced and exposed only during low tide. The discrepancy in the total area for the 1940-1979 air photos is a result of the photos taken at different tidal elevations, difficulty in accurately locating registration points on all air photos, and difficulty in discerning the developing spit platform and swash bars on the grayscale photos. Sprague Neck Bar extended farther north into the head of Machias Bay and had a broader gravel flat in the 1940 air photo. More recent air photos show that the recurve system and new sediment sink is growing in a southeasterly direction and the developing spit platform is increasing in size, suggesting sediment reworking of the cuspate spit tip and active current recurved spit tip.

Incoming waves and subsequent refraction around numerous islands, subaqueous barriers and ledges, and the rocky headlands of Sprague Neck are visible on the 1966 and 1979 air photos. Incoming wave crests are oriented parallel to Davis Beach at these times. Refraction around Sprague Neck changes the orientation of the waves to a more northeasterly direction. The (November) 1991 air photo shows that the wave direction is from northwest to southeast, directing wave energy around the spit tip to the south and southeast.

Large- and small-scale geomorphic elements are discernible on the 1991 air photo, scale of 1 in. = 500 ft. (Figure 50). Sprague Neck Bar is in the same shape and orientation as depicted in the earlier maps and air photos. The broad flat (A in Figure 50), rounded tip (B in Figure 50), progressive narrowing to the south, and the distinct
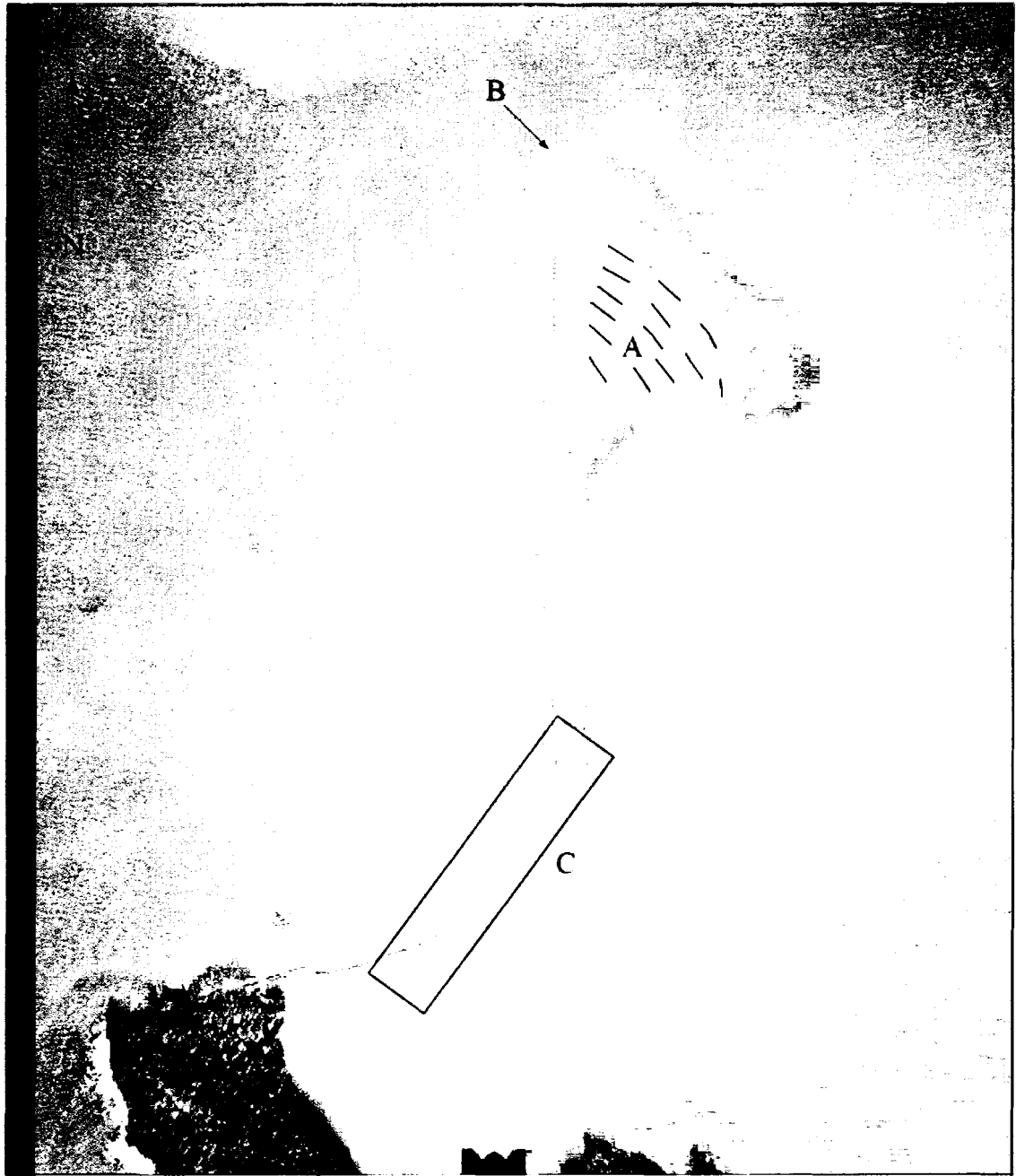
Figure 50. Air photo of Sprague Neck Bar, November 1991. Approximate scale is 1 cm = 60 m. Letters A, B, and C are described in the text. The dashed lines indicate the main gravel ridges on the flat.

bend (C in Figure 50) near the Pond Ridge Moraine are clearly identified. Equally

prominent on the 1991 air photo are wave refraction around the spit tip and the seven

gravel ridges comprising the preserved recurve system (see A in Figure 50).

DISCUSSION

Tidal Currents

Tidal currents for most mesotidal channels and inlets along the U.S. Atlantic coast are ebb dominated. Ebb domination results in a net sediment transport in the direction of the ebbing tide (FitzGerald and Nummedal, 1983). Dominance of the ebb tide is a factor of the water elevation at maximum ebb and flood tides and channel/inlet efficiency during the complete tidal cycle (FitzGerald and Nummedal, 1983). However, FitzGerald et al. (1984) found flood-dominated inlets on the mesotidal coast of Maine. A stronger current at the inlet throat creates a significant net landward transfer of sediment into the backbarrier environment. The steepening of the tidal wave in the embayment and the shallow ebb-tidal delta and spit platform causes flood-dominance.

FitzGerald and Nummedal (1983) described the efficiency of a channel in transporting water from the ocean and bay as a relationship between the bay surface area (A_b) and inlet cross-sectional volume (A_c) during the tidal cycle. The A_c/A_b ratio reaches a maximum value at low tide and a minimum value at high tide. The ratio reaches a minimum value at high tide because the bay surface area increases during flooding tides. During ebbing tides the bay surface area decreases, and the A_c/A_b ratio increases. Therefore, at times of flooding tide the tidal channel is the least efficient, resulting in a lag time between high tide at the mouth and head of an embayment. There is less of a lag time during ebbing tide because the channel can more efficiently transport water. The difference in lag time indicates a greater duration of the flood tide and greater ebb velocities, which is often necessary if the flood- and ebb-tidal prisms are to remain balanced (FitzGerald and Nummedal, 1983). In the head of Machias Bay the times of

93

high and low tide lag behind the mouth by 12-37 minutes.

The lag time in Machias Bay affects the tidal currents near Sprague Neck. During the sampling period winds ranged between 0-0.5 m/s from the southwest, with no significant wind gusts. Data obtained from the current meters provided limited information on the influence of tidal currents on Sprague Neck Bar. Ideally, the tidal regime would have been sampled during storm events, winter months, and calm weather when the wind approached Sprague Neck from alternate directions.

Flood tidal currents along the western side of Sprague Neck Bar are to the northeast, and ebb tide is to the southwest. Along the active recurve, flood tidal currents flow to the southeast, and the ebbing tide is to the northwest. Ebb tidal currents along the recurve obtained maximum velocities of 25 cm/s, which is greater than the maximum velocity (9 cm/s) of the ebb tidal currents along the western side of Sprague Neck Bar. Flood-tidal current velocities along Sprague Neck Bar ranged between 4-12 cm/s, with greater flood current velocities occurring along the modern recurve. Flood-tidal current velocities along the recurve, 5-12 cm/s, are comparable to the flood-tidal current velocities FitzGerald et al. (1984) found in flood-dominated systems, 10-20 cm/s. This suggests the flood-tidal current at Sprague Neck Bar transports a significant amount of mud and fine/medium sand to the backbarrier environment, which accounts for the accumulation of mud in the backbarrier and the higher minimum elevation on the topographic profiles (Figure 35). The higher minimum elevation of the landward facing slope indicates the long-term stability of Sprague Neck Bar.

During slack high tide, tidal currents along the recurve and western side of Sprague Neck Bar are moving at similar horizontal scalar speeds. Horizontal and total

scalar speeds during flooding and ebbing tides are greater along the recurve. Transient

horizontal and total scalar speeds do not occur within one specific time and indicate

bursts of the tidal current or wave slap during submergence and emergence. Greater total

scalar speed is a product of higher up velocities, indicating faster and more turbulent flow

during flooding and ebbing tides along the recurve. The recurve is constricted so higher

speeds are expected. Under these conditions, waves resuspend more material in the outer

beach and transport sediment to the backbarrier environment. Overall, tidal currents are

probably not the dominant sediment transport mechanism, and storm waves may

dominate. This conjecture was not tested, however.

Ground Penetrating Radar

GPR transects provided limited data due to the high saltwater content of Sprague

Neck Bar. At low tide, the saltwater content was expected to be negligible and have only

minor affects on the EM signal. However, a significant amount of saltwater is retained

within the barrier spit. The saltwater within the barrier prevented the EM signal from

penetrating deeply into the substrate. The attenuated EM signal produced multiples of

the surface.

Saltwater retention within Sprague Neck Bar may indicate a finer-grained

sediment core. Coarse-clastic beaches are typically highly permeable due to an

openwork beachface surface and the degree of pore space. Carter and Orford (1993)

found that the degree of permeability within coarse systems may be reduced as a result of

a fine, interstitial component common at all depths. The internal structure of a coarse

barrier system often exhibits a coarse/fine unit stratification, which reduces the

permeability of the system (Carter and Orford, 1993).

The feature located at 220 m along the northward extension of Sprague Neck Bar (Figure 37) occurs approximately 1 m below the surface and may be explained by: 1) a tidal inlet or 2) a topographic low on the barrier crest. The location of the dipping reflector corresponds with the distinct increase in elevation observed on the modern-day spit. The shallow nature of the reflector suggests the feature formed within recent Holocene time. Historic analysis of Sprague Neck Bar, ca. 1776 to present, shows no evidence of a tidal inlet at this location. It is, therefore, likely that this feature represents a washover channel on a low, embayed segment of the barrier.

Algae and Ice Processes

Fifty clasts were painted and labeled on November 14, 2000 to determine the role of algae and ice in shaping Sprague Neck Bar. Monitoring the movement of these clasts throughout the winter months would have been ideal. However, Sprague Neck Bar was not accessible until May 2001. In May 2001, none of the clasts were located. Abrasion by ice and other clasts is not considered great enough to remove paint from the labeled rocks. Thus, the clasts were either transported offshore or buried beneath other clasts by storm events or ice processes. Their disappearance, at least, indicates that much of the sediment, including coarse clasts, is mobile during the winter.

Barrier Evolution

Coastal systems are constantly changing over various time scales. Dynamic equilibrium is represented by the evolution of landforms over geologic time, whereas steady-state equilibrium operates on a shorter time scale. During steady-state equilibrium landforms are considered to be in a constant state of equilibrium until a limiting threshold is reached. Coastal evolution is a function of accommodation space and sediment supply

in relation to relative sea level change. As the rate of relative sea-level rise slows, the role of sediment availability dominates. The relationship between the two is difficult to observe when both are "small" and act together.

Walsh (1988) postulated that the rate of sea-level rise controls the evolution of coastal morphology within the Lubec Embayment, with increased shoreline dynamics related to accelerated rates of relative sea-level rise. Retreat within the embayment has been episodic through time as a result of rising relative sea level and fluctuating sediment supply (Walsh, 1988). When supply is insufficient to nourish the barrier system during transgression, the barrier must either increase the rate of landward migration or be overstepped by rising sea level (Swift, 1975). Barrier evolution within the Lubec Embayment from 1785 to present has involved the formation and partial destruction of at least two ancestral barriers, followed by the development of the modern-day Lubec Spit. Similar shoreline dynamics exist along the eastern shore of Nova Scotia, where episodic barrier retreat results from isolated sediment supplies (eroding drumlins) and headland anchor points (Boyd et al., 1987; Figure 4). The four stages of barrier evolution (barrier genesis and progradation, barrier retreat, barrier destruction, barrier reestablishment) are similar to the evolutionary history Walsh (1988) inferred for the Lubec Embayment. The Lubec Embayment clearly fits the evolutionary model by Boyd et al. (1987).

Low wave energy, meso- to macro-tidal conditions, and a 2-3 mm/yr rate of relative sea-level rise characterizes Machias Bay and the Lubec Embayment. Tidal range within the Lubec Embayment is approximately 2 m greater than the tidal range for Machias Bay, with proportionally greater tidal currents. The initial hypothesis for the evolutionary history of Sprague Neck Bar was the stepwise retreat model by Boyd et al.

(1987), placing the barrier system in the barrier genesis and progradation stage. Sprague Neck (the Pond Ridge Moraine) was considered to be the headland anchor point and main sediment source. Additional sediment sources for the modern-day barrier system included three washboard moraines located along the western side of Sprague Neck and Sprague Neck Bar, transgressive retreat of Sprague Neck Bar, and erosion of the now-submerged moraines (Shipp, 1989) in the middle of Machias Bay.

An evolutionary model developed for Sprague Neck Bar must explain five unknowns: 1) the longshore changes in grain size, 2) the growth of Sprague Neck Bar occurring along the modern recurve, 3) the lack of significant long-term morphological change observed in the historical analysis, 4) the deposition of the eroded sediment from central Machias Bay, and 5) initial marsh growth and it's subsequent cessation. Two hypotheses were formulated to describe the evolution of Sprague Neck Bar: 1) two sediment sources/attachment points, and 2) multiple sediment sources with transport to the north and subsequent recurving to the southeast.

Model one (Figure 51) involves two discrete sediment sources, Sprague Neck and a large till deposit north of Sprague Neck, that serve as anchor points for barrier attachment and growth. Longshore drift transported sediment to the north-northeast from Sprague Neck and central Machias Bay, creating a barrier system extending to the north. While the barrier spit began growing to the north, the large till deposit was reworked to supply sediment to two separate barrier systems, one system extending to the south and the second growing to the southeast. A tidal inlet separated the two barrier spits oriented north-south. During the early Holocene, the tidal inlet closed. Self-cannibalization near Sprague Neck and relative sea-level rise created the distinct bend in Sprague Neck Bar
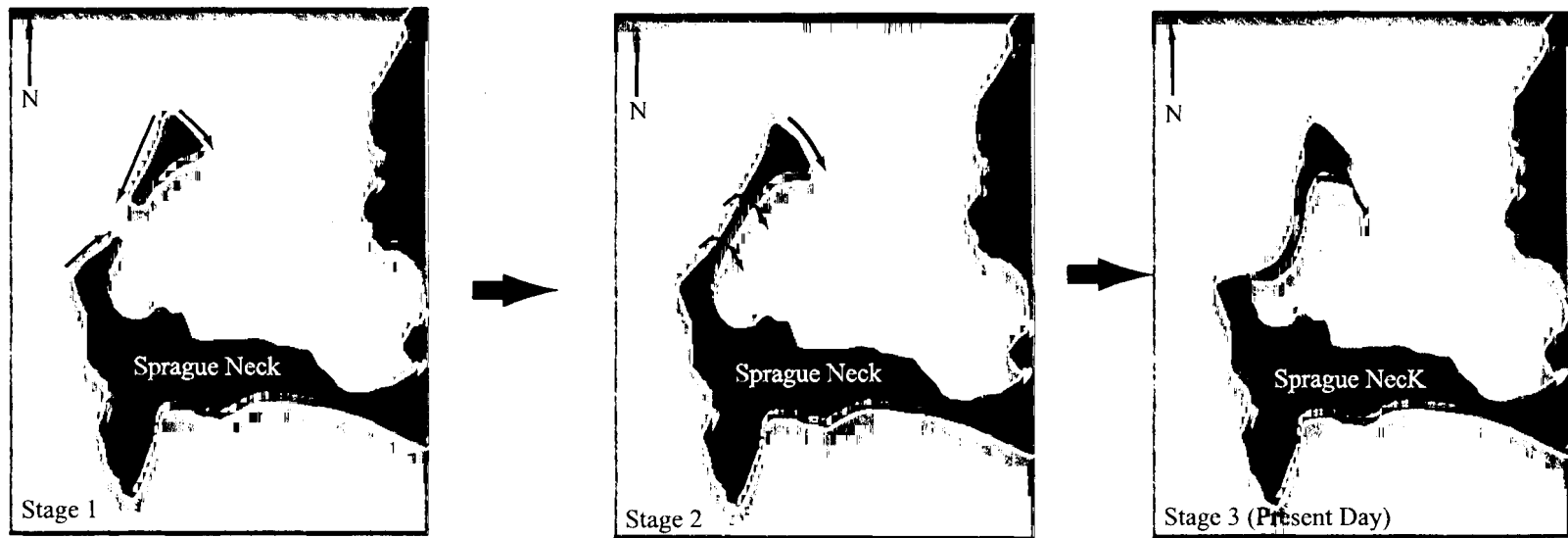
Figure 51. Evolutionary model of Sprague Neck Bar. This model describes the formation and evolution of Sprague Neck Bar in terms of two distinct sediment sources/attachment points and three separate barrier systems. Arrows indicate the direction of sediment transport.

proximal to the Pond Ridge Moraine.

In model two (Figure 52) the Pond Ridge Moraine is the headland anchor point and principle sediment source. Additional sediment sources exist in central Machias Bay, forming barrier islands separated by tidal inlets. Waves and tidal currents reworked the local deposits and transported material to the north-northeast by longshore drift. Longshore sediment transport closed the inlets, forming a single, drift-aligned barrier spit extending toward the head of Machias Bay. Sprague Neck Bar recurved to the southeast as bathymetric lows were filling with sediment.

The evolutionary model of Sprague Neck Bar extending to the north and recurving to the southeast is most supported by the existing data (Figure 52). Sprague Neck (Pond Ridge Moraine) divides Machias Bay in half and serves as the main attachment point and principle sediment source for the developing Sprague Neck Bar. Flood and ebb tidal current velocities around Sprague Neck Bar are nearly equal in magnitude. Fine sediment in the more exposed, open central portion of Machias Bay eroded earlier than the Pond Ridge Moraine. Wave and tidal currents transported the eroded material to the east-northeast, where the sediment entered an energy well and sediment sink. Sprague Neck Bar derived additional sediment, both directly and indirectly, from the coastal bluffs bordering the northern and western sides of Sprague Neck and eroded moraines and associated boulder ramps. The pocket beaches located along the western side of Sprague Neck Bar are not sediment sources per se but are residual deposits left from larger, more extensive till deposits.

Clast size varies along the western side of Sprague Neck Bar (Figure 31), with no coarsening or fining trend along the northward extension. Surface sediment of Sprague
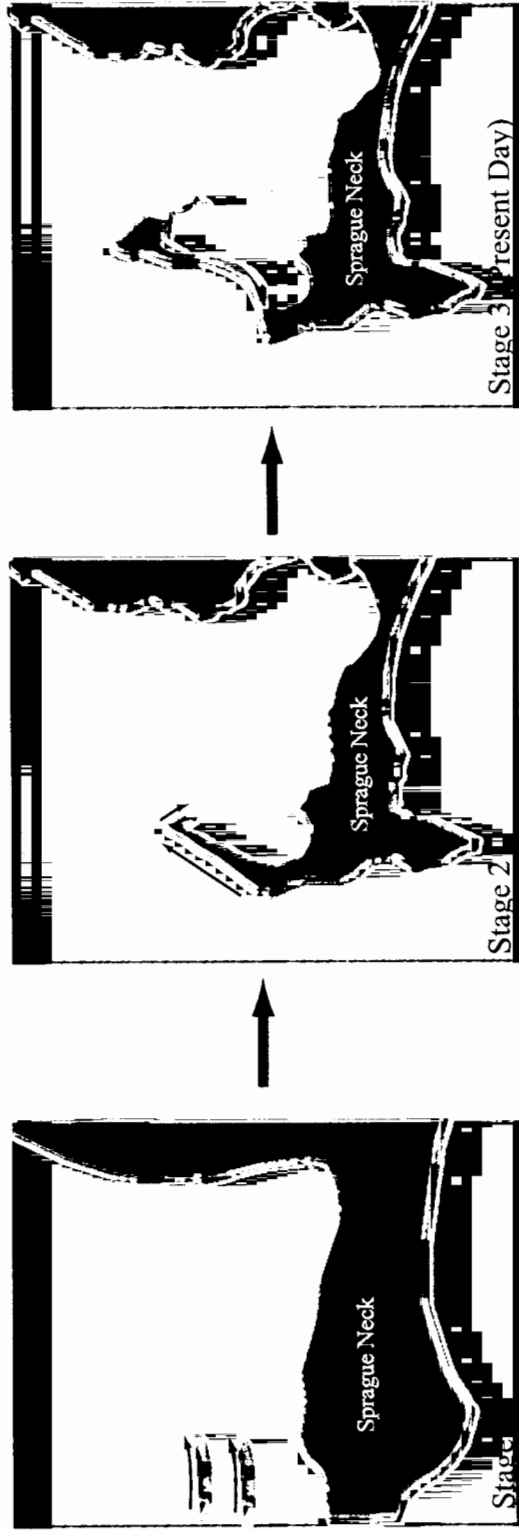
Figure 52. Evolutionary model for Sprague Neck Bar. This model relies on multiple sediment sources and describes barrier evolution according to northward growth and recurving to the southeast. Sprague Neck Bar stops growing to the north when a topographic low is encountered. While the topographic low is being filled with sediment, wave refraction creates the recurve to the southeast. The arrows in the diagram depict the direction of sediment transport.

101

Neck Bar is coarsest at the spit tip. The heterogeneous nature of the surface sediment suggests multiple sources, i.e., the linear extensions oriented normal to Sprague Neck and Sprague Neck Bar. The source of the sediment comprising the extensions is unclear. Several options exist: 1) tombolo-like features, 2) eroded moraines, and 3) sediment entrapment behind the rock outcrops in the nearshore environment as the shoreline migrated landward. The recurve to the southeast does have a fining trend away from the tip of Sprague Neck Bar because the spit tip is the only sediment source for the recurve.

The trends in grain size distribution along the northward extension are explained by the hypothesis of multiple sediment sources. One question remains unanswered: Why is the coarsest sediment located at the spit tip? Surface sediment is typically expected to fine in the direction of longshore sediment transport. Therefore, with longshore drift to the north the tip of Sprague Neck Bar was expected to be composed of the finest sediment. However, on coarse-grained systems, the largest clast sizes can be transported the greatest distance. The tip of Sprague Neck Bar is directly exposed to winds from the north, which are frequent and have the greatest fetch available to Sprague Neck Bar. The deep tidal channel (Figure 16) minimizes wave attenuation due to frictional losses.

A fluctuating sediment supply is not necessarily needed to create a recurved barrier spit. Wave refraction and variations in the underlying topography cause Sprague Neck Bar to recurve to the southeast. Sprague Neck Bar stops growing to the north when a bathymetric low is encountered. While a bathymetric low is being filled, the system recurves. During the historic evolution of Sprague Neck Bar, the spit recurved six times. The recurves do not extend farther southeast because of transgressive retreat.

The lack of long-term change observed in the historical analysis for the northward

extension of Sprague Neck Bar may be attributed to self-cannibalization and reworking of the surface sediment into cross-shore and alongshore zones. Sediment reworking and washover processes produced the distinct bend in Sprague Neck Bar proximal to the moraine. An overwash channel may be revealed in the GPR transect along the northward extension at 220 m north of Sprague Neck.

Sprague Neck Bar is geomorphically and dynamically different from other barrier systems in the eastern Gulf of Maine, i.e., the Lubec Embayment. The Lubec Embayment is a closed system, and barrier spits within the embayment have a lower ability (than Sprague Neck Bar) to absorb stress. Therefore, relative sea-level rise, fluctuations in sediment availability, and accommodation space drive conditions to limiting thresholds. Sprague Neck Bar is not as obvious an example of the model by Boyd et al. (1987) due to the large evolutionary time-scale, lack of significant observable change within historic time, and variations from the model. Sprague Neck Bar differs from the Boyd et al. (1987) model by the number and location of sediment sources. The stepwise retreat model describes barrier evolution in terms of two discrete point sources (drumlins). A barrier spit grows by longshore transport from each sediment source, with a tidal inlet separating the two spit systems. Sprague Neck Bar can not be accurately explained by the stepwise retreat model and is more easily explained in terms of morphodynamics.

CONCLUSIONS

Sprague Neck Bar has evolved slowly throughout historic times. The Pond Ridge

Moraine served as the main sediment source and attachment point. Multiple sediment

sources located in central Machias Bay contributed sediment to Sprague Neck Bar. Tidal

currents and longshore transport reworked and transported material from each of these

sources, forming barrier islands separated by tidal inlets. Longshore drift transported

sediment to the north-northeast to create a single, drift-aligned barrier system. Sprague

Neck Bar recurved to the southeast each time a bathymetric low was encountered. A

bathymetric low acts as a sediment sink that takes a longer period of time to accumulate

sediment and aggrade above mean low water, thus preventing the barrier system to grow

northward. While the system is accumulating sediment, wave refraction transports

sediment to the southeast. Wave and tidal currents are the principle sediment transport

mechanisms. Overwash during storm events and ice-rafting are additional mechanisms

important in transporting the larger clast sizes. Based on observations of attached algae

and dragmarks on the beachface the attachment of algal fronds to individual clasts does

play a minor role in sediment transport.

The model by Boyd et al. (1987) developed for the southern coast of Nova Scotia

can not explain the evolution of Sprague Neck Bar. The stepwise retreat model explains

barrier evolution according to two sediment sources and anchor points. Sprague Neck

Bar consists of one attachment point (Sprague Neck) and multiple sediment sources.

Sprague Neck Bar has remained stable for three primary reasons: 1) the nature of the

local, discrete source deposits, 2) sediment reworking, and 3) accommodation space.

Additional work needs to be done in order to better understand the evolutionary history of Sprague Neck Bar. Tidal currents need to be sampled during the winter months, various storm events, and again during calm conditions. Barrier stratigraphy also needs to be determined. Coring along the crest would determine if the evolutionary model proposed for Sprague Neck Bar accurately explains the system and if Sprague Neck Bar is composed of a fine sediment core. Coring the backbarrier mudflat would reveal if the system has been stable in the current configuration for an extended time period.

REFERENCES

Anderson, R.S. and Borns, H.W., Jr., 1983, Evidence for late Holocene sea-level rise in New England: A summary of available data derived from salt marshes and other organic materials: In: Thompson, W.B. and Kelley, J.T., eds., New England seismotectonic study activities in Maine during fiscal year 1982, MGS Report to U.S. Nuclear Regulatory Commission, Augusta, p. 121-136.

Anderson, R.S., Miller, N.G., Davis, R.B., and Nelson, R.E., 1990, Terrestrial fossils in the marine Presumpscot Formation; implications for late Wisconsinan paleoenvironments and isostatic rebound along the coast of Maine: Canadian Journal of Earth Science, v. 27, n. 9, p. 1241-1246.

Anderson, R.S. and Race, C.D., 1981, Evidence for late Holocene and recent sea-level rise along coastal Maine utilizing salt marsh data: In: Thompson, W.B., ed., New England seismotectonic study activity in Maine during fiscal year 1981: MGS Report to U.S. Nuclear Regulatory Commission, Augusta, p. 79-96.

Anderson, W.A., Borns, H.W., Jr., Kelley, J.T., and Thompson, W.B., 1989, Neotectonic activity in coastal Maine: In: Anderson, W.A. and Borns, H.W., Jr., eds., Neotectonics of Maine: Maine Geological Survey Bulletin 40, p. 1-10.

Anderson, W.A., Kelley, J.T., Thompson, W.B., Borns, H.W., Jr., Sanger, D., Smith, D.C., Tyler, D.A., Anderson, R.S., Bridges, A.E., Crossen, K.J., Ladd, J.W., Anderson, B.G., and Lee, F.T., 1984, Crustal warping in coastal Maine: Geology, v. 12, p. 677-680.

Ashley, G.M., Boothroyd, J.C., and Borns, H.W., Jr., 1991, Sedimentology of late Pleistocene (Laurentide) deglacial-phase deposits, eastern Maine; An example of a temperate marine grounded ice-sheet margin: Geological Society of America, Special Paper 261, p. 107-125.

Barnhardt, W.A., Belknap, D.F., and Kelley, J.T., 1997, Sequence stratigraphy of submerged river-mouth deposits in the northeastern Gulf of Maine: responses to relative sea level changes: Geological Society of America Bulletin, v. 109, p. 612-630.

Barnhardt, W.A., Gehrels, W.R., Belknap, D.F., and Kelley, J.T., 1995, Late Quaternary relative sea-level change in the western Gulf of Maine: Evidence for a migrating glacial forebulge: Geology, v. 23, p. 317-320.

Barnhardt, W.A. and Kelley, J.T., 1995, Carbonate accumulation on the inner continental shelf of Maine: A modern consequence of Late Quaternary glaciation and sea-level change: Journal of Sedimentary Research, v. A65, n. 1, p. 195-207.

Belknap, D.F., unpublished (1988), University of Maine rapid sediment analyzer manual.

Belknap, D. F., 1991, Preservation potential of the Delaware Atlantic coast barrier-backbarrier system: In: Kraus, N. C., Gingerich, K. J., and Kriebal, D. L., eds., ASCE, Virginia, Coastal Sediment '91, v. 2, p. 1269-1283.

Belknap, D. F., Anderson, B. G., Anderson, R. S., Anderson, W. A., Borns, H. W., Jr., Jacobson, G. L., Kelley, J. T., Shipp, R. C., Smith, D. C., Stuckenrath, R., Jr., Thompson, W. B. and Tyler, D. A., 1987a, Late Quaternary sea-level changes in Maine: Society of Economic Paleontologists and Mineralogists, p. 72-86.

Belknap, D.F., Kelley, J.T., and Shipp, R.C., 1987b, Quaternary stratigraphy of representative Maine estuaries: initial examination by high-resolution seismic reflection profiling: In: FitzGerald, D.M. and Rosen, P.S., eds., Glaciated Coasts, Academic Press, San Diego, p. 177-207.

Belknap, D.F. and Kraft, J.C., 1981, Preservation potential of transgressive coastal lithosomes on the U.S. Atlantic shelf: Marine Geology, v. 42, p. 429-442.

Belknap, D.F. and Kraft, J.C., 1985, Influence of antecedent geology on stratigraphic preservation potential and evolution of Delaware's barrier systems: Marine Geology, v. 63, p. 235-262.

Belknap, D.F., Kraft, J.C., and Dunn, R.K., 1994, Transgressive valley-fill lithosomes: Delaware and Maine: In: Boyd, R., Zaitlin, B.A. and Dalrymple, R., eds., Incised Valley Fill Systems, SEPM Special Pub. 51, p. 303-320.

Belknap, D.F., Shipp, R.C., and Kelley, J.T., 1986, Depositional setting and Quaternary stratigraphy of the Sheepscot Estuary, Maine: Geographie physique et Quaternaire, v. 40, p. 55-69.

Belknap, D.F., Shipp, R.C., Stuckenrath, R., Kelley, J.T., and Borns, H.W., Jr, 1989, Holocene sea-level change in coastal Maine: In: Anderson, W.A. and Borns, H.W., Jr., eds., Neotectonics of Maine, Maine Geological Survey Bulletin, v. 40, p. 85-105.

Bloom, A.L., 1963, Late Pleistocene fluctuations of sea level and postglacial crustal rebound in coastal Maine: American Journal of Science, v. 261, p. 862-879.

Bluck, B.J., 1967, Sedimentation in beach gravels: examples from South Wales: Journal of Sedimentary Petrology, v. 37, p. 128-156.

Bothner, M.H. and Spiker, E.C., 1980, Upper Wisconsinan till recovered on the continental shelf southeast of New England: Science, v. 210, p. 423-425.

Boyd, R., Bowen, A.J., and Hall, R.K., 1987, An evolutionary model for transgressive sedimentation on the Eastern Shore of Nova Scotia: In: FitzGerald, D.M. and Rosen, P.S., eds., Glaciated Coasts, Academic Press, San Diego, p. 87-114.

Boyd, R. and Honig, C., 1992, Estuarine sedimentation on the Eastern Shore of Nova Scotia: Journal of Sedimentary Petrology, v. 62, n. 4, p. 569-583.

Brenninkmeyer, B.M. and Nwankwo, A.F., 1987, Source of Pebbles at Mann Hill Beach, Scituate, Massachusetts: In: FitzGerald, D.M. and Rosen, P.S., eds., Glaciated Coasts, Academic Press, San Diego, p. 251-278.

Buynevich, I. and FitzGerald, D.M., 1999, Structural Controls on the development of a coarse sandy barrier, Reid State Park, Maine: In: Krauss, N.C. and McDougal, W.G., eds., Coastal Sediments '99, ASCE, Virginia, p. 1256-1267.

Carr, A.P., 1969, Size grading along a gravel beach: Chesil Beach, England: Journal of Sedimentary Petrology, v. 39, p. 297-311.

Carter, C.H. and Guy, D.E., 1988, Coastal erosion: timing and magnitude at the bluff toe: Marine Geology, v. 84, p. 1-17.

Carter, R.W.G., Forbes, D.L., Jennings, S.C., Orford, J.D., Shaw, J., and Taylor, R.B., 1989, Barrier and lagoon coast evolution under differing relative sea-level regimes: ex. for Ireland and Nova Scotia: Marine Geology, v. 88, p. 221-242.

Carter, R.W.G. and Orford, J.D., 1988, Conceptual model of coarse-clastic barrier formation from multiple sediment sources: The Geographical Review, v. 78, p. 219-238.

Carter, R.W.G. and Orford, J.D., 1991, The sedimentary organization and behavior of drift-aligned gravel barriers: In: Kraus, N.C., Gingerich, K.J. and Kriebal, D.L., eds., Coastal Sediments '91, ASCE, New York, p. 934-948.

Carter, R.W.G. and Orford, J.D., 1993, The morphodynamics of coarse clastic beaches and barriers: a short- and long-term perspectives: Journal of Coastal Research, Special Issue 15, Spring, p. 158-179.

Carter, R.W.G. and Woodroffe, C.D., 1994, Coastal evolution: an introduction: In: Carter, R.W.G. and Woodroffe, C.D., eds., Coastal Evolution: Late Quaternary Shoreline Morphodynamics, Cambridge University Press, Cambridge, p. 1-32.

Cowell, P.J. and Thom, B.G., 1994, Morphodynamics of coastal evolution: In: Carter, R.W.G. and Woodroffe, C.D., eds., Coastal Evolution: Late Quaternary Shoreline Morphodynamics, Cambridge University Press, Cambridge, p. 33-86.

Davis, R.A., Jr., 1994, Barrier island systems-a geologic overview: In: Davis, R.A., Jr., ed., Geology of Holocene Barrier Island Systems, Springer-Verlag, New York, p. 1-46.

Davis, R.B. and Jacobson, G.L., Jr., 1985, Late glacial and early Holocene landscapes in northern New England and adjacent areas of Canada: Quaternary Research, v. 23, p. 341-368.

deBeaumont, E., 1845, Lecons de geologie pratique: In: Hoyt, J.H., 1967, Barrier Island Morphology: Geological Society America Bulletin, v. 78, p. 1125-1136.

Dionne, J., 1965, Sedimentologie littorale; le role des algues comme agents d'erosion et de transport: Annales de l'ACFAS, v. 31, p. 58-59.

Dorion, C.C., 1997, An updated high resolution chronology of deglaciation and accompanying marine transgression in Maine: Unpublished M.S. thesis, Dept. of Geological Sciences, University of Maine, Orono, Maine, 147 p.

Dorion, C.C., Balco, G.A., Kaplan, M.R., Kreutz, K., Wright, J.D., and Borns, H.W., Jr., in press, Stratigraphy, paleoceanography, chronology and environment during the deglaciation of eastern Maine: In: Weddle, T.K. and Retelle, M.V., eds., Deglacial history and relative sea level changes, northern New England and adjacent Canada: Boulder, Colorado, Geological Society of America Special Paper 351.

Duffy, W., Belknap, D.F., and Kelley, J.T., 1989, Morphology and stratigraphy of small barrier-lagoon systems in Maine: Marine Geology, v. 88, p. 243-262.

Evans, M.W., Hine, A.C., Belknap, D.F., and Davis, R.A. Jr, 1985, Bedrock control on barrier island development: west-central Florida Coast: Marine Geology, v. 63, p. 263-283.

Falmouth Scientific Instruments, 2000, 3D Acoustic Current Meter Manual, Version 7.1.

Fefer, S.I. and Schettig, P.A., 1980, An ecological characterization of coastal Maine: U.S. Fish and Wildlife Service Report FWS/OBS-80/29.

Fields, J.W., Katuna, M.P., and Mirecki, J.E., 1999, Relationship of Geologic Framework to Origin of Barrier Island Coast, South Carolina: In: Krauss, N.C. and McDougal, W.G., eds., Coastal Sediments '99, ASCE, Virginia, p. 588-596.

Fisher, J.J., 1968, Barrier island formation: discussion: Geological Society of America Bulletin, v. 79, p. 1421-1426.

FitzGerald, D.M., Fink, and Lincoln, 1984, A flood-dominated mesotidal inlet: GeoMarine Letters, v. 3, n. 1, p. 17-22.

FitzGerald, D.M. and Nummedal, D., 1983, Response characteristics of an ebb-dominated tidal inlet channel: Journal of Sedimentary Petrology, v. 53, n. 3, p. 833-843.

FitzGerald, D.M., Rosen, P.S., and van Heteren, S., 1994, New England Barriers: In: Davis, R.A., Jr., ed., Geology of Holocene Barrier Island Systems, Springer-Verlag, New York, p. 305-394.

FitzGerald, D.M. and Van Heteren, S., 1999, Classification of paraglacial barrier systems: coastal New England, USA: Sedimentology, v. 46, p. 1083-1108.

Forbes, D.L. and Taylor, R.B., 1987, Coarse-grained beach sedimentation under paraglacial conditions, Canadian Atlantic Coast: In: FitzGerald, D.M. and Rosen, P.S., eds., Glaciated Coasts, Academic Press, San Diego, p. 51-86.

Forbes, D.L. and Syvitski, J.P.M., 1994, Paraglacial coasts: In: Carter, R.W.G. and Woodroffe, C.D., eds., Coastal Evolution: Late Quaternary Shoreline Morphodynamics, Cambridge University Press, Cambridge, p. 373-424.

Forbes, D.L., Orford, J.D., Carter, R.W.G., Shaw, J., and Jennings, S.C., 1995a, Morphodynamic evolution, self-organization, and instability of coarse-clastic barriers on paraglacial coasts: Marine Geology, v. 126, p. 63-85.

Forbes, D.L., Shaw, J., and Taylor, R.B., 1995b, Differential preservation of coastal structures on paraglacial shelves: Holocene deposits on southeastern Canada: Marine Geology, v. 124, p. 187-201.

Forbes, D.L., Taylor, R.B., Orford, J.D., Carter, R.W.G., and Shaw, J., 1991, Gravel-barrier migration and overstepping: Marine Geology, v. 97, p. 305-313.

Gehrels, W.R., 2000, Using foraminiferal transfer functions to produce high resolution sea-level records from salt-marsh deposits, Maine, USA: The Holocene, v. 10, n. 3, p. 367-376.

Gehrels, W.R. and Belknap, D.F., 1993, Neotectonic history of eastern Maine evaluated from historic sea-level data and ^{14}C dates on salt-marsh peats: Geology, v. 21, p. 615-618.

Gehrels, W.R., Belknap, D.F., and Kelley, J.T., 1996, Integrated high-precision analyses of Holocene relative sea-level changes: Lessons from the coast of Maine: Geological Society of America Bulletin, v. 108, n. 9, p. 1073-1088.

Gilbert, G.K., 1885, The topographic feature of lake shores: U.S.G.S. 5th Annual Report, p. 69-123.

Haines, J. W., Howd, P., and Hanson, K., 1999, Cross-shore transport and profile evolution at Duck, North Carolina: In: Krauss, N.C. and McDougal, W.G., eds., Coastal Sediments '99, ASCE, Virginia, p. 1050-1064.

Halsey, S.D., 1979, Nexus: new model of barrier island development: In: Leatherman, S.P., ed., Barrier Islands: From the Gulf of St. Lawrence to the Gulf of Mexico, Academic Press, New York, p. 185-210.

110

Hayes, M.O., 1975, Morphology of sand accumulations in estuaries: In: Cronin, L.E., ed., Estuarine Research, v. 3, p. 3-22, Academic Press, New York.

Hoekstra, P., Houwman, K., and Ruessink, G., 1999, The role and time scale of cross-shore sediment exchange for a barrier island shoreface: In: Krauss, S.P. and McDougal, W.G., eds., Coastal Sediments '99, ASCE, Virginia, p. 519-534.

Hoyt, J.H., 1967, Barrier island formation: Geological Society of America Bulletin, v. 78, p. 1125-1136.

Hume, T.M., Beamsley, B., Green, M.O., de Lange, W., and Hicks, D.M., 1995, Influence of seabed topography and roughness on longshore wave processes: In: Dally, W.R. and Zeidler-Ryszard, B., eds., Coastal Dynamics '95, ASCE, Virginia, p. 975-986.

Johnson, D.W., 1919, Shore processes and shoreline development: New York, 397 p.

Kaplan, M.R., 1994, The deglaciation of southeastern Washington County, Maine: Unpublished M. S. thesis, Dept. of Geological Sciences, University of Maine, Orono, Maine, 112 p.

Kaplan, M.R., 1999, Retreat of a tidewater margin of the Laurentide ice sheet in eastern coastal Maine between ca. 14,000 and 13,000 ^{14}C yr. B.P.: Geological Society of America Bulletin, v. 111, n. 4., p. 620-632.

Kelley, J.T., 1987, An Inventory of Coastal Environments and Classification of Maine's Glaciated Shoreline: In: FitzGerald, D.M. and Rosen, P.S., eds., Glaciated Coasts, Academic Press, San Diego, p. 51-86.

Kelley, J.T., Belknap, D.F., and Shipp, R.C., 1989, Sedimentary framework of the southern Maine inner continental shelf; influence of glaciation and sea-level change: Marine Geology, v. 90, n. 1-2, p. 139-147.

Kelley, J.T. and Dickson, S.M., 2001, Low-cost bluff-stability mapping coastal Maine; providing geological hazard information without alarming the people: Environmental Geosciences, v. 7, n. 1, p. 46-56.

Kelley, J.T., Dickson, S.M., Belknap, D.F., and Stuckenrath, R., 1992, New radiocarbon-dated sea-level indicators from inner continental shelf vibracores, western Gulf of Maine: Geological Society of America-Abstracts with Programs, v. 23, n. 1, p. 51.

King, L.H., 1996, Late Wisconsinan ice retreat from the Scotian Shelf: Geological Society of America Bulletin, v. 108, n. 8, p. 1056-1067.

Komar, P.D., 1974, Beach processes and sedimentation, second edition: Prentice Hall, New Jersey, 544 p.

Komar, P.D. and Cui, B., 1984, The analysis of grain-size measurements by sieving and settling-tube techniques: Journal of Sediment Petrology, v. 54, n. 2, p. 603-614.

Kraft, J.C., Allen, E.A., Belknap, D.F., John, C.J., and Maurmeyer, E.M., 1979, Processes and morphologic evolution of an estuarine and coastal barrier system: In: Leatherman, S.P., ed., Barrier Islands, Academic Press, New York, p. 149-183.

Kraft, J.C. and John, C.J., 1979, Lateral and vertical facies relations of transgressive barriers: American Association of Petroleum Geologists Bulletin, v. 63, n. 12, p. 2145-2163.

LePage, C., 1982, The composition and origin of the Pond Ridge Moraine, Washington County, Maine: Unpublished M. S. thesis, Dept. of Geological Sciences, University of Maine, Orono, Maine, 74 p.

List, J.H. and Farris, A.S., 1999, Large-scale shoreline response to storms and fair weather: In: Krauss, N.C. and McDougal, W.G., eds., Coastal Sediments '99, ASCE, Virginia, p. 1324-1338.

McNinch, J.E., Wells, J.T., and Snyder, S.W., 1999, The long-term contribution of Pre-Holocene sands to transgressing barrier islands: In: Krauss, N.C. and McDougal, W.G., eds., Coastal Sediments '99, ASCE, Virginia, p. 786-801.

Mickelson, D.M. and Borns, H.W., Jr., 1972, Chronology of a kettle-hole peat bog, Cherryfield, Maine: Geological Society of America Bulletin, v. 83, p. 827-832.

Moss, A.L., 1963, The physical nature of common sandy and pebbly deposits - Part 2: American Journal of Science, v. 261, p. 297-343.

NOS (National Ocean Service), 2000, Tide Table-High and low water predictions: East Coast of North and South America: National Oceanic and Atmospheric Administration, U.S. Dept. of Commerce, Washington, D.C., 290 p.

Orford, J.D., Carter, R.W.G., and Jennings, S.C., 1996, Control Domains and morphological phases in gravel-dominated coastal barriers Nova Scotia: Journal of Coastal Research, v. 12, n. 3, p. 589-604.

Orford, J.D., Carter, R.W.G., Johnston, T.W., and Hansom, J.D., 1983, Discussion of size grading along a shingle beach in Wicklow, Ireland: Journal of Earth Sciences, v. 5, n. 2, p. 247-253.

Orford, J.D., Carter, R.W.G., McKenna, J., and Jennings, S.C., 1995, The relationship between the rate of mesoscale sea-level rise and the rate of retreat of swash-aligned gravel-dominated barriers: Marine Geology, v. 124, p. 177-186.

Osberg, P.H., Hussey, A.M., II, and Boone, G.M., 1985, Bedrock geologic map of Maine: Maine Geological Survey, Augusta, Maine, 1:500,000.

Ostrowski, R., Pruszak, Z., Rozynski, G., and Zeidler, R. B., 1995, Stochastics of Sediment transport, shore evolution and their input: In: Dally, W.R. and Zeidler, R.B., eds., Coastal Dynamics '95, ASCE, New York, p. 963-974.

Otvos, E.G., 1970, Development and migration of barrier islands, northern Gulf of Mexico: Geological Society of America Bulletin, v. 81, p. 241-246.

Quick, M.C. and Ametepe, J., 1991, Relationship between longshore and cross-shore transport: In: Kraus, N.C., Gingerich, K.J. and Kriebel, D.L., eds., Coastal Sediments '91, ASCE, New York, p. 184-196.

Rosen, P.S. and Leach, K., 1987, Sediment Accumulation Forms, Thompson Island, Boston Harbor, Massachusetts: In: FitzGerald, D.M. and Rosen, P.S., eds., Glaciated Coasts, Academic Press, San Diego, p. 234-250.

Roy, P.S., Cowell, P.J., Ferland, M.A., and Thom, B.G., 1994, Wave-dominated coasts: In: Carter, R.W.G. and Woodroffe, C.D., eds., Coastal Evolution: Late Quaternary shoreline morphodynamics, Cambridge University Press, Cambridge, p. 121-186.

Schwartz, M.L., 1971, The multiple causality of barrier islands: Journal of Geology, v. 79, p. 91-94.

Scott, D.B. and Greenberg, D.A., 1982, Relative sea-level rise and tidal development in the Fundy tidal system: Canadian Journal of Earth Science, v. 20, p. 1554-1564.

Selley, R.C., 1994, Applied Sedimentology: Academic Press, United States, 446 p.

Shepard, F.P., 1960, Gulf Coast Barriers: In: Shepard, F.P., Phleger, F.B. and van Andel, Tj.H. (eds.), Recent Sediments, Northwest Gulf of Mexico, American Association of Petroleum Geologists, Tulsa, Ok., p. 56-81.

Shipp, R.C., 1989, Late Quaternary sea-level fluctuations and geologic evolution of four embayments and adjacent inner shelf along the northwestern Gulf of Maine: Unpublished Ph.D. dissertation, Dept. of Geological Sciences, University of Maine, Orono, Maine, chapter 6.

Smith, R.V., 1990, Geomorphic trends and shoreline dynamics in three Maine embayments: Unpublished M.S. thesis, Dept. of Geological Sciences, University of Maine, Orono, Maine, 338 p.

Soulsby, R., 1991, Sediment transport by strong wave-plus-current flows: In: Kraus, N.C., Gingerich, K.J. and Kriebel, D.L., eds., Coastal Sediments '91, ASCE, New York, p. 405-417.

Stuiver, M. and Borns, H.W., Jr., 1975, Late Quaternary marine invasion in Maine: Its chronology and associated crustal movement: Geological Society of America Bulletin, v. 86, p. 99-104.

Swift, D.J.P., 1975, Barrier island genesis: evidence from the central Atlantic shelf, eastern U.S.A.: Sedimentary Geology, v. 14, p. 1-43.

Terrain Navigator, 1998, Map Tech, Coastal Maine CD.

Thompson, S.N., 1973, Sea-level rise along the Maine coast during the last 3000 years: Unpublished M.S. thesis, Dept. of Geological Sciences, University of Maine, Orono, Maine, 78 p.

Thompson, W.D., and Borns, H.W., Jr., 1985, Surficial Geologic Map of Maine: Maine Geological Survey, Augusta, 1:500,000.

Timson, B., 1976, Coastal Maine Geological Maps, Maine Geological Survey Open File Report 77-1, Augusta, Maine, 113 maps at 1:24,000 scale.

Tucker, M.E., 1991, Sedimentary Petrology: An Introduction to the Origin of Sedimentary Rocks: Blackwell Science, United Kingdom, 260 p.

Van Heteren, S., FitzGerald, D.M., McKinlay, P.A., and Buynevich, I.V., 1998, Radar facies of paraglacial barrier systems: coastal New England, USA: Sedimentology, v. 45, p. 181-200.

Walsh, J.A., 1988, Sedimentology and Late Holocene evolution of the Lubec Embayment: Unpublished M.S. thesis, Dept. of Geological Sciences, University of Maine, Orono, Maine, 434 p.

Zenkovitch, V.P., 1967, Processes of coastal development: Oliver and Boyd, Edinburgh, 738 p.

BIOGRAPHY OF THE AUTHOR

Rebecca A. Nestor was born in Rochester, Pennsylvania on February 22, 1977. She was raised in Zelienople, Pennsylvania and graduated from Seneca Valley High School in 1995. She attended Juniata College and graduated in 1999 with a B.S. in Geological Sciences. She moved to Maine to enter the Geological Sciences program at The University of Maine in the fall of 1999 with the hope of obtaining a Master's degree, concentrating in coastal sedimentology.

After completing her degree, Rebecca will be attending the University of New Hampshire to obtain her Ph.D. in Earth Sciences, concentrating in atmospheric sciences. Rebecca is a candidate for the Master of Science degree in Geological Sciences from the University of Maine in December, 2001.